Stony Brook University

Surface Remodeling of Lentiviral and Adeno-Associated Viral Vectors via Metabolically

Introduced Bioorthogonal Functionalities

A Dissertation Presented

by

Yanjie Chu

to

The Graduate School

in Partial Fulfillment of the

Requirements

for the Degree of

Doctor of Philosophy

in

Chemistry

Stony Brook University

August 2015

Stony Brook University

The Graduate School

Yanjie Chu

We, the dissertation committee for the above candidate for the

Doctor of Philosophy degree, hereby recommend

acceptance of this dissertation.

Isaac S. Carrico, Ph.D. - Dissertation Advisor
Associate Professor, Department of Chemistry

Kathlyn A. Parker, Ph.D. - Chairperson of Defense
Professor, Department of Chemistry

Orlando D. Sch ärer, Ph.D. - Third Member of Defense
Professor, Department of Chemistry

Patrick Hearing, Ph.D. - Outside Member of Defense
Professor, Department of Molecular Genetics and Microbiology

This dissertation is accepted by the Graduate School

Charles Taber
Dean of the Graduate School

ii

Abstract of the Dissertation

Surface Remodeling of Lentiviral and Adeno-Associated Viral Vectors via Metabolically

Introduced Bioorthogonal Functionalities

by

Yanjie Chu

Doctor of Philosophy

in

Chemistry

Stony Brook University

2015

As the most effective means to transfer genetic material into cells and tissues, viral vectors have been widely used for both therapeutic and basic biological applications. Extensive effort has been invested in the modification of viral surfaces to generate vectors with enhanced properties such as restricted cell tropism, easier purification and reduced immunogenicity. In particular, targeted gene transduction of specific cells has been a highly desirable goal and attempted by various strategies. Bioorthogonal chemical reactions such as Cu(I)-catalyzed azide-alkyne cycloaddition (CuAAC), strain-promoted azide-alkyne cycloaddition (SPAAC) and Staudinger ligation have significantly facilitated the study of biomolecules in their native environment due to the fast rates and superior selectivity under physiological conditions. We modified the surface of two frequently used viral gene delivery vehicles, lentiviral and adeno-associated viral (AAV) vectors, by a two-step labeling method. The viral particles were first metabolically labeled during production with unnatural substrates carrying the bioorthogonal azide group and subsequently

modified via click reactions, allowing the attachment of a variety of ligands. This strategy exhibited minimal perturbation on virus physiology and demonstrated remarkable flexibility.

For lentiviral vectors, the unnatural sugar *N*-azidoacetyl sialic acid (SiaNAz) was metabolically incorporated into viral envelope glycoproteins simply by addition of the precursor peracetylated *N*-α-azidoacetylmannosamine (Ac$_4$ManNAz) into the cell culture medium during virus production. Ligands targeting high-profile cancer associated receptors were functionalized with the strained alkyne bicyclo-[6.1.0]-nonyne (BCN) and introduced onto the viral surface through SPAAC, leading to enhanced transduction toward targeted cells *in vitro*. Furthermore, this general, versatile labeling technique is expected to be easily extended to the surface modification of other retroviruses.

For AAV vectors, the unnatural amino acid azidohomoalanine (Aha), a methionine surrogate, was added to the methionine-depleted cell growth medium during virus production for metabolic incorporation into the viral capsid. The impact of Aha on viral production and transduction efficiency was assessed by analyzing viruses produced in the presence of Aha in various concentrations using quantitative real time PCR assays and transduction assays. Successful incorporation of Aha onto viral surface was suggested by SDS-PAGE and western blotting analysis on virus samples modified with a reporter ligand through CuAAC.

This dissertation is dedicated to my parents.

Table of Contents

List of Figures

List of Schemes

List of Tables

List of Abbreviations

AAV	adeno-associated virus
Ac$_4$ManNAz	peracetylated *N*-α-azidoacetylmannosamine
ADA	adenosine deaminase deficiency
Aha	azidohomoalanine
BCN	bicyclononyne
CuAAC	Cu(I)-catalyzed azide-alkyne cycloaddition
DCC	*N*,*N'*-dicyclohexylcarbodiimide
DCM	dichloromethane
DHF	dihydrofolate
DIC	*N*,*N'*-diisopropylcarbodiimide
DIPEA	*N*,*N*-diisopropylethylamine
DMB	1,2-diamino-4,5-methylenedioxy-benzene
DMSO	dimethyl sulfoxide
FBS	fetal bovine serum
Fmoc	9-fluorenylmethyloxycarbonyl
FR	folate receptor
GFP	green fluorescent protein
GPI	glycosylphosphatidylinositol
HA	hemagglutinin
HBTU	2-(1H-benzotriazol-1-yl)-1,1,3,3-tetramethyluronium hexafluorophosphate
HIV	human immunodeficiency virus
HOBt	hydroxybenzotriazole
HRP	horseradish peroxidase
ITR	inverted terminal repeat
LTR	long terminal repeats
NHS	*N*-hydroxysuccinimide
ORF	open reading frame
PBS	phosphate buffered saline
PCFT	proton-coupled folate transporter
PCR	polymerase chain reaction
PEG	polyethylene glycol
PSMA	prostate-specific membrane antigen
RFC	reduced folate carrier
RGD	arginine-glycine-aspartate
SiaNAz	*N*-azidoacetyl sialic acid
SPAAC	strain-promoted alkyne-azide cycloaddition
SPANC	strain-promoted alkyne-nitrone cycloaddition
TEA	triethylamine
THF	tetrahydrofolate
VEGFR	vascular endothelial growth factor receptor
VSV-G	vesicular stomatitis virus glycoprotein

Acknowledgments

First and foremost I would like to thank my advisor Prof. Isaac Carrico for his constant support, encouragement and guidance. I had very little experience in chemical biology when I joined his group, or in any field of scientific research in general. He has taught me, both consciously and unconsciously, how to be an explorer in science and how good research is done. His academic enthusiasm and warm personality were contagious and motivational for me, especially during tough times in the Ph.D. pursuit. I shall forever be grateful for his contributions of time and ideas, without which nothing in this dissertation would have been possible.

I would also like to express my gratitude to Prof. Kathlyn Parker and Prof. Orlando Schärer, members of my dissertation committee, for their insightful comments and valuable advices, which have been immensely helpful for my research. Furthermore, I would like to thank Prof. Patrick Hearing for being the outside member of my committee, and giving helpful suggestions on the writing of this dissertation.

The members of the Carrico group have been such great colleagues and friends. During my stay in Stony Brook, they have been an inexhaustible source of professional advice as well as great fun. I shall forever cherish the memories we made together, the late night experiments, the loud K-pop in the lab, the beach party, and all the ups and downs of life.

I would also like to thank the members of the other groups in the chemistry department for generously sharing their knowledge and experimental resources.

Finally, to my parents, thank you for your endless love and support, and all the sacrifices you have made to give me a better life.

Chapter 1. Introduction

1.1 Viral vectors

1.1.1 Gene therapy

The understanding that many human diseases have a genetic origin, and the complete sequencing of the human genome established the molecular basis of gene therapy strategies. Generally defined as "the use of genes as medicine", gene therapy provides a rational therapeutic technique, which aims at eliminating the underlying biochemical defects of inherited and acquired diseases, rather than a symptomatic treatment. A therapeutic or working gene is transferred into specific cells of a patient in order to replace a faulty gene, or to introduce a new gene in order to prevent, cure or favorably modify the clinical course of a particular condition [1]. Since the first phase I trials treating adenosine deaminase deficiency (ADA) and malignant melanoma using retroviral vectors in 1990 [2, 3], more than 2200 gene therapy clinical trials have been reported, exploring novel approaches to the treatment of many genetic disorders, cancers, infectious diseases and other ailments (Figure 1-1). In this context, gene transfer systems are needed to deliver the desired gene to the target cells or tissues.
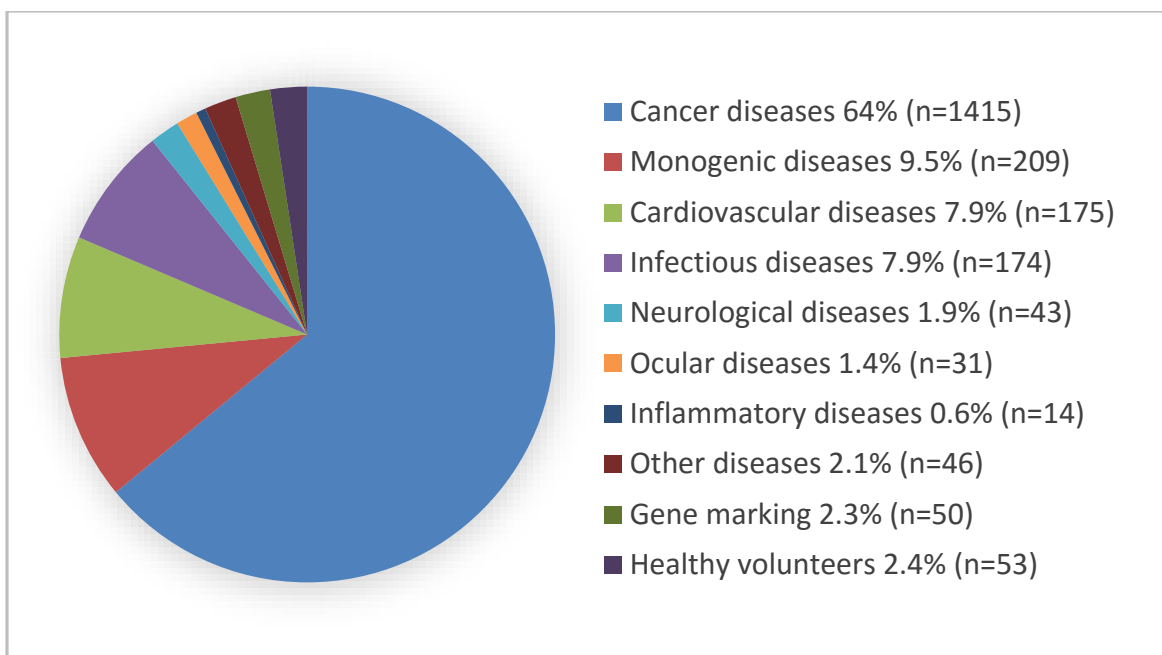
Figure 1-1. Indications addressed by gene therapy clinical trials (until July 2015).
Data reproduced from the *Journal of Gene Medicine*. Updated information available at www.wiley.co.uk/genmed/clinical.

1.1.2 Gene transfer vectors

Generally, gene transfer systems can be categorized into two groups: viral and non-viral vectors [4]. Non-viral vectors include naked DNA that is injected alone or in combination with physical methods [5-8], and a variety of synthetic delivery vectors such as lipids and liposomes [9, 10], polymers [11-13], polymersomes [14], cell-penetrating peptides [15] and inorganic nanoparticles [16]. Compared to viral vectors, non-viral delivery systems possess the advantages of easier and cheaper production, more effective cell/tissue targeting, lower immunogenicity and the capacity to transfer larger genes [4, 9, 17]. Nevertheless, the clinical usefulness of non-viral vectors is limited due to their low transduction efficiency relative to viral vectors [17, 18].
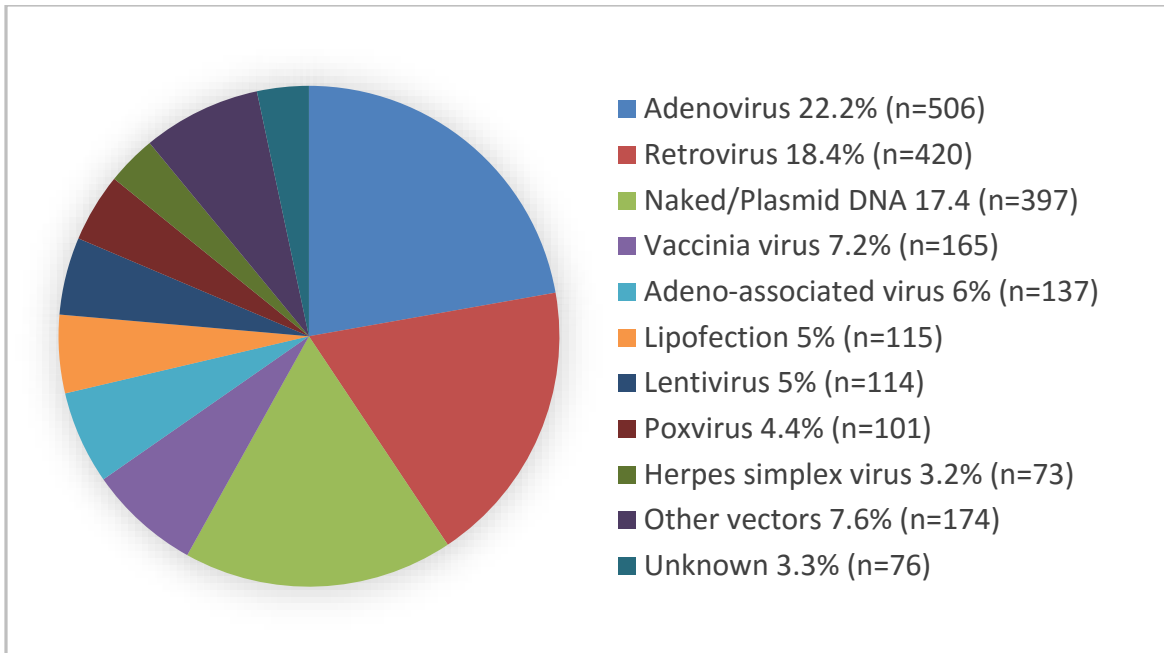
Figure 1-2. Vectors used in gene therapy clinical trials (until July 2015).
Data reproduced from the Journal of Gene Medicine. Updated information available at www.wiley.co.uk/genmed/clinical.

Viruses have evolved to effectively transport their genetic material into host cells. Viral vectors are generally viruses genetically modified to eliminate viral genes essential for replication and virulence, and make space to carry heterologous genes [19]. As a result, they are among the most efficient gene transfer vehicles. Nearly 70% of gene therapy clinical trials worldwide have used viral vectors derived from retroviruses, lentiviruses, adenoviruses, adeno-associated viruses, herpesviruses and poxviruses (Vaccinia viruses) (Figure 1-2). In addition to therapeutic applications such as correction of genetic defects, vaccination against cancer and infectious diseases, viral vectors are also used in many other areas for various goals including but not limited to functional gene studies and generation of experimental animal models. Yet, several limitations are associated with viral vectors, including the risk of insertional mutagenesis [20], toxicity [4], immunogenicity [21], restricted target cell specificity [22], limited gene packaging capacity [4, 23]

and difficulty of vector production [24]. Many efforts are still needed to develop viral vectors that are safe, efficient and capable of mediating well controlled expression of therapeutic genes in specific target cells/tissues.

1.2 Bioorthogonal chemistry

To understand the molecular details of extremely complicated biological processes in living organisms, various labeling strategies have been developed to probe diverse classes of biomolecules in real time. Genetically encoded reporters such as GFP represent typical biological tools to elucidate the roles of specific proteins in dynamic cellular processes, yet they are not suited for the study of other types of biomolecules such as glycans, lipids, nucleic acids, small molecule metabolites, as well as posttranslational modification [25-27]. To overcome this limitation, a general platform termed "bioorthogonal chemistry" has been developed over the past two decades. Biorthogonal reaction pairs react readily with each other but are inert to surrounding molecules under physiological conditions. The reaction pair and their products are stable and nontoxic to the biological system. Applications of bioorthogonal chemistries as bioconjugation strategies typically involve a two-step approach (Figure 1-3). First, a biomolecule is installed with a biocompatible functional group as the "chemical reporter". A variety of strategies have been developed to selectively introduce these chemical handles into the biomolecules of interest, including chemical or enzymatic modifications [28], residue-specific incorporation using the cell's biosynthetic machinery (metabolic labeling) [29, 30], and site-specific incorporation by an exogenous tRNA/aminoacyl-tRNA synthetase pair [31, 32]. Most notably, the metabolic incorporation method by hijacking native biosynthetic pathways greatly facilitated the study of biomolecules not directly encoded by the genome.
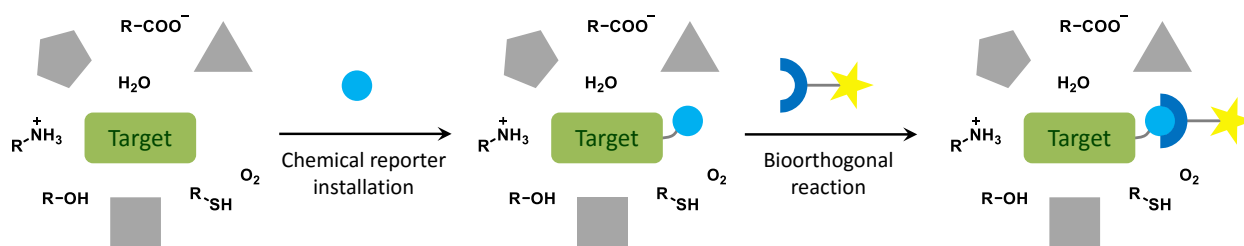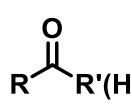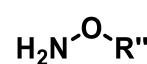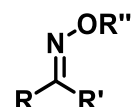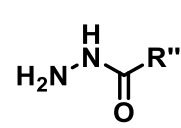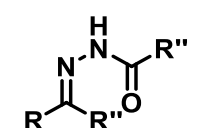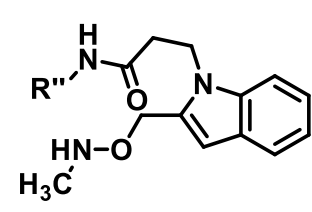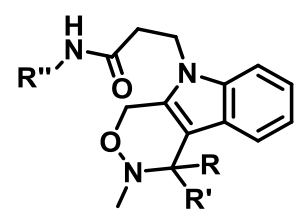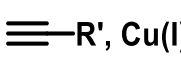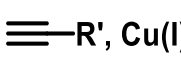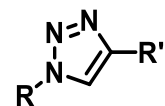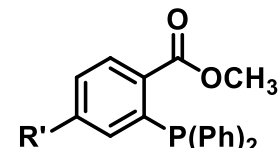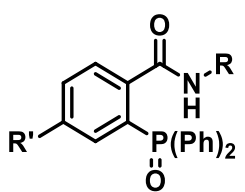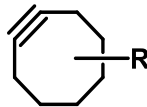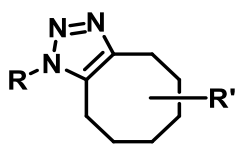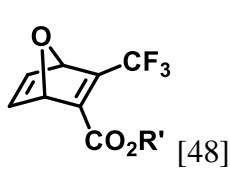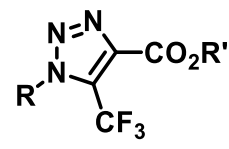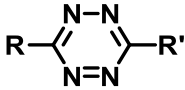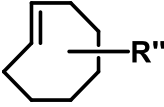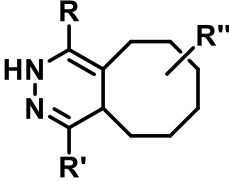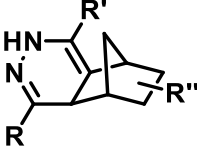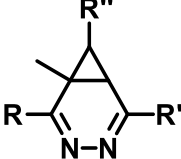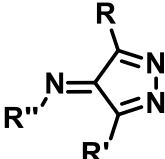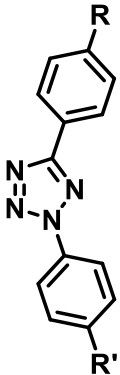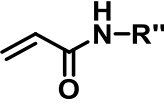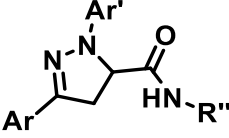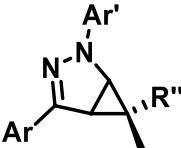
Figure 1-3. Bioorthogonal chemical reporter system for biomolecule tagging.
Figure modified from reference [33].

The second step of the bioorthogonal strategy involves the selective reaction between the chemical reporter and the complementary probe *in situ*. Several bioorthogonal reactions have been developed since introduction of the term by Bertozzi, C.R. [34], including Staudinger ligation [35], Cu(I)-catalyzed azide-alkyne cycloaddition (CuAAC) [36], strain-promoted azide−alkyne cycloaddition (SPAAC) [37], tetrazine ligation [38-41], photoinduced tetrazole-alkene cycloadditon [42-44], strain-promoted alkyne-nitrone cycloaddition (SPANC) [45] and many other reactions. (Table 1-1). In the past decade, many efforts have been made to optimize existing bioorthogonal reactions and develop new biorthogonal pairs, particularly in the aspect of reaction kinetics improvement, expansion of the pool of unnatural substrates, fluorogenic reactions for robust imaging and photoinducible reactions for improved spatial and temporal control. In addition, increasing efforts have been directed to the development of mutually exclusive bioothogonal reactions for multiple modification of a single target [46, 47].

Table 1-1. Bioorthogonal reactions used in the modification of biomolecules

Reactant A	Reactant B	Product
	[48]	

R ⌖ R' (tetrazine)	R" [38]	R / HN-N / R' / R"
	R" [39]	HN-N / R' / R / R"
	R" [41]	R" / R / N-N / R'
	R"—N≡C [40]	R / N-N / R" / R'
R / tetrazole / UV / R'	R" [42]	Ar' / N-N / Ar / R"
	H / N-R" / O [43]	Ar' / N-N / Ar / O / HN-R"
	R" [44]	Ar' / N-N / Ar / R"

R'–N⁺(–O⁻)=CH–R	⬡ ～～R'' [45]	R'–N–O ring with R and R''

1.3 Surface modification of viral vectors using bioorthogonal chemistry

The ideal gene transfer vectors are capable of efficiently transducing the desired gene to the target cells or tissues for the appropriate period of time without causing adverse effects. Extensive effort has been invested in the modification of viral surfaces to generate vectors with enhanced properties such as specific cell tropism, easier production/purification and reduced immunogenicity. In this context, various chemical and biological strategies have been developed. Bioorthogonal chemical reactions have significantly facilitated the study of biomolecules in their native environment due to the fast rates and superior selectivity under physiological conditions. In this thesis we aimed to modify the surface of two frequently used viral gene delivery vehicles, lentiviral and adeno-associated viral (AAV) vectors, by the aforementioned two-step conjugation method. The viral particles were first metabolically labeled during production with unnatural substrates and subsequently modified via highly chemoselctive bioorthogonal reactions, allowing the attachment of a variety of ligands. This strategy exhibited minimal perturbation on virus physiology and demonstrated remarkable flexibility, making it a powerful tool to develop novel viral vectors with desired surface properties.

Chapter 2. Engineering lentiviral surface via bioorthogonal chemistry

2.1 Introduction

2.1.1 The biology of lentivirus

Retroviruses are enveloped viruses possessing an RNA genome. They rely on the enzyme reverse transcriptase (RT) to convert viral genomic RNA into DNA, which is then integrated into the host's genome via the action of viral integrase (IN) [19, 49]. The viral genome then replicates as part of the host genome, leading to maintained expression in daughter cells. Lentivirus is a genus of slow viruses of the *Retroviridae* family, characterized by a long incubation period [50]. Unlike other retroviruses, lentiviruses can replicate in both dividing and non-dividing cells [51-53]. This is due to the ability of the lentiviral pre-integration complex to actively transport the reverse transcribed viral genome into the nucleus through nuclear pore complexes in an ATP-dependent manner, without the requirement of mitosis [54].

Several types of lentiviruses have been engineered to construct gene delivery vectors [55-58]. The most commonly used lentiviral vectors in both laboratory and clinical studies are based on human immunodeficiency virus type 1 (HIV-1) [59, 60], whose molecular biology has been extensively studied [61, 62]. Each HIV-1 virion contains two copies of the single-stranded positive-sense RNA genome approximately 9 kb in length, encoding nine different gene products (Table 2-1, Figure 2-1).

Table 2-1. Proteins encoded by the HIV genome

Class	Gene name	Protein products
Viral structural proteins and enzymes	gag	**MA (p17), CA (p24), NC (p7), p6**
	pol	**RT, RNase H, IN, PR**
	env	**SU (gp120), TM (gp41)**
Essential regulatory factors	tat	**Tat**
	rev	**Rev**
Accessory proteins	nef	**Nef**
	vpr	**Vpr**
	vif	**Vif**
	vpu	**Vpu**
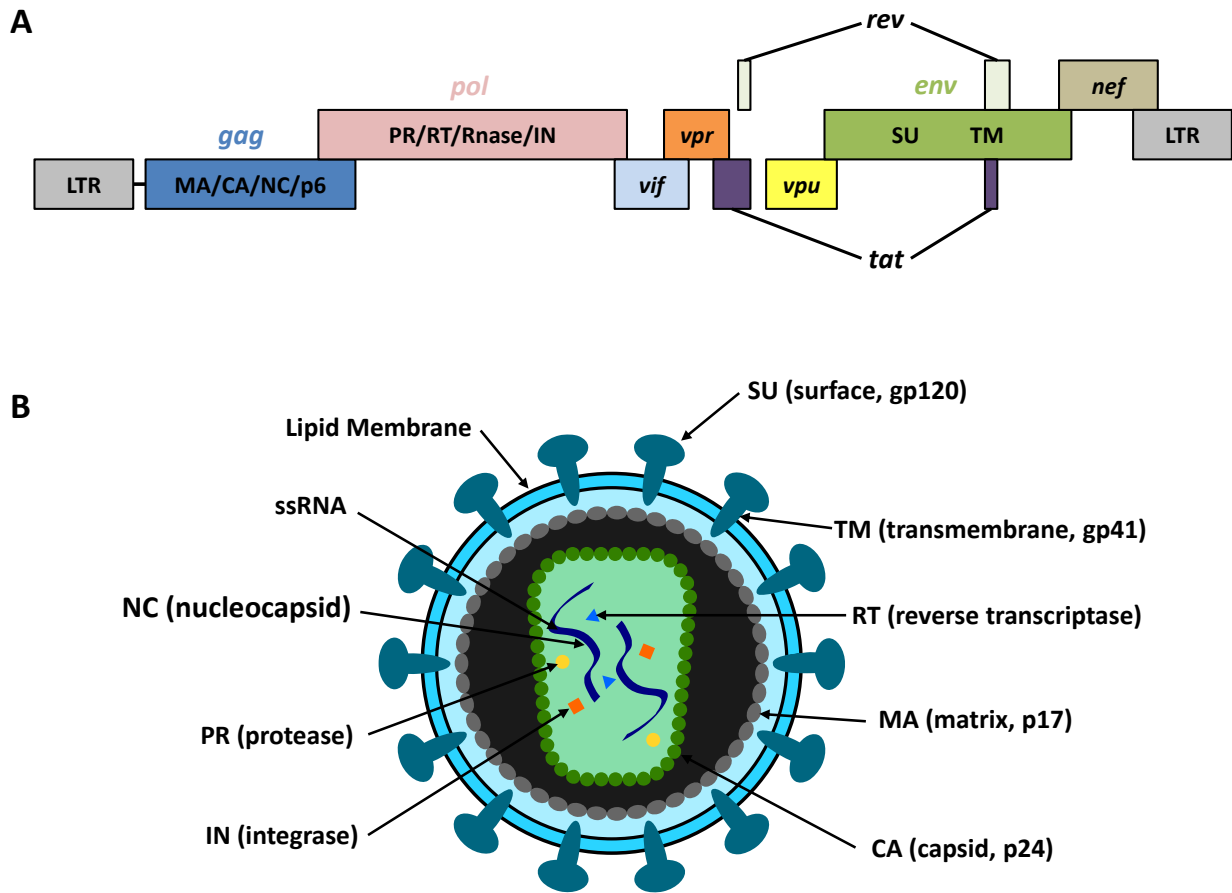
Figure 2-1. HIV-1 genome map and structure of HIV-1 virion.

(A) Schematic representation of the HIV-1 viral genome, which encodes the three structural, regulatory, and accessory genes flanked by LTRs. (B) Structure and major components of the HIV-1 virion. Figure modified from reference [59].

The three major structural proteins, Gag, Pol, and Env, are encoded in the three largest open-reading frames. The *gag* gene encodes viral core proteins that provide the basic physical infrastructure of the virus. The Gag precursor is the myristoylated p55 protein, which is processed by the viral protease during virion maturation to the matrix protein (MA), capsid protein (CA), nucleocapsid protein (NC) and p6 protein. The *pol* gene encodes the viral enzymes protease (PR), reverse transcriptase (RT), and integrase (IN). These enzymes are produced as a Gag-Pol precursor polyprotein, which is processed by the viral protease. The *env* gene encodes the viral surface

glycoprotein gp160, which is eventually cleaved by viral protease into gp120 and gp41. Gp120 is referred to as the surface subunit (SU), which attaches to its primary receptor CD4 and co-receptors on the cell surface. Gp41 is referred to as the transmembrane subunit (TM). The Env proteins can be replaced by surface glycoproteins of another virus to expand/alter vector tropism [63].

In addition to these major proteins, the HIV genome also encodes the essential regulatory proteins Tat and Rev. Tat transactivates and amplifies transcription of other structural viral proteins and Rev facilitates nuclear exports of viral transcripts. HIV-1 also encodes four other accessory proteins, Vif, Vpr, Vpu and Nef. Although these accessory proteins are generally not necessary for viral propagation in tissue culture, their conservation in the different isolates and experimental observations suggest important roles *in vivo*.

The HIV genome is flanked by two long terminal repeats (LTRs) at 5' and 3' extremities that contain important regulatory regions, required for viral transcription and integration. The genome dimerization and packaging signal Ψ, a set of 4 stem-loop structures preceding and overlapping the Gag start codon, is found in unspliced genomic transcripts, but absent from spliced viral mRNAs.

2.1.2 Lentivirus as gene delivery vehicles

Over the past two decades, lentiviral vectors have been used widely as a gene delivery system for both therapeutic and basic biological applications[59, 60, 64], largely due to their ability to mediate stable, long term transgene expression by integrating into the genome of both dividing and non-dividing cells. Compared to their counterpart γ-retroviruses, lentiviruses are less prone to insertional mutagenesis [65, 66], capable of accommodating larger genes [67], and have the unique advantage of transducing target cells without complete cell division [53, 68], a feature especially

suited for resting and differentiated cells such as hematopoietic stem cells [69], macrophages [70] and neurons [71] (Table 2-2). With demonstrable clinical safety [72], these vectors present an attractive alternative therapy for a variety of genetic diseases [73, 74], cancer [75] as well as infectious diseases [76, 77]. In addition to the introduction of complementary therapeutic genes into target cells, lentiviral victors have been developed to induce gene silencing by siRNAs [71, 78, 79], and deliver genetic material to antigen-presenting cells for vaccination[80]. In the context of laboratory and preclinical applications, lentiviral vectors have been widely used in functional genetics, cell engineering and generating animal model systems [59, 60].

Table 2-2. Advantages and disadvantages of lentiviral vectors

Advantages	**Disadvantages**
Transduce non-dividing and dividing cells	Possible insertional mutagenesis
Integration into host cell genome	Transient expression of transgene with integration-defective vectors
Carry up to 9 Kbp heterologous DNA	
Prolonged expression of transgene	
Integration-defective vectors available	

Modified from reference [19].

2.1.3 Surface remodeling of lentiviral vectors

Extensive effort has been invested in the modification of the envelope glycoprotein of lentivirus to generate vectors with enhanced properties such as restricted cell tropism [81-86], easier purification [87] and reduced immunogenicity [88, 89]. Surface glycoproteins of lentivirus can be substituted by those of another virus, commonly referred to as pseudotyping, which is often used to alter the cell specificity of the vector or to improve particle stability and production [63].

13

Other methods for surface engineering of lentiviral vectors include genetic manipulation of the envelope protein sequence [81-83, 87, 90-93], non-covalent modification with bridging moieties such as antibodies [81, 90] or adaptor ligands [83], co-enveloping of virus vectors with a fusogenic protein and a membrane-bound targeting protein [85, 94-97], and chemical modification through the primary amino groups on surface exposed lysine residues [86, 88]. Low virus titer and transductional efficiency can result from genetic modification of the lentiviral envelope, and the types of motifs that can be introduced are limited. The targeting molecules in the co-enveloping strategies are limited to membrane-bound proteins [85, 94-97]. Although the bridging adaptor approach demonstrates wide substrate scope, it requires multistep procedures and the *in vivo* stability of these complexes is debatable. Lysine acylation also allows access to a wide variety of effector moieties, however, efficiency is relatively low, specificity is problematic and the chemistry will be adversely affected by the presence of other nucleophiles in the sample. As a result, additional methods of surface functionalization that are flexible, efficient, broadly applicable, and highly specific would aid in the development of next generation lentiviral vectors.

2.1.4 Chemoselective modification of lenriviral surface via the metabolically introduced unnatural sugar SiaNAz

Unlike more conventional *in vitro* bioconjugation methods, such as electophilic modification of free lysines and cysteines, azide-alkyne cycloaddition [36, 37, 98-100] and Staudinger ligation [35] reactions are highly selective, well-controlled and fast, making them preferable in complex biological systems. Metabolic incorporation of unnatural substrates bearing azide or terminal alkyne functionalities have been utilized to label glycans [101, 102], lipids [103], DNA [104] and proteins [30]. Specifically noteworthy for the work in this thesis, unnatural ManNAc analogs can be taken up by the sialic acid biosynthetic pathway and converted to

14

unnatural sialic acid analogs on the cell surface [29] (Figure 2-2). Bertozzi and coworkers have demonstrated the metabolic incorporation of the azido sialic acid analogue, N-azidoacetyl sialic acid (SiaNAz), onto cell surface glycoproteins as a chemical reporter for both *in vitro* and *in vivo* studies [35, 37, 105, 106].
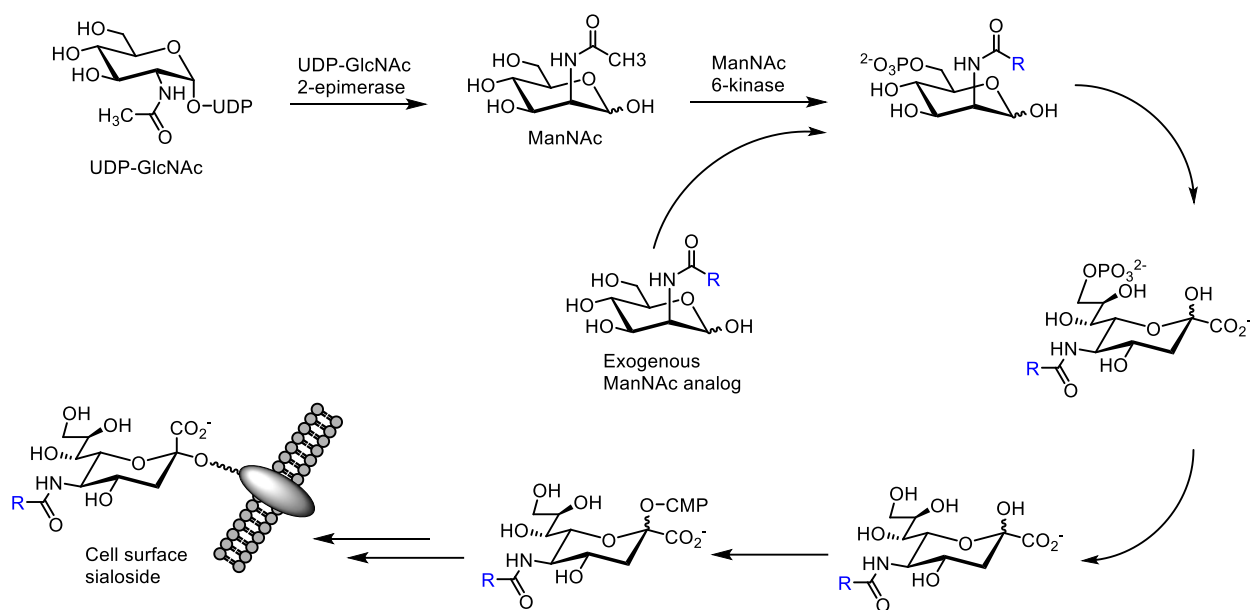
Figure 2-2. The sialic acid biosynthetic pathway is permissive of unnatural ManNAc analogs. Figure modified from reference [29].

As the envelopes of lentiviruses are derived from portions of the host cell membranes, with the viral glycoproteins generated by the cellular biosynthetic machinery, we hypothesized that sialylated viral glycoproteins could be labeled through the same strategy used to label cellular proteins. As chemical "handles", the introduced azide groups are small, inert and expected to have little impact on virus assembly and function. Several azide-specific chemical reactions can be employed for subsequent modification of the viral surface, including the Staudinger ligation, Cu(I)-catalyzed azide-alkyne cycloaddition (CuAAC), and strain-promoted azide−alkyne cycloaddition (SPAAC), giving access to virtually any functionality desired. For SPAAC, the

15

novel reagent bicyclo[6.1.0]nonyne (BCN) featuring the combination of easy preparation, high

reactivity and relatively low lipophilicity was used in this work [107].
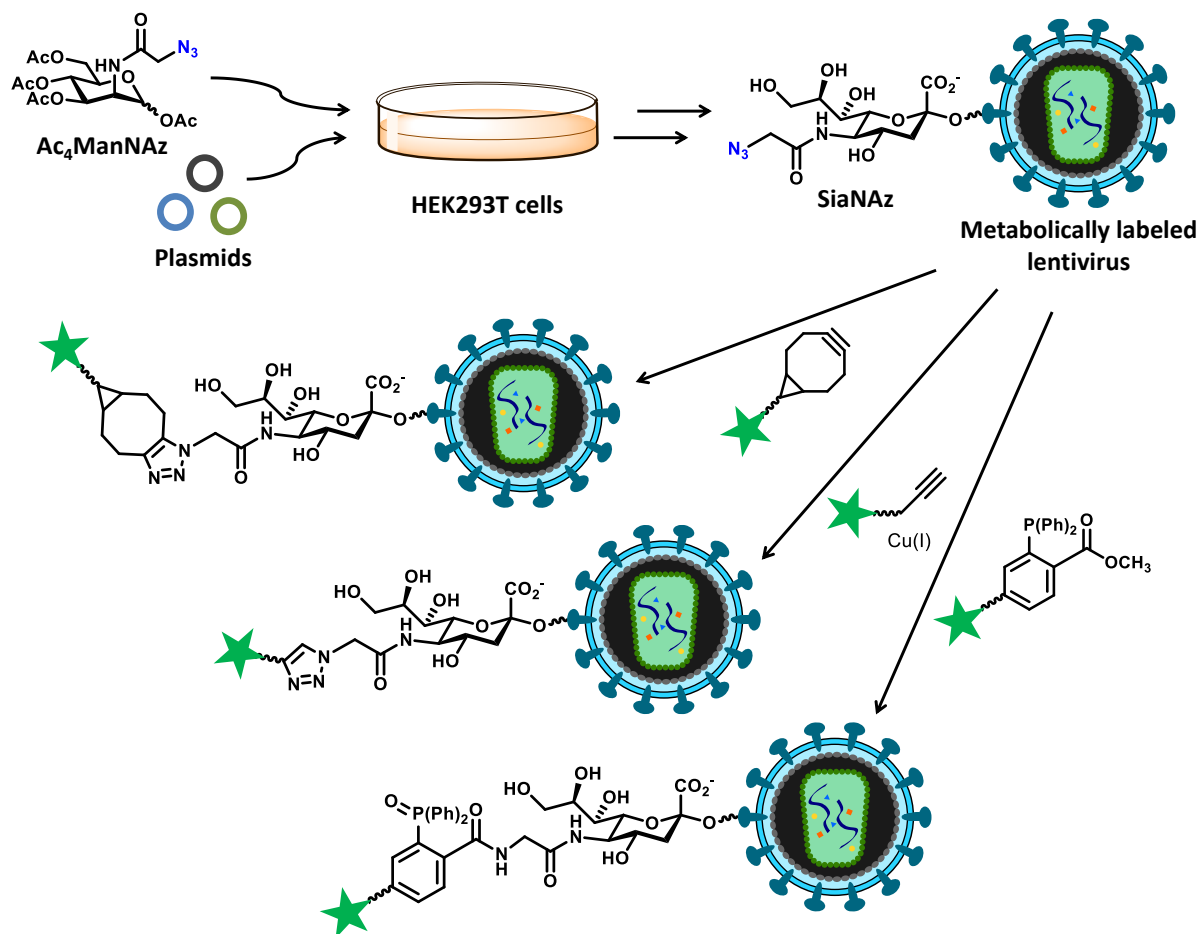
Figure 2-3. Two step labeling method for surface modification of lentiviral vectors.

Production of lentivirus in the presence of Ac₄ManNAz leads to incorporation of SiaNAz onto
viral surface glycans. Further modification via bioorthogonal reactions such as SPAAC, CuAAC
and Staudinger ligation facilitates installation of various functional molecules.

2.2 Results

2.2.1 Metabolic incorporation of SiaNAz onto lentiviral surface

Vesicular stomatitis virus glycoprotein (VSV-G) is the most commonly used glycoprotein for pseudotyping lentiviruses due to its broad tropism, and ability to enable high-titer vector preparation [63]. As a result, VSV-G pseudotyped lentiviruses were chosen as a platform to test SiaNAz mediated surface labeling. Each pseudotyped lentivirus particle is encapsulated with approximately 216 copies of VSV-G [88], containing two complex N-linked oligosaccharides at amino acids 179 and 336 [108]. Both the extent of sialylation of the oligosaccharides and the ability of SiaNAz to replace sialic acid depends on the cell line in which the virus proteins are produced [109, 110]. Sialic acid analogs have been shown to be directly incorporated into surface sialoglycoconjugates by mammalian cells [111, 112]. Yet, the more synthetically accessible precursor peracetylated N-α-azidoacetylmannosamine (Ac$_4$ManNAz) has demonstrated similar metabolic efficiency as the corresponding sialic acid analog has [113], and was therefore preferred in this work. When grown in medium with an initial Ac$_4$ManNAz concentration of 50 μM, the lentivirus producing cell HEK293T exhibited about 27% substitution of cell surface sialic acid by SiaNAz [102]. However, it is unknown whether the incorporation plateaus at this concentration. In addition, the labeling efficiency of a single glycoprotein species, VSV-G in the case of this work, may vary from the average of the whole glycoprotein population of the cell.

Lentiviral vectors were produced using the calcium phosphate transfection method [114]. In a reported test of calcium phosphate transfection on HEK293 cells, it has been shown that plasmid expression, when tested 48 hours after transfection, reached a plateau after 5-7 hours of coincubation with the DNA/Ca-Pi coprecipitates [115]. Although the required coincubation time

may vary for a different cell line, we used this data as a guideline and applied Ac4ManNAz 7 hours

after beginning of transfection, in an effort to avoid possible complications the unnatural substrate

and ethanol (solvent of the stock solution) may impose on plasmid uptake. Transfection medium

was then replaced with fresh medium also containing 75 μM of Ac4ManNAz 16 to 18 hours after

beginning transfection. Virus containing supernatant was collected and concentrated 48 hours after

transfection.
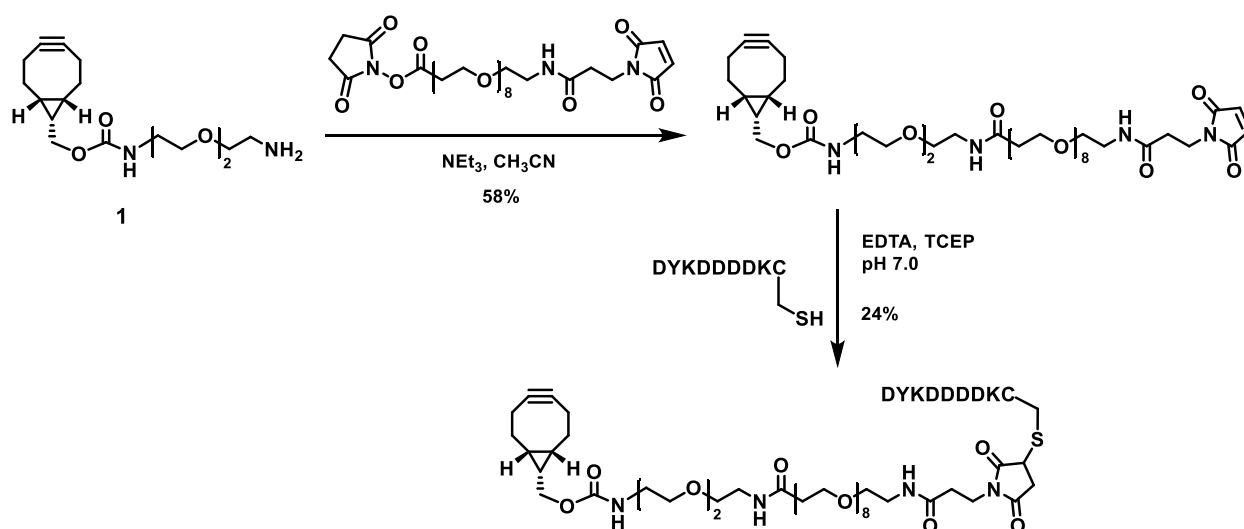
Scheme 2-1. Synthesis of BCN-PEG-FLAG.
FLAG-Cys peptide (DYKDDDDKC) was synthesized using a CEM microwave peptide
synthesizer (model No. 908505). (1*R*,8*S*,9*s*)-bicyclo[6.1.0]non-4-yn-9-ylmethyl 3,6,9-trioxa-12-
azadodecylcarbamate (*endo*-**1**) was synthesized by Fred Rubino as previously described [107].

Strain promoted "click" chemistry (SPAAC) has the advantage of being fast, highly

selective for azides, and does not require the addition of a toxic catalyst. In order to access this

chemistry, labeling/targeting moieties were modified with a previously described strained alkyne,

bicyclo[6.1.0]nonyne (BCN) (Scheme 2-1).   To demonstrate SiaNAz incorporation, viruses

produced in the presence of Ac4ManNAz were exposed to a BCN armed FLAG epitope (300 μM

BCN-FLAG; 6 hours at room temperature) and analyzed by anti-FLAG western blot. The result indicated successful installation of SiaNAz onto the surface of VSV-G pseudotyped lentivirus (Figure 2-4). Notably there is a complete loss in signal with omission of either the azido sugar or BCN-FLAG. Neuraminidase treatment prior to SPAAC reaction also completely abrogates signal, indicating the azide specific labeling is directly associated with sialic acid residues.

kDa					
175 —					
80 —					
58 —					
46 —					
Ac$_4$ManNAz	+	+	+	-	-
FLAG-PEG-BCN	+	-	+	+	-
Neuraminidase	-	-	+	-	-
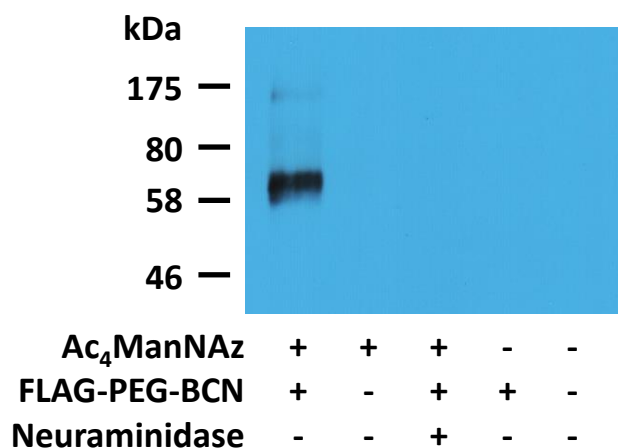
Figure 2-4. Confirmation of SiaNAz incorporation onto the surface of VSV-G pseudotyped lentiviral vectors.

The BCN-PEG-FLAG ligand was used to selectively modify SiaNAz residues on the surface of VSV-G pseudotyped lentiviral vectors. Prior to SPAAC modification, each virus sample was suspended in G1 reaction buffer (50 mM sodium citrate, pH 6.0, 10X buffer supplied with neuraminidase) and incubated with neuraminidase (2.5 U/ μL, New England BioLabs, Cat. No. P0720) or merely the buffer at 37 ℃ for 1 hour. Each reaction sample was then run through a size-exclusion spin column (Princeton Separations, Cat. No. CS-901) equilibrated in PBS, and incubated with BCN-FLAG (300 μM) or only the buffer at room temperature for 6 hours. The reaction samples were subsequently analyzed by electrophoresis on 10% SDS-polyacrylamide gels followed by western blotting with the monoclonal ANTI-FLAG® M2-Peroxidase (HRP) antibody (Sigma-Aldrich, Cat. No. A8592). FLAG-positive signal was observed on the western blot for the experimental reaction sample, whereas complete loss in signal was observed with omission of either the azido sugar or BCN-FLAG. Removal of sialic acid residues by neuraminidase prior to SPAAC reaction also completely abrogated signal. The molecular weight of VSV-G is ~67 kDa [116].

Alternatively, the incorporation of SiaNAz was also confirmed by CuAAC using an alkyne functionalized FLAG ligand (alkyne-FLAG). Reaction samples were analyzed by anti-FLAG tag

19

and anti-VSVG western blot. As expected the results again suggested successful conjugation of

the FLAG motif onto the viral surface (Figure 2-5).
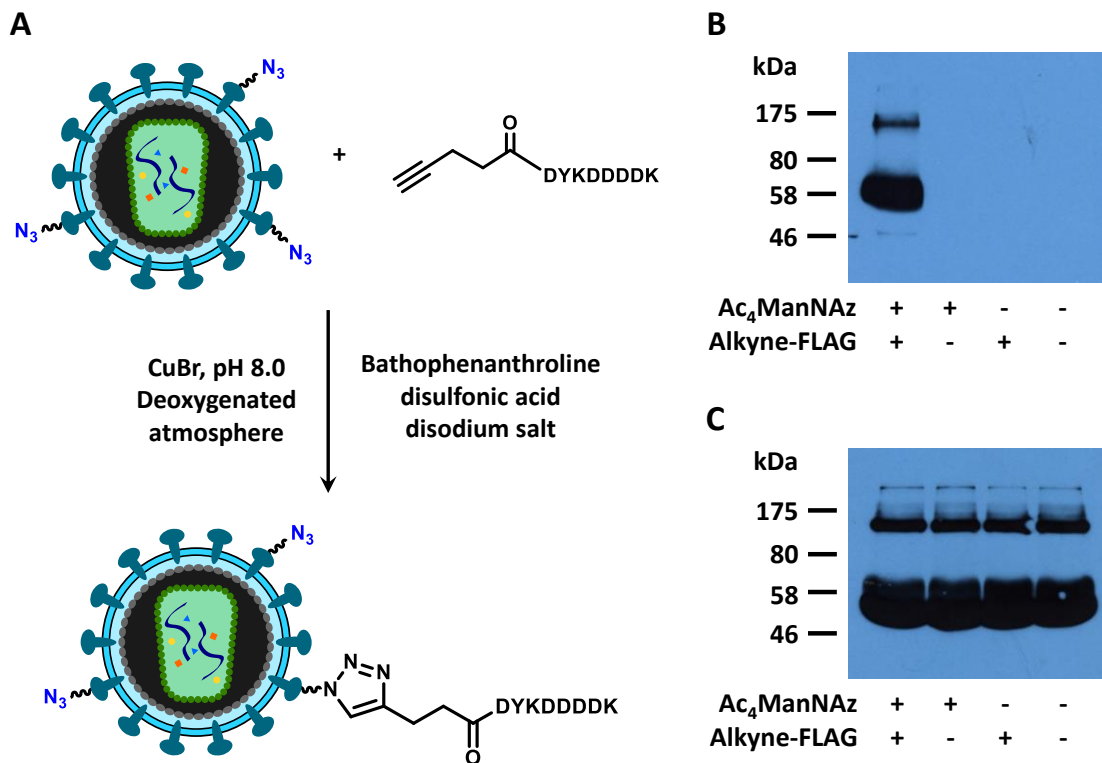
Figure 2-5. Confirmation of SiaNAz incorporation by CuAAC.

The terminal alkyne functionalized FLAG ligand alkyne-FLAG (synthesized by Isaac Carrico) was used to selectively modify SiaNAz residues on the surface of VSV-G pseudotyped lentiviral vectors. (A) Each virus sample was suspended in a reaction mixture containing tris (100mM, pH 8.0), bathophenanthroline disulfonic acid disodium salt (final conc. 3 mM, MP Biomedicals, Cat. No. 150112) and alkyne-FLAG (final conc. 200 μM or 0 μM). Each reaction mixture was kept in a deoxygenated glove bag for 12 hours to ensure full exclusion of oxygen, before CuBr (final conc. 1 mM, Alfa Aecar, Cat. No. 40752, 100 mM stock in DMSO freshly made before reaction) was added. The reaction mixtures were then incubated for another 12 hours at room temperature in deoxygenated atmosphere. Each sample was subsequently analyzed by electrophoresis on 10% SDS-polyacrylamide gels followed by western blotting with (B) monoclonal ANTI-FLAG® M2-Peroxidase (HRP) antibody (Sigma-Aldrich, Cat. No. A8592) to detect FLAG tag labeled proteins, or (C) anti-VSVG tag antibody (Abcam, Cat. No. ab49610) to detect VSV-G protein. FLAG-positive signal was observed on the western blot for the experimental reaction sample, whereas complete loss in signal was observed with omission of either the azido sugar or BCN-FLAG. Anti-VSV-G western blot revealed essentially equal amount of VSV-G protein in each reaction sample.

2.2.2 Impact of SiaNAz incorporation on virus production and infectivity

In contrast to genetic manipulations of envelope proteins, introduction of SiaNAz is post-translational and results in the addition of only 3 atoms per site of incorporation. As a result, SiaNAz introduction is expected to cause minimal impact on the physiology of labeled lentiviral vectors. The impact of SiaNAz incorporation on both viral particle production and infectivity was determined. The former was assayed via p24 titer, whereas the latter was measured by quantifying gene delivery to cells via flow cytometry. With the addition of Ac$_4$ManNAz during virus production, p24 ELISA demonstrated a reduction of titer (ng p24/mL) by 26% for unconcentrated samples and 22% for samples concentrated by ultracentrifugation (Figure 2-6 A and B). Transduction assays examining expression of the GFP transgene in HEK293T cells exhibited a reduction of functional titer (TU/mL) by 11% for unconcentrated samples and 7% for concentrated (Figure 2-6 C and D). Surprisingly, transduction efficiency values (TU/ng p24) calculated from these two types of titers indicated an increase of infectivity by 20% for unconcentrated samples and 19% for concentrated (Figure 2-6 E and F), for which no obvious explanation is currently available.
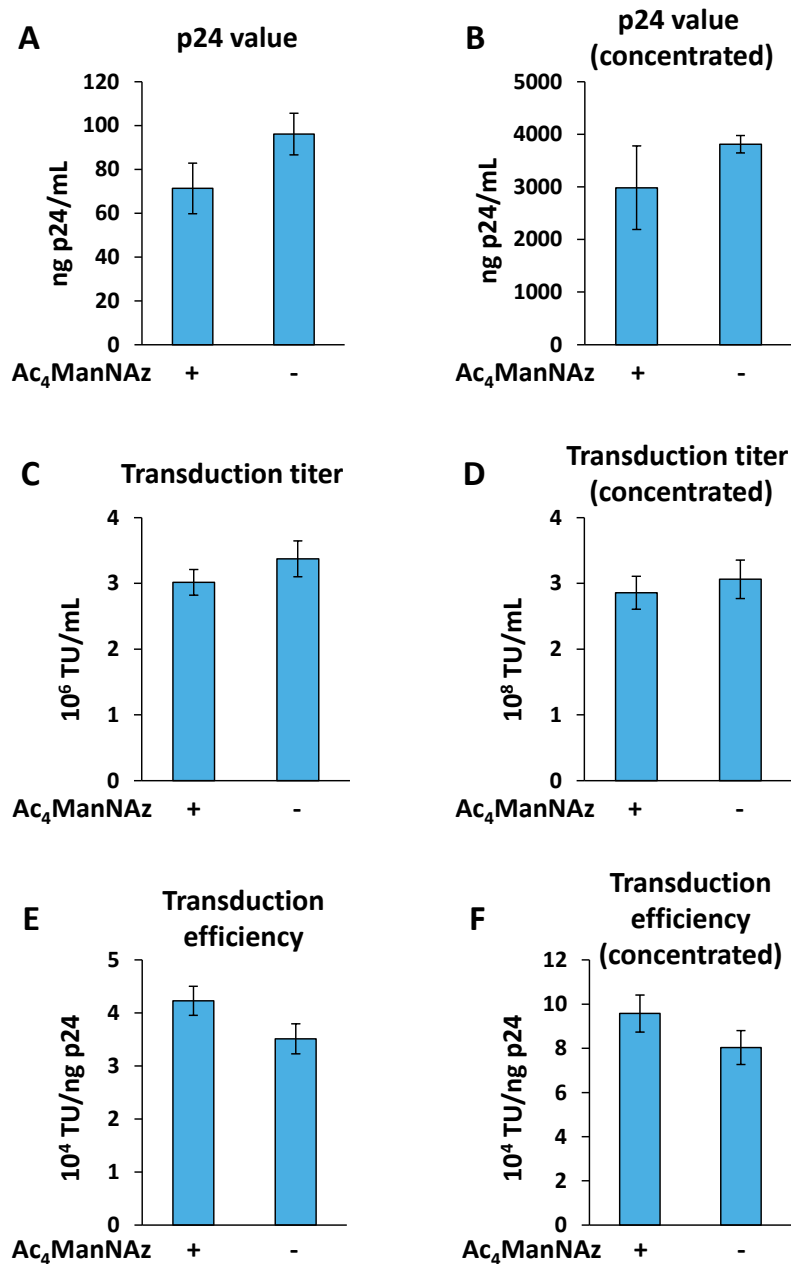
Figure 2-6. Impact of the metabolically introduced azides on virus production and transduction efficiency.

Production of virus particles with or without addition of Ac4ManNAz was examined by p24 ELISA assay on the (A) unconcentrated virus containing supernatant and (B) virus samples concentrated by ultracentrifugation. Each virus sample was assayed in triplicate and average value was reported. Error bars indicate standard deviation. Transduction titers of the virus samples were examined by infecting HEK293T cells and detecting transgene (GFP) expression by flow cytometry. Titers of the (C) unconcentrated and (D) concentrated virus samples were calculated based on percentage of GFP positive cells. 2.5 μL, 5 μL and 10 μL aliquots of each unconcentrated virus sample and 100-fold diluted concentrated virus sample was used in transduction, each

amount was assayed in triplicate. Average value of all the calculated TU titers of each virus sample was reported. Error bars indicate standard deviation. Transduction efficiency values (TU/ng p24) of (E) unconcentrated and (F) concentrated virus samples were calculated by dividing the transduction titer values in (C) and (D) by the average p24 concentrations in (A) and (B) respectively.

These results indicate that neither the production of viral particles nor the gene delivery function of labeled lentiviral vectors is significantly affected by the metabolically incorporated SiaNAz. It is also evident that physical stress from ultracentrifugation did not result in larger difference in functional titers between azide (+) and azide (-) samples, suggesting that the stability of labeled lentiviral particles was not compromised by the metabolic incorporation of SiaNAz (Figure 2-6 C and D).

2.3 Conclusion and discussion

SiaNAz was successfully incorporated onto lentiviral surface with addition of $Ac_4ManNAz$ in the virus production culture. The azides can then be specifically modified by a variety of bioorthogonal reactions, providing a simple, versatile tool for lentiviral surface remodeling.

One advantage of our proposed technique is the minimal impact on viral fitness. Production of concentrated functional lentiviral vectors was affected by less than 10% with the addition of unnatural substrate (Figure 2-6 D). This reduction is more likely to be a result of hindered viral production rather than compromised infectivity of SiaNAz labeled virus. This assumption is supported by the fact that transduction efficiency (TU/ng p24) was not undermined by the inclusion of $Ac_4ManNAz$ during viral production (Figure 2-6 E and F). Possible reasons for the negative impact on viral production include cytotoxic effect of the unnatural substrate on virus producing cells and impeded viral particle assembly. Whether the metabolism of $Ac_4ManNAz$ saturates at the concentration that we used in the virus producing HEK293T cells is not yet known,

23

nor the potential toxicity. Incorporation percentage of SiaNAz in total virus samples can be obtained using protocols previously reported for cell lysate and recombinant glycoproteins, where sialic acids and analogs were derivatized with 1,2-diamino-4,5-methylenedioxy-benzene (DMB) and analyzed by HPLC with fluorescence detection [117]. However, data from this assay may not fairly represent the sialic acid composition on intact lentiviral particles, mainly due to the inherent contamination by cellular components and free viral proteins from the virus production.

2.4 Materials and methods

Synthesis of Ac₄ManNAz (1,3,4,6-tetra-*O*-acetyl-*N*-azidoacetyl-α,β-D-mannosamine)

Azidoacetic acid was synthesized as described by Luchansky *et al*.[118] D-mannosamine hydrochloride (0.216g, 1.0mmol, Totonto Reseach Chemicals Inc) was added to a solution of azidoacetic acid (0.145g, 1.4mmol) in methanol (10ml). Triethylamine (0.36ml, 2.4mmol) was then added and the reaction mixture stirred for 5 minutes at room temperature. The solution was cooled to 0 ℃ and N-hydroxybenzotriazole (HoBt) (0.159g, 1.0mmol, Advanced ChemTech) was added followed by 1-[3-(dimethylamino)propyl]-3-ethylcarbodiimide hydrochloride (DIC) (0.31mL, 2.0mmol, Acros Organics). The reaction was allowed to warm to room temperature overnight when TLC with ceric ammonium nitrate showed the reaction to be complete. The solution was concentrated and the crude ManNAz was purified by silica gel chromatography (Alfa Aesar, 230-400 mesh) twice, eluting with 10% methanol in dichloromethane, with a 30% yield.

Acetic anhydride (1.0ml, 11mmol) was added to a solution of ManNAz (27.5mg, 1.05mmol) in pyridine (2ml) and the reaction mixture stirred overnight at room temperature. The solution was then concentrated and resuspended in ethyl acetate, followed by washing with 1M HCl, saturated NaHCO₃ and saturated NaCl. The organic layer was dried, filtered and

concentrated. The crude peracetylated ManNAz was purified by silica gel chromatography eluting with 1:2 ethylacetate-hexane, with a 65% yield. ^{1}H NMR (300MHz, CDCl$_3$): δ 2.01 (3H, s), 2.02 (3H, s), 2.08 (6H, s), 2.13 (6H, s), 2.14 (3H, s), 2.19 (3h, s), 3.83 (1H, ddd), 4.03-4.18 (7H, m), 4.21-4.29 (2H, m), 4.64 (1H, ddd), 4.74 (1H, ddd), 5.07 (1H, dd), 5.18 (1H, app t), 5.24 (1H, app t), 5.36 (1H, dd), 5.90 (1H, d), 6.06 (1H, d), 6.59 (1H,d), 6.65 (1H, d) ppm.

Synthesis of BCN-PEG-FLAG

FLAG-Cys peptide (DYKDDDDKC) was synthesized on a 0.25 mmol scale using a CEM Liberty microwave peptide synthesizer (model No. 908505) utilizing Fmoc chemistry. Solvents used were ACS-grade. Fmoc-Cys(trt)-Wang resin (500mg, 100-200 mesh, Novabiochem) was used as the starting reagent for the solid phase synthesis. Standard Fmoc reaction cycles were used. In each cycle, 5 equiv. (1.25 mmol) of an Fmoc amino acid (Fmoc-Asp(OtBu)-OH, Fmoc-Lys(Boc)-OH or Fmoc-Tyr(tBu)-OH) was activated by DIPEA and HBTU and attached to the growing peptide in a single coupling step (300 sec, 75 ˚C), followed by removal of the Fmoc group in two deprotection steps (30 sec and 180 sec, 75 ˚C) by 20% piperidine in DMF with HOBt. Resin was washed with DCM and collected by vacuum filtration before cleavage of the peptide using a mixture (10 mL) of 90% TFA, 5% thioanisole, 3% EDT and 2% anisole for 2 hours. Resin was then removed by vacuum filtration through a sintered glass funnel, and washed twice with TFA. The resulting solution was concentrated to ~ 2 mL by blowing Ar on the surface, and added drop wise into diethyl ether to precipitate the peptide. The precipitate was re-dissolved in 10% acetic acid (30 mL) and lyophilized to afford 310.7 mg of crude FLAG-Cys peptide. A portion of the crude peptide (87.4 mg) was then purified by reversed-phase HPLC using a Phenomenex Jupiter C12 semi-preparative column (250 x 10 mm, part No. 00G-4396-N0), eluting with a gradient of acetonitrile in water (5-25% over 40 min, flow rate 4 ml/min). TFA (0.1%) was included in the

mobile phase as the ion-pairing reagent. Subsequent lyophilization afforded purified FLAG-Cys peptide (21.3 mg, 27%). MS (MALDI+): m/z calcd for $[C_{44}H_{66}N_{11}O_{21}S]^+$ $[M + H]^+$: 1116.415, found: 1117.229.

(1R,8S,9s)-Bicyclo[6.1.0]non-4-yn-9-ylmethyl 3,6,9-trioxa-12-azadodecylcarbamate (*endo*-**1**) was synthesized as previously described [107]. To a solution of *endo*-**1** (10.3 mg, 31.7 µmol) in anhydrous acetonitrile (400 µL) was added triethylamine (4 µL) and NHS-PEG$_8$-maleimide (20 mg, 29.0 µmol, Thermo Scientific). The reaction was then allowed to proceed at room temperature for 12 hours with rotation (Scheme 2-1). The resulting BCN-PEG-maleimide was purified by reversed-phase HPLC using a Phenomenex Jupiter C12 semi-preparative column (250 x 10 mm, part No. 00G-4396-N0), eluting with a gradient of acetonitrile in water (10-50% over 40 min, flow rate 4 ml/min). TFA (0.1%) was included in the mobile phase as the ion-pairing reagent. Subsequent removal of solvent by lyophilization afforded purified BCN-PEG-maleimide (15 mg, 58%). MS (ESI+): m/z calcd for $[C_{43}H_{71}N_4O_{16}]^+$ $[M + H]^+$: 899.486, found: 899.35.

Purified FLAG-Cys peptide (8.0 mg, 7.2 µmol) was dissolved in reducing buffer (500 µL, 20 mM EDTA, 10 mM TCEP, 50 mM sodium phosphate pH 7.0) and rotated on a Labquake Shaker Rotisserie (Thermo Scientific) at room temperature for 1 hour. To a suspension of BCN-PEG-maleimide (6.4 mg, 7.1 µmol) in 500 µL of CH_3CN/H_2O (4:1) was added the FLAG-Cys containing solution. After the reaction mixture was rotated at room temperature for 2 hours, DMSO (200 µL) and an additional aliquot of BCN-PEG-maleimide (2.2 mg, 2.4 µmol) was added. The reaction mixture was then rotated for an additional 6 hours (Scheme 2-1). The product BCN-PEG-FLAG was purified by reversed-phase HPLC using a Phenomenex Jupiter C12 semi-preparative column (250 x 10 mm, part No. 00G-4396-N0), eluting with a gradient of acetonitrile in water (5% for 5 min, then 5-45% over 40 min, flow rate 4 ml/min). TFA (0.1%) was included in the mobile

phase as the ion-pairing reagent. Subsequent removal of solvent by lyophilization afforded purified BCN-PEG-FLAG (3.5 mg, 1.7 μmol, 24%). MS (MALDI+): *m/z* calcd for $[C_{87}H_{136}N_{15}O_{37}S]^+$ [M + H]$^+$: 2014.894, found: 2015.337 (Appendix 1).

Cells and viruses

All cell lines used in this work were grown at 37 ˚C in a 5% CO_2 environment in a humidified incubator. HEK 293T cells (gift of Dr. Soosan Ghazizadeh, Stony Brook University) were maintained at low passage in Dulbecco's modified Eagle's medium (DMEM) with 10% fetal bovine serum (FBS), 100 U/ml penicillin and 100 μg/ml streptomycin. To produce VSV-G glycoprotein pseudotyped lentivirus, HEK 293T cells were seeded into 10-cm tissue culture dishes at the density of 3.3 x 10^6 cells per dish. Twenty four hours later, each dish of cells were transfected with 10 μg of pMD.G (VSV-G), 20 μg of pCMVΔR8.91, and 20 μg of pHR.EF1α.GFP.WPRE.sin (all three plasmids were gift of Dr. Soosan Ghazizadeh, Stony Brook University) using standard calcium phosphate transfection [119]. For production of SiaNAz labeled virus, Ac4ManNAz in 50 mM stock solution was added into culture medium to the final concentration of 75 μM 7 hour after initiation of transfection. Medium was removed by aspiration 16-18 hours after beginning of transfection, and cells were washed once with fresh medium before 7 ml of complete DMEM was added per dish. Again, for the production of SiaNAz labeled virus, 75 μM of Ac4ManNAz was included in culture medium. Virus containing medium was collected after another 48 hours and filtered through 0.45 μm sterile filter (VWR, Cat. No. 28145-481) to remove cell debris. Resulting virus samples was further concentrated by ultracentrifugation using a SW41 rotor for 2 hours 20 min at 25,000 rpm (82,700 g). The virus was stored at – 80 ˚C until use [114].

p24 ELISA assay

The p24 value of lentiviral vectors was obtained by an ELISA assay using the Lenti-X^{TM} p24 Rapid Titer Kit (Clontech, Cat. No. 632200), following the instruction provided in the kit. For standard curve, a series of 2 fold dilutions of p24 protein (0 pg/ml, 12.5 pg/ml, 25 pg/ml, 50 pg/ml, 100 pg/ml, 200 pg/ml) were made with complete DMEM. To fit into the concentration range of the standards, unconcentrated virus samples were diluted 10^3 fold, and virus samples concentrated by ultracentrifugation were diluted 10^5 fold. Each dilution of standard was assayed in duplicate, and each virus sample was assayed in triplicate. Assay was read on a PerkinElmer VICTOR™ X5 Multilabel Plate Reader.

Transduction assay

Virus titer by transducing unit (TU) was obtained by a flow cytometry method detecting expression of the GFP transgene in transduced HEK 293T cells. Briefly, HEK 293T cells were seeded at the density of 5 x 10^4 cells per well in 6-well plates 24 hours before transduction, and the number of cells per well was counted again using a hemacytometer immediately before transduction. Cells were then transduced by adding 0 μl, 2.5 μl, 5 μl and 10 μl aliquots of an unconcentrated virus stock, or of a 100 fold diluted concentrated virus stock. Each dilution was assayed in triplicate. Cells were harvested 2 days later and analyzed by flow cytometry.

Western blotting

The BCN-PEG-FLAG peptide was used to selectively modify SiaNAz labeled lentiviral vectors through SPAAC. In each reaction, control or experimental, a 16 ng p24 value of virus sample was suspended in 40 μl G1 reaction buffer (50 mM sodium citrate, pH 6.0, 10X buffer supplied with neuraminidase) and incubated in the presence or absence of 100 U of neuraminidase

(New England BioLabs, Cat. No. P0720) at 37 ℃ for 1 hour. Each reaction mixture was then run through a size-exclusion spin column (Princeton Separations, Cat. No. CS-901) equilibrated in PBS. BCN-FLAG at a final concentration of 300 μM was added into the corresponding reactions, and the total volume of each reaction was adjusted to 50 μl by PBS. The reaction mixtures were then incubated in room temperature for 6 hours before they were analyzed by electrophoresis on 10% SDS-polyacrylamide gels followed by western blotting. Monoclonal ANTI-FLAG® M2-Peroxidase (HRP) antibody (Sigma-Aldrich, Cat. No. A8592) was used to detect FLAG peptide labeled proteins.

The alkyne-FLAG peptide (synthesized by Isaac Carrico) was used to selectively modify SiaNAz labeled lentiviral vectors through CuAAC. To each suspension of virus in tris buffer (100 mM, pH 8.0) was added bathophenanthroline disulfonic acid disodium salt (MP Biomedicals, Cat. No. 150112) at a final concentration of 3 mM, and alkyne-FLAG at a final concentration of 200 μM or 0 μM. Each reaction mixture was kept in a deoxygenated glove bag for 12 hours in order to ensure full exclusion of oxygen, before CuBr (Alfa Aecar, Cat. No. 40752, 100 mM stock in DMSO freshly made before reaction) was added to a final concentration of 1 mM. The reaction mixtures were then incubated for another 12 hours at room temperature in deoxygenated atmosphere. Each sample was subsequently analyzed by electrophoresis on 10% SDS-polyacrylamide gels followed by western blotting. Monoclonal ANTI-FLAG® M2-Peroxidase (HRP) antibody (Sigma-Aldrich, Cat. No. A8592) was used to detect FLAG peptide labeled proteins, and anti-VSVG tag antibody (Abcam, Cat. No. ab49610) was used to detect VSV-G protein.

Chapter 3. Targeted lentiviral transduction of cancer cells via ligands introduced by bioorthogonal reactions

3.1 Introduction

Transductional targeting of lentiviral vectors towards specific cells or tissues is an attractive goal, particularly for *in vivo* applications. Towards this goal, we designed and synthesized several targeting ligands for bioorthogonal modification of SiaNAz labeled viral surfaces. In order to restrict endogenous cell tropism, we used lentiviruses pseudotyped with mutant Sindbis glycoproteins.

Sindbis virus envelope proteins, composed of two ~50 kDa transmembrane glycoproteins E1 and E2 [120], contain two complex N-glycans at amino acid 196 on E2 and aa 139 on E1, both exposed [121]. Chen and coworkers introduced a series of mutations into the Sindbis virus envelope proteins that resulted in reduced binding to the natural cell surface receptors, heparan sulfate and laminin receptor, while maintaining relatively high lentiviral vector production [81]. One of these "detargeted" mutants containing a 14 aa flexible linker inserted at the original receptor binding region and termed as "2.2 1L1L" [82] was used in this work. This scaffold of detargeted Sindbis glycoproteins was adopted by the Wang group who developed several variants of these mutants [85, 94, 95], including one termed "SINmu" that was also used in this work on several occasions. SINmu has essentially the same mutations as 2.2 1L1L, except for the replacement of the 14 aa linker by a 10 aa hemagglutinin (HA) tag to facilitate detection, and the absence of the mutations A226S and K227G in E1 that allows cholesterol-independent fusion in the target membrane. Importantly, the glycosylation sites are unperturbed in all of these mutants[121].

Lentiviral vectors have long been explored for cancer gene therapy, where they have been used to deliver cytotoxic genes [122-124], RNAi [79], or antigenic genes designed for cancer immunotherapy [80, 125]. The therapeutic potential of lentiviral vectors can be greatly improved through targeting of the vectors to tumor cells, facilitating direct *in vivo* application [81, 96]. Five high-profile cancer associated receptors were targeted in the context of this approach, vascular endothelial growth factor receptor 2 (VEGFR2), tyrosine kinase receptor Tie2, $\alpha_v\beta_3$ integrin, prostate-specific membrane antigen (PSMA) and folate receptors (FRs). Ligands for these receptors have been extensively developed and, as a result, have facile modification routes for installation of functionalities capable of bioorthogonal reactions with azide.

3.2 Results

3.2.1 Metabolic incorporation of SiaNAz onto the surface of Sindbis envelope protein pseudotyped lentiviral vectors

Akin to VSV-G pseudotyped lentiviral vectors, the extent of sialylation of Sindbis glycoproteins depends on the cell lines in which they are produced [126]. Sindbis envelope protein pseudotyped vectors were produced by the same procedures used for VSV-G pseudotyped vectors, differing only in the envelope encoding plasmid used in transfection. Incorporation of SiaNAz onto the surface of 2.2 1L1L pseudotyped vectors was confirmed by reaction with 300 μM BCN-FLAG and following anti-FLAG western blot. (Figure 3-1). Complete loss in signal with omission of either the azido sugar or BCN-FLAG was observed. Removal of sialic acid residues by neuraminidase prior to SPAAC reaction also completely abrogated signal.
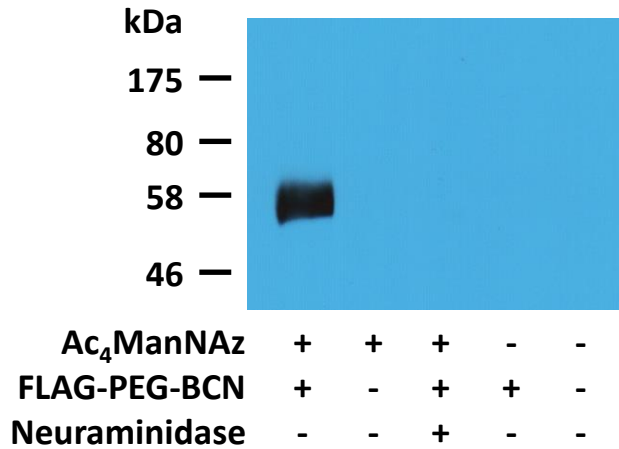
Figure 3-1. Confirmation of SiaNAz incorporation onto the surface of lentiviral vectors pseudotyped with mutant Sindbis glycoproteins.

The BCN-PEG-FLAG ligand was used to selectively modify SiaNAz residues on the surface of 2.2 1L1L pseudotyped lentiviral vectors. Prior to SPAAC modification, each virus sample was suspended in G1 reaction buffer (50 mM sodium citrate, pH 6.0, 10X buffer supplied with neuraminidase) and incubated with neuraminidase (2.5 U/μL, New England BioLabs, Cat. No. P0720) or merely the buffer at 37 ℃ for 1 hour. Each reaction sample was then run through a size-exclusion spin column (Princeton Separations, Cat. No. CS-901) equilibrated in PBS, and incubated with BCN-FLAG (300 μM) or only the buffer at room temperature for 6 hours. The reaction samples were subsequently analyzed by electrophoresis on 10% SDS-polyacrylamide gels followed by western blotting with the monoclonal ANTI-FLAG® M2-Peroxidase (HRP) antibody (Sigma-Aldrich, Cat. No. A8592). FLAG-positive signal was observed on the western blot for the experimental reaction sample, whereas complete loss in signal was observed with omission of either the azido sugar or BCN-FLAG. Removal of sialic acid residues by neuraminidase prior to SPAAC reaction also completely abrogated signal. The molecular weight of both Sindbis glycoprotein E1 and E2 are ~50 kDa [120].

The impact of SiaNAz incorporation on production of 2.2 1L1L pseudotyped viral particles was evaluated via p24 titer. With the addition of Ac4ManNAz during virus production, p24 ELISA assay demonstrated a reduction of titer (ng p24/mL) by 18% for virus samples concentrated by ultracentrifugation (Figure 3-2), similar to what was observed for VSV-G pseudotyped vectors.
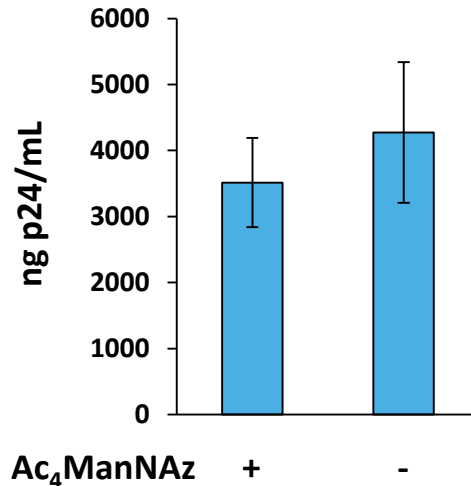
Figure 3-2. Impact of SiaNAz incorporation on viral particle production of Sindbis glycoprotein pseudotyped lentiviral vectors.

The p24 titers of 2.2 1L1L pseudotyped lentiviral vectors produced with or without the addition of Ac4ManNAz was obtained by an ELISA assay using the Lenti-X™ p24 Rapid Titer Kit (Clontech, Cat. No. 632200). For standard curve, a series of 2 fold dilutions of p24 protein (0 pg/ml, 12.5 pg/ml, 25 pg/ml, 50 pg/ml, 100 pg/ml, 200 pg/ml) were made with complete DMEM. To fit into the concentration range of the standards, virus samples concentrated by ultracentrifugation were diluted 10^5 fold. Each dilution of standard was assayed in duplicate, and each virus sample was assayed in triplicate. Assay was read on a PerkinElmer VICTOR™ X5 Multilabel Plate Reader. The result is reported as mean ± standard deviation.

3.2.2 Targeting lentiviral vectors to vascular endothelial growth factor 2 (VEGFR2)

Tumor angiogenesis is a prominent process that accompanies the development of solid tumors and the formation of cancer cell metastasis [127]. Neovasculature in tumors represents an attractive target for the activity and delivery of cancer therapeutics. As an angiogenic factor, vascular endothelial growth factor (VEGF) plays a crucial role in facilitating tumor vascularization and presents an important target for anticancer therapy [128]. Through phage display Mazié and colleagues identified an effective peptide antagonist of VEGF, ATWLPPR [129]. A nitrophenyl carbonate of BCN (*endo*-**2**) was synthesized as described by van Delft and coworkers [107], and used in the coupling reaction with the amine terminus of this peptide antagonist, which contains

two extra glycine residues as a short spacer (Scheme 3-1). The resulting VEGFR2 targeting ligand BCN-GGATWLPPR was used in surface modification of 2.2 1L1L pseudotyped lentiviral vectors and tested for elevated transduction on a VEGFR2 over-expressing cell line HUVEC (Figure 3-3).
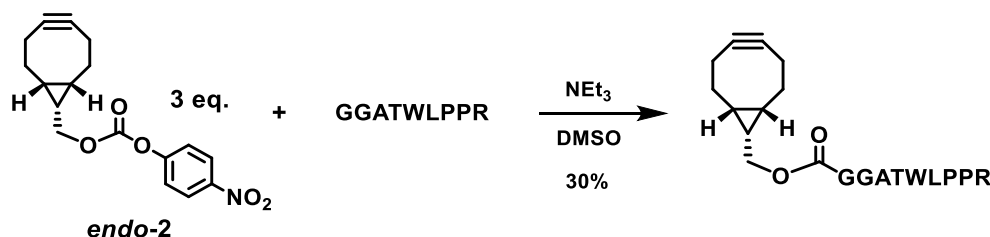
Scheme 3-1. Synthesis of the VEGFR2 targeting ligand BCN-GGARWLPPR.
The VEGFR2 targeting peptide GGATWLPPR was synthesized by Yoon Hyeun Oum on a CEM Liberty microwave peptide synthesizer (model No. 908505).

SiaNAz labeled lentiviral vectors were incubated with BCN-GGATWLPPR (600 μM) for 6 hours at room temperature and used in transduction of HUVEC cells immediately after removal of excess ligand by size exclusion spin columns. Expression of the GFP transgene was analyzed by flow cytometry two days later. As controls, virus samples produced in the absence of Ac$_4$ManNAz or incubated without BCN-GGATWLPPR were assayed under otherwise identical conditions. Viral surface conjugation with the BCN-ligand effectively enhanced the transduction efficiency toward target cells without extensive optimization of reaction conditions. Labeled vectors exhibited ~11-fold increased levels of transgene expression, which was specific to both azide labeling and SPAAC modification. Incubation of HUVEC cells with free GGATWLPPR peptide (300 μM) as inhibitors one hour prior to infection attenuated ligand enhanced gene delivery (Figure 3-3).

Ac$_4$ManNAz (75 µM)	+	+	+	-	-
BCN-GGATWLPPR (600 µM)	+	+	-	+	-
GGATWLPPR inhibition (300 µM)	-	+	-	-	-

Figure 3-3. Modification of lentiviral vectors with BCN-GGATWLPPR led to enhanced transduction of a VEGFR2 over-expressing cell line HUVEC.

HUVEC cells were seeded in 6-well plates at a density of 2×10^4 cells/well one day prior to transduction and counted again right before infection. 90 ng p24 value of concentrated 2.2 1L1L pseudotyped lentivirus was used in each reaction, experimental or control, and incubated at room temperature for 6 hours. Each sample was then desalted by a size-exclusion spin column, and used immediately in the 2 hours infection of three wells of HUVEC cells (3×10^4 cells/well). As a control, 300 µM of GGATWLPPR peptide was added into three wells, and cells were incubated for 1 hour at 37 ˚C before infection to block cell surface receptors. Expression of the GFP transgene in transduced cells was analyzed by flow cytometry two days later and the mean value of the resulting percentages of GFP positive cells for each illustrated virus sample was reported. Error bars indicate standard deviation.

3.2.3 Targeting lentiviral vectors to the tyrosine kinase receptor Tie2

The tyrosine kinase receptor Tie2 and its natural ligands, angiopoietins, play a crucial role in several vascular changes under both physiological and pathological conditions [130]. Elevated expression of Tie2 has been observed not only in the endothelium of the neovasculature in numerous solid tumors [131-135], but also in non-vascular cells in several types of cancer [130, 136-138]. The expression of Tie2 in different tumoral compartments makes it an attractive target

for cancer therapy. The RLVAYEGWV peptide was identified from phage display libraries as a substrate to inhibit the kinase activity of the Tie2 receptor [139]. Naturally, the Tie2 targeting ligand BCN-GGRLVAYEGWV, which again contains two extra glycine residues as a short spacer, was synthesized following the same protocol used in the synthesis of the VEGFR2 ligand (Scheme 3-2).
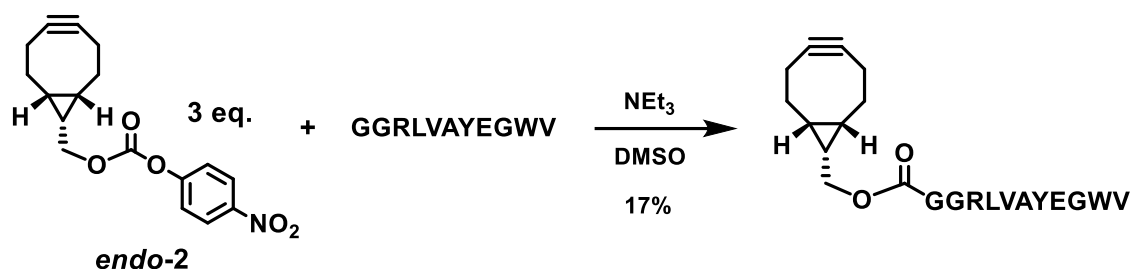
Scheme 3-2. Synthesis of the Tie2 targeting ligand BCN-GGRLVAYEGWV.
The Tie2 targeting peptide GGATWLPPR was synthesized by Yoon Hyeun Oum on a CEM Liberty microwave peptide synthesizer (model No. 908505).

SiaNAz labeled lentiviral vectors were incubated with BCN-GGRLVAYEGWV (600 μM) for 6 hours at room temperature and used in transduction of HUVEC cells immediately after removal of excess ligand by size exclusion spin columns. Expression of the GFP transgene was analyzed by flow cytometry two days later. As controls, virus samples produced in the absence of $Ac_4ManNAz$ or incubated without BCN-GGRLVAYEGWV were assayed under otherwise identical conditions. Viral surface conjugation with the BCN-ligand enhanced transduction efficiency toward target cells. Labeled vectors exhibited ~2-fold increased levels of transgene expression, which was specific to both azide labeling and SPAAC modification (Figure 3-4).

36
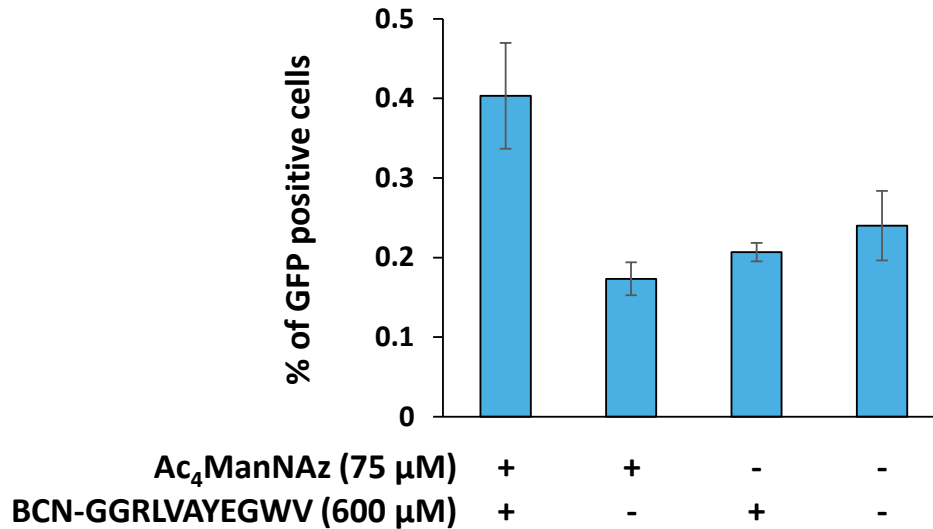
Figure 3-4. Modification of lentiviral vectors with BCN-GGRLVAYEGWV led to enhanced transduction of a Tie2 over-expressing cell line HUVEC.

HUVEC cells were seeded in 6-well plates at a density of 1.2×10^4 cells/well one day prior to transduction and counted again right before infection. 29 μL of concentrated 2.2 1L1L pseudotyped lentivirus was used in each reaction, experimental or control, and incubated at room temperature for 6 hours. Each sample was then desalted by a size-exclusion spin column, and used immediately in the 3 hours infection of three wells of HUVEC cells (3.6×10^4 cells/well). Expression of the GFP transgene in transduced cells was analyzed by flow cytometry two days later and the mean value of the resulting percentages of GFP positive cells for each illustrated virus sample was reported. Error bars indicate standard deviation.

3.2.4 Targeting lentiviral vectors to integrin $\alpha_v\beta_3$

Cell adhesion $\alpha_v\beta_3$ integrin, over-expressed in blood vessels of tumors, is required in tumor-induced angiogenesis and tumor metastasis. We developed a bicyclononyne functionalized integrin $\alpha_v\beta_3$ targeting ligand based on a highly potent and selective antagonist first designed and synthesized by Kessler's group, the cyclic pentapeptide c(RGDfK) [140]. Compared to the RGD-4C version of cyclic RGD, where the RGD motif is cyclized through disulfide bonds, the c(RGDfK) peptide, which contains a D-phenylalanine and is cyclized via an amide bond, has higher affinity and specificity toward integrin $\alpha_v\beta_3$. The cyclic peptide was synthesized by Yoon Hyeun Oum using Fmoc solid-phase chemistry according to the scheme described by the Liu

37

group[141]. The diastereomeric *exo*-isomer of the BCN nitrophenyl carbonate (*exo*-**2**) was used in the coupling reaction with the primary amino group on the lysine residue contained in the c(RGDfK) (Scheme 3-3). The resulting ligand BCN-c(RGDfK) was used in surface modification of 2.2 1L1L pseudotyped letiviral vectors. The transduction efficiency of the modified vectors was then tested on an integrin $\alpha_v\beta_3$ over-expressing cell line U-87 MG (Figure 3-5).
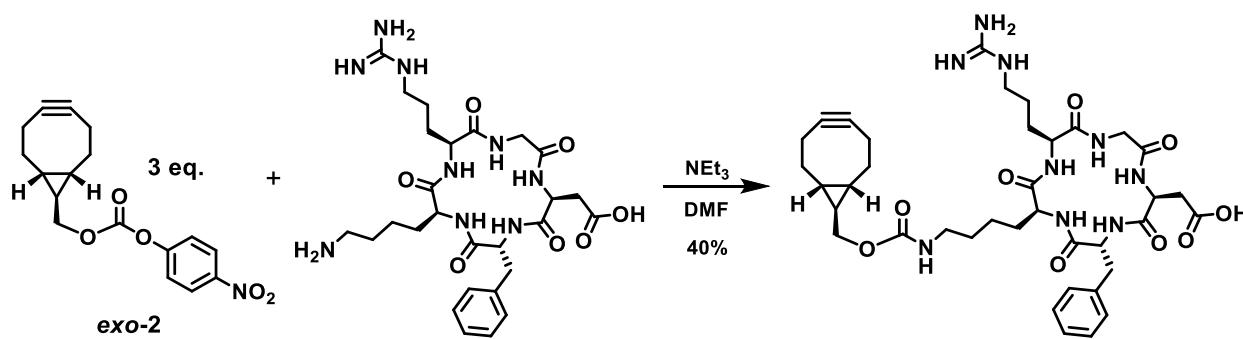
Scheme 3-3. Synthesis of the integrin $\alpha_v\beta_3$ targeting ligand BCN-c(RGDfK).
Cyclo (-Arg-Gly-Asp-D-Phe-Lys-) peptide was synthesized manually by Yoon Hyeun Oum based on published procedures [141].

SiaNAz labeled lentiviral vectors were incubated with BCN-c(RGDfK) (600 μM) for 6 hours at room temperature and used in transduction of U-87 MG cells immediately after removal of excess ligand by size exclusion spin columns. Expression of the GFP transgene was analyzed by flow cytometry two days later. As controls, virus samples produced in the absence of Ac₄ManNAz or incubated without BCN-c(RGDfK) were assayed under otherwise identical conditions. Viral surface conjugation with the BCN-ligand effectively enhanced the transduction efficiency toward target cells without extensive optimization of reaction conditions. Labeled vectors exhibited a more than 3-fold increase in levels of transgene expression, which was specific to both azide labeling and SPAAC modification. Incubation of U-87 MG cells with free c(RGDfK)

peptide (200 μM) as inhibitors one hour prior to infection attenuated ligand enhanced gene delivery
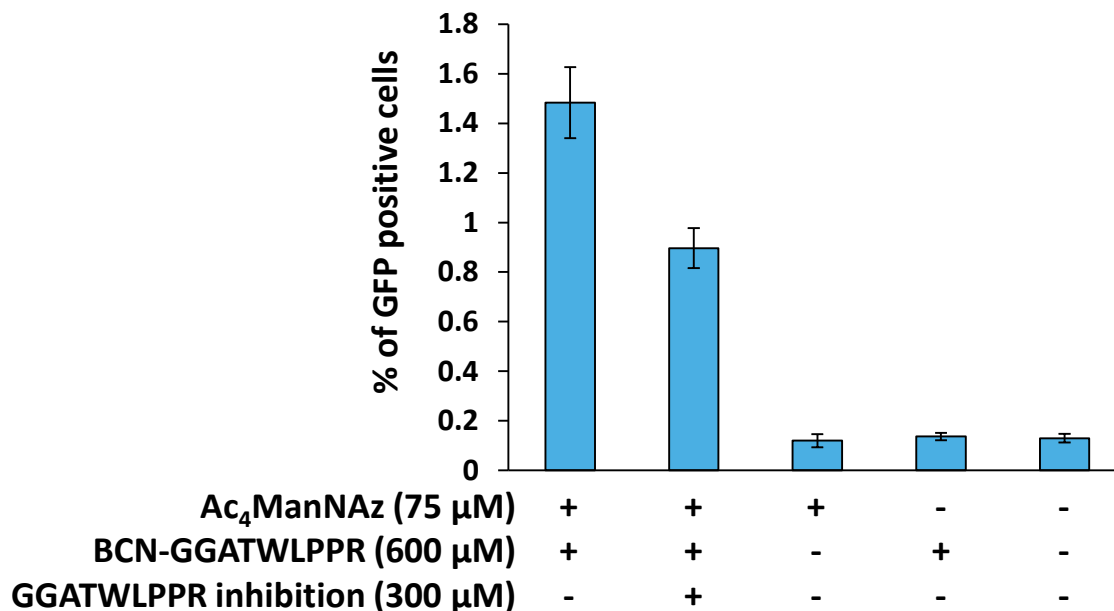
(Figure 3-5).

Ac$_4$ManNAz (75 μM)	+	+	+	-	-
BCN-cRGD (600 μM)	+	+	-	+	-
cRGD inhibition (200 μM)	-	+	-	-	-
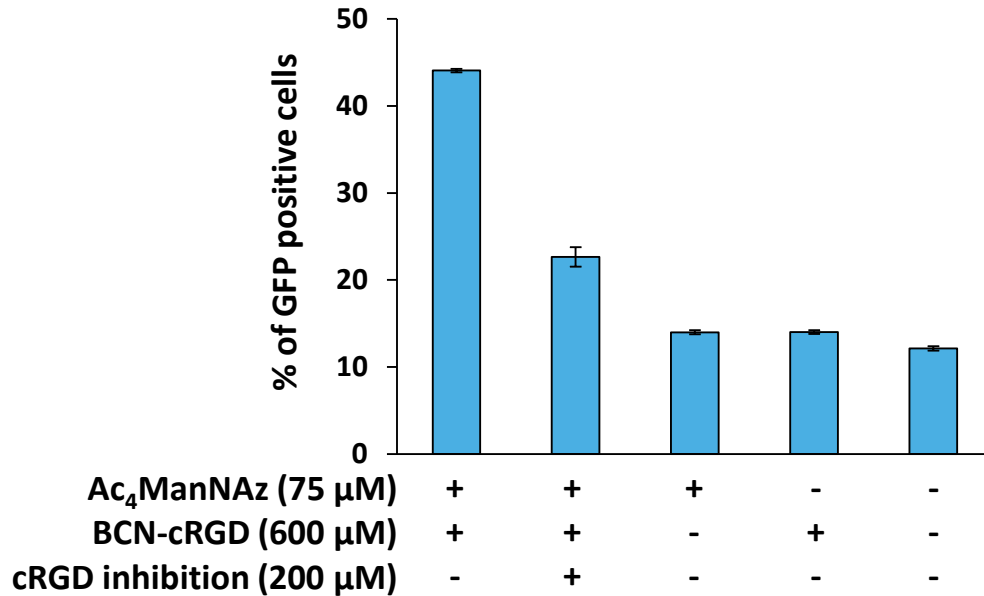
Figure 3-5. Modification of lentiviral vectors with cyclic RGD led to enhanced transduction of an integrin α$_v$β$_3$ over-expressing cell line U-87 MG.

U-87 MG cells were seeded in 6-well plates one day prior to transduction. 90 ng p24 value of concentrated 2.2 1L1L pseudotyped lentivirus was used in each reaction, experimental or control, and incubated at room temperature for 6 hours. Each sample was then desalted by a size-exclusion spin column, and used immediately in the 3 hours infection of three wells of U-87 MG cells. As a control, 200 μM of cyclic(RGDfK) peptide was added into three wells, and cells were incubated for 1 hour at 37 ˚C before infection to block cell surface receptors. Expression of the GFP transgene in transduced cells was analyzed by flow cytometry two days later and the mean value of the resulting percentages of GFP positive cells for each illustrated virus sample was reported. Error bars indicate standard deviation.

3.2.5 Targeting lentiviral vectors to prostate-specific membrane antigen (PSMA)

PSMA is a type II transmembrane protein expressed in all types of prostate tissues and at

increased levels in prostate cancer tissues [142, 143]. Additionally, it is also robustly expressed in

the neovasculature of various nonprostatic solid malignancies [144, 145]. Kozikowski and

coworkers synthesized and tested a series of glutamate urea derivatives designed to inhibit PSMA.

39

An analog bearing a γ-tetrazole on one of the glutamic acid moieties was identified as the most potent inhibitor with a K_i of 0.9 nM [146]. Spiegel and coworkers adopted this design and proposed a 1-butyl-4-alkyl-1,2,3-triazole analog for the construction of the cell-binding terminus in their antibody recruiting small molecule [147]. This scaffold was synthesized using a similar route to that described by Spiegel and colleagues, with a slightly different linker region, and conjugated to BCN via the same coupling scheme used for the three peptide ligands (Scheme 3-4). The resulting PSMA targeting ligand BCN-PEG-glutamate urea was tested on a human prostate cancer cell line LNCaP (Figure 3-6).
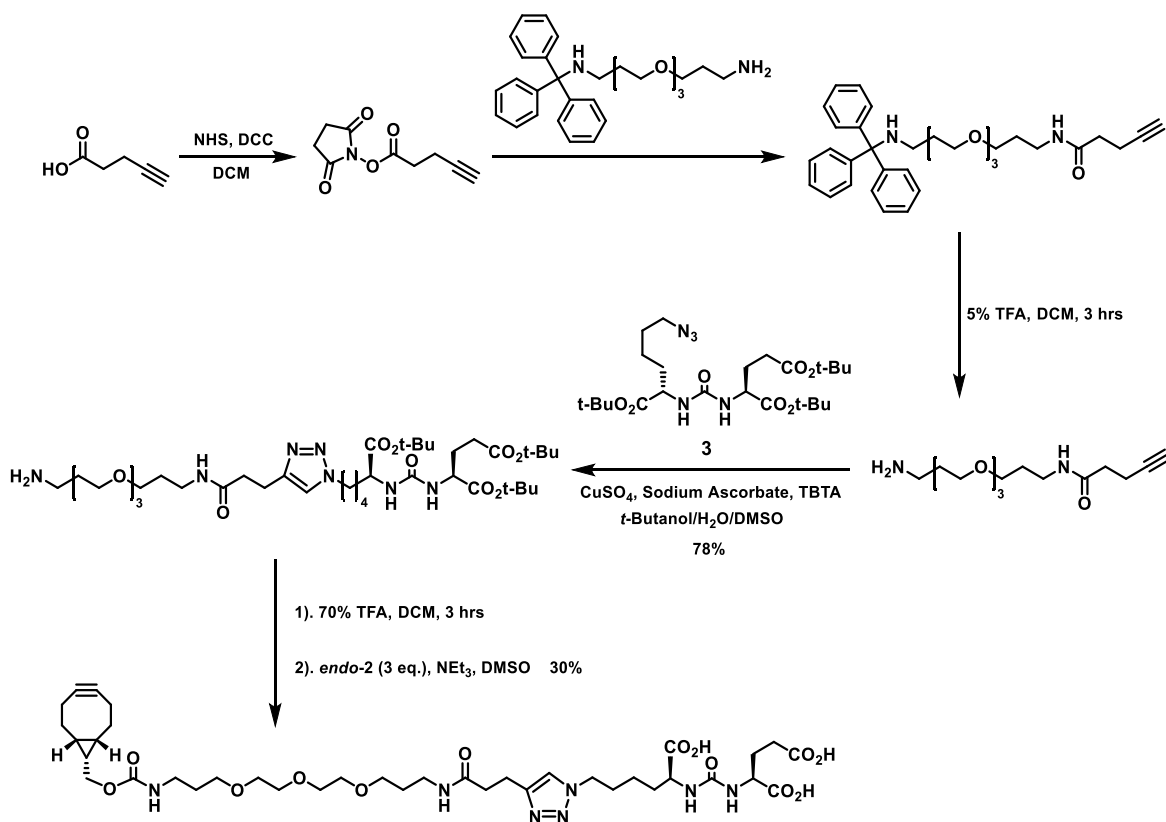
Scheme 3-4. Synthesis of the PSMA targeting ligand BCN-PEG-glutamate urea.

Compound **3** was synthesized by Paul Gelfand according to the procedure described by D. A. Spiegel, *et al.* [147].

SiaNAz labeled lentiviral vectors were incubated with BCN-PEG-glutamate urea (600 μM) for 6 hours at room temperature and used in transduction of LNCaP cells immediately after removal of excess ligand by size exclusion spin columns. Expression of the GFP transgene was analyzed by flow cytometry two days later. As controls, virus samples produced in the absence of Ac$_4$ManNAz or incubated without BCN-PEG-glutamate urea were assayed under otherwise identical conditions. Viral surface conjugation with the BCN-ligand effectively enhanced the transduction efficiency toward target cells without extensive optimization of reaction conditions. Labeled vectors exhibited 16 to 18 fold increased levels of transgene expression, which was specific to both azide labeling and SPAAC modification. Incubation of LNCaP cells with NH$_2$-PEG-glutamate urea (200 μM) as inhibitors one hour prior to infection attenuated ligand enhanced gene delivery (Figure 3-6).

Ac$_4$ManNAz (75 μM)	+	+	+	-	-
BCN-Glu-Urea (600 μM)	+	+	-	+	-
Glu-Urea inhibition (200 μM)	-	+	-	-	-
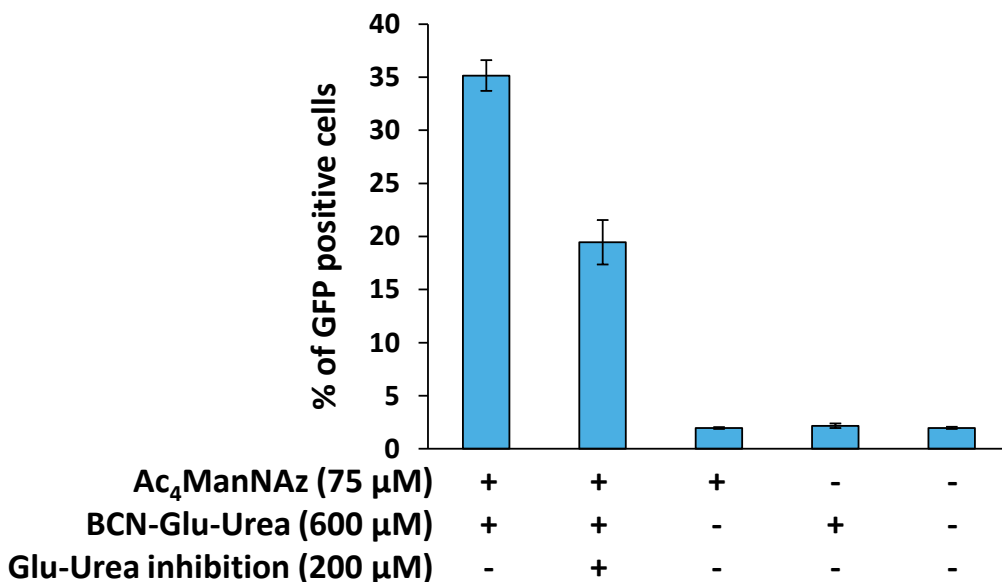
Figure 3-6. Modification of lentiviral vectors with a glutamate urea derived ligand led to enhanced transduction of a prostate cancer cell line LNCaP.

LNCaP cells were seeded in 6-well plates one day prior to transduction. 90 ng p24 value of concentrated 2.2 1L1L pseudotyped lentivirus was used in each reaction, experimental or control, and incubated at room temperature for 6 hours. Each sample was then desalted by a size-exclusion

spin column, and used immediately in the 3 hours infection of three wells of LNCaP cells. As a control, 200 μM of NH₂-PEG-glutamate urea was added into three wells, and cells were incubated for 1 hour at 37 ˚C before infection to block cell surface receptors. Expression of the GFP transgene in transduced cells was analyzed by flow cytometry two days later and the mean value of the resulting percentages of GFP positive cells for each illustrated virus sample was reported. Error bars indicate standard deviation.

3.2.6 Targeting lentiviral vectors to folate receptors

Folates, also known as the B9 vitamins, are required in multiple crucial biosynthetic pathways including *de novo* biosynthesis of purines and thymidylate, amino acid metabolism, and methylation reactions, and consequently, are essential for cell growth, proliferation and survival [148]. Folates can be found in an oxidized form as folic acid, or in naturally occurring reduced forms as the partially reduced intermediate 7,8-dihydrofolate (DHF) or the biologically active 5,6,7,8-tetrahydrofolate (THF) and derivatives [148, 149]. Mammalian cells lack the metabolic enzymes necessary for folate biosynthesis, therefore all folate requirements must be obtained through diet [150, 151].

Cellular uptake of folates occurs through three genetically distinct and functionally diverse transport systems, including the proton-coupled folate transporter (PCFT), the reduced folate carrier (RFC) and the folate receptors (FRs) [151]. PCFT is a proton-folate symporter that facilitates intestinal folate absorption at the acidic pH of the upper small intestine [151-154]. RFC is a ubiquitously expressed anion exchanger and serves as the primary pathway for the transport of reduced folates into various cells and tissues under physiological pH [155].

FRs bind folic acid, reduced folates, many antifolates and folate conjugates with high affinities (low nanomolar) [149, 151, 156-161], and facilitate internalization via receptor-mediated endocytosis [162, 163]. The two major isoforms of human FR, FRα and FRβ, are cell surface

glycosylphosphatidylinositol (GPI)-anchored glycoproteins [164]. In normal tissues and organs, FRα expression is confined to the apical (luminal) surface of polarized epithelial cells where it is inaccessible to circulating folates or intravenously administered folic acid conjugates [164-166], and FRβ expression is restricted mainly to the placenta and white blood cells of myeloid lineage, including activated macrophages [164, 167-170]. However, marked overexpression of FRα has been observed on many types of solid tumor cells, including ovarian, kidney, lung, brain, endometrial, colorectal, pancreatic, gastric, prostate, testicular, bladder, head and neck, and breast cancers, and non-small cell lung cancer [149, 157, 158, 166, 171-177]. FRβ has also been reported to express on the surface of a substantial fraction of chronic and acute myelogenous leukemia cells [176, 178]. As a result of this tumor associated overexpression, FR has emerged as an appealing target for cancer therapy, and a wide spectrum of folate conjugates has been developed as therapeutic and diagnostic agents [149, 161].

A short diamino-PEG spacer was conjugated to folic acid by Partha Banerjee through an NHS ester reaction scheme. The resulting NH_2-PEG-folate was purified by reversed-phase HPLC and used in the coupling reaction with the BCN nitrophenyl carbonate (*exo*-**2**) to generate BCN-PEG-folate (Scheme 3-5). This FR targeting ligand then was used in surface modification of 2.2 1L1L pseudotyped letiviral vectors. The transduction efficiency of the modified vectors was tested on an FR over-expressing cell line ID8 (Figure 3-7).
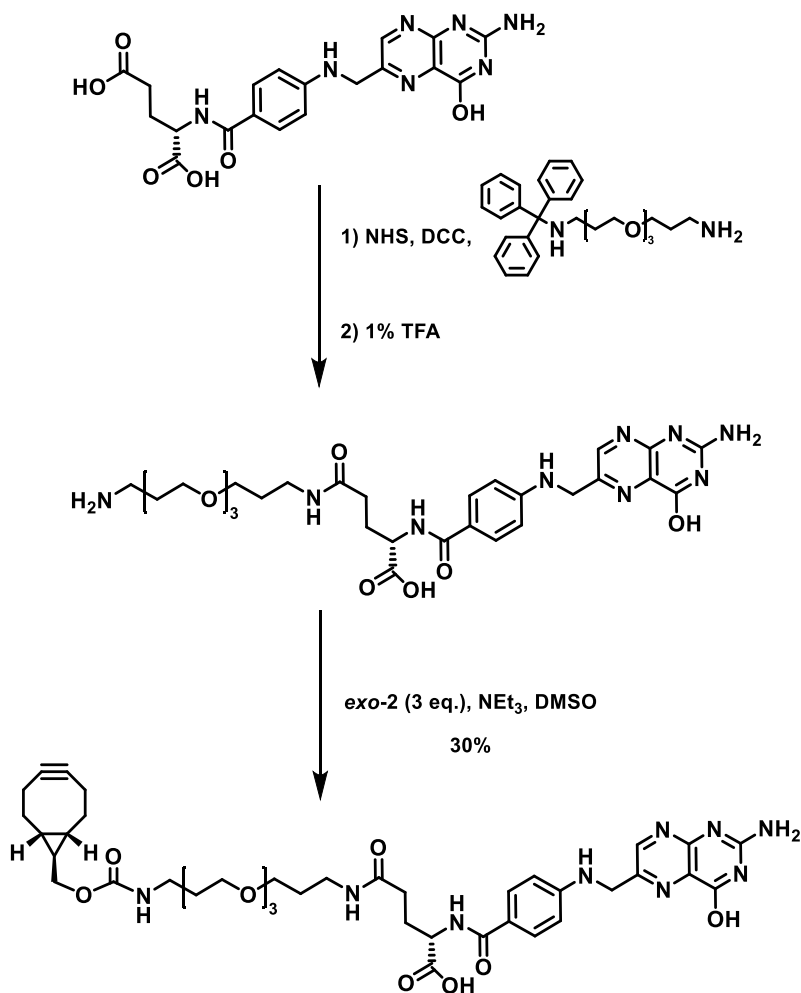
Scheme 3-5. Synthesis of the FR targeting ligand BCN-PEG-folate.

Crude NH_2-PEG-folate was synthesized by Partha Banerjee.

Ac$_4$ManNAz (75 µM)	+	+	+	-	-
BCN-PEG-folate (600 µM)	+	+	-	+	-
Folic acid inhibition (10 µM)	-	+	-	-	-
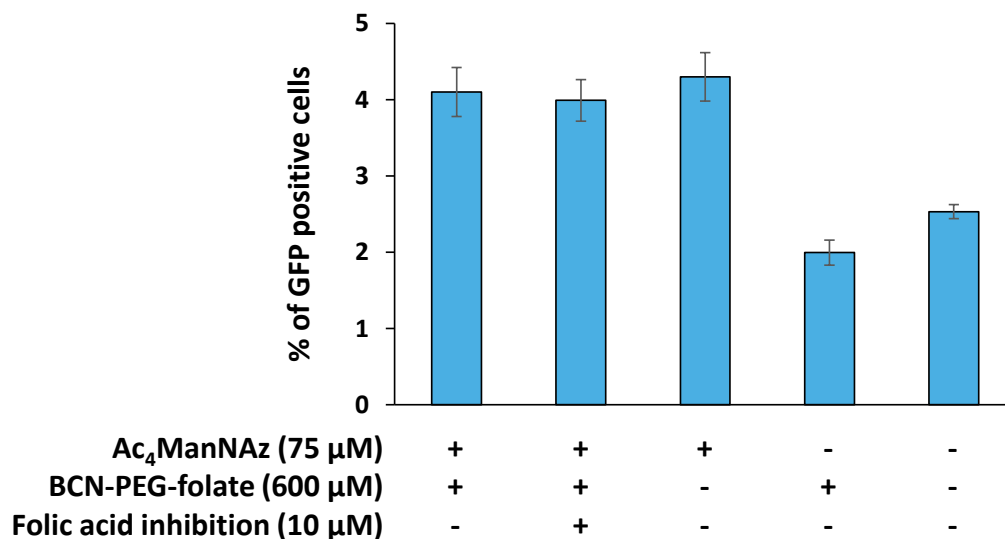
Figure 3-7. Targeting lentiviral vectors to folate receptors through conjugation with BCN-PEG-folate.

ID8 cells were cultivated in (-) folate media for two weeks, and seeded in 6-well plates at a density of 4×10^4 cells/well one day prior to transduction. 32 µL of concentrated 2.2 1L1L pseudotyped lentivirus was used in each reaction, experimental or control, and incubated at room temperature for 5 hours. Each sample was then desalted by a size-exclusion spin column, and used immediately in the 2 hours infection of three wells of ID8 cells (9.4×10^4 cells/well). As a control, 10 µM of folic acid was added into three wells, and cells were incubated for 1 hour at 37 ˚C before infection to block cell surface receptors. Expression of the GFP transgene in transduced cells was analyzed by flow cytometry two days later and the mean value of the resulting percentages of GFP positive cells for each illustrated virus sample was reported. Error bars indicate standard deviation.

SiaNAz labeled lentiviral vectors were incubated with BCN-PEG-folate (600 µM) for 5 hours at room temperature and used in transduction of ID8 cells immediately after removal of excess ligand by size exclusion spin columns. Expression of the GFP transgene was analyzed by flow cytometry two days later. As controls, virus samples produced in the absence of Ac4ManNAz or incubated without BCN-PEG-folate were assayed under otherwise identical conditions. Unexpectedly, viral surface conjugation with the BCN-ligand did not obviously enhanced the transduction efficiency toward target cells. The difference in transduction efficiency between (+) SiaNAz and (-) SiaNAz vectors is likely inherited from the difference in TU titers between the

stock viruses in this particular batch, instead of a result of the chemical labeling. Incubation of ID8

cells with folic acid (10 μM) as inhibitors one hour prior to infection did not show any effect either.

Alternatively, two other folate conjugates, alkyne-PEG-folate and phosphine-PEG-folate

(designed and synthesized by Partha Banerjee [179-181]), were also used in modification of

SiaNAz labeled lentiviral vectors via CuAAC and Staudinger ligation, respectively (Figure 3-8).
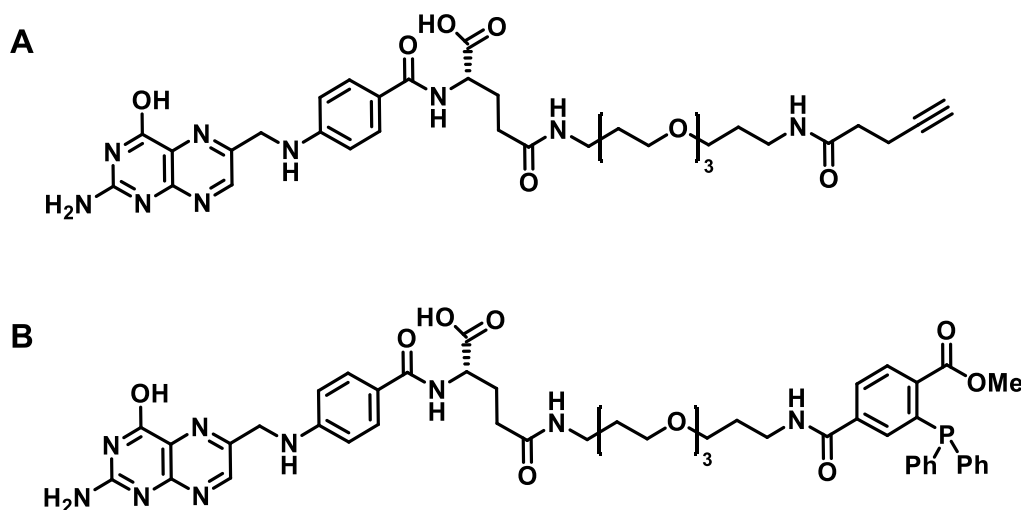
Figure 3-8. Structures of alkyne-PEG-folate and phosphine-PEG-folate.
Both folate conjugates, (A) alkyne-PEG-folate and (B) phosphine-PEG-folate, were designed and
synthesized by Partha Banerjee [179-181].

Alkyne-PEG-folate was used in surface modification of SINmu pseudotyped letiviral

vectors via CuAAC. The transduction efficiency of the modified vectors was tested on an FR over-

expressing cell line 4T1 (Figure 3-9).
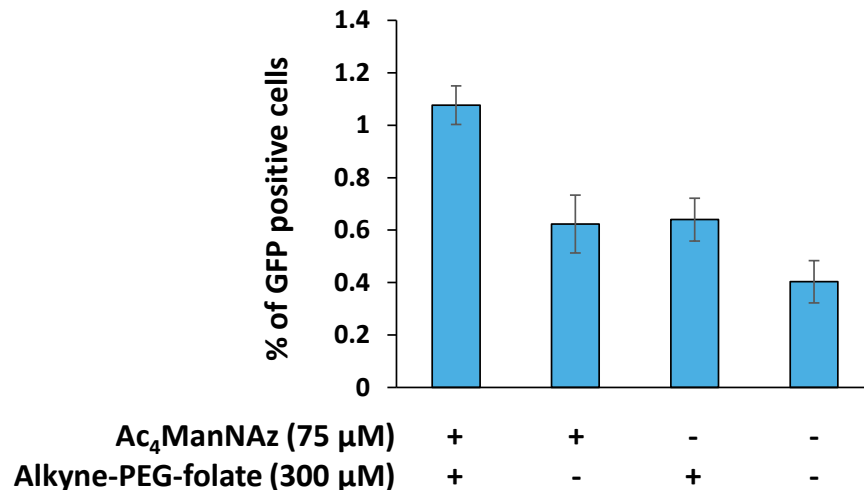
Figure 3-9. CuAAC modification of lentiviral vectors with alkyne-PEG-folate led to enhanced transduction of an FR over-expressing cell line 4T1.

4T1 cells were cultivated in (-) folate media for two weeks, and then seeded in 6-well plates at a density of 5×10^4 cells/well one day prior to transduction. 50 μL of concentrated SINmu pseudotyped lentivirus was suspended in a reaction mixture (total vol. 100 μL) containing tris (100 mM, pH 8.0), bathophenanthroline disulfonic acid disodium salt (3 mM) and alkyne-PEG-folate (300 μM or 0 μM). Each reaction mixture was kept in a deoxygenated glove bag for 12 hours to ensure full exclusion of oxygen before CuBr (1 mM) was added, followed by incubation at room temperature for another 6 hours in deoxygenated atmosphere. Each sample was then desalted by a size-exclusion spin column, and used immediately in the 3 hours infection of three wells of 4T1 cells (5×10^4 cells/well). Expression of the GFP transgene in transduced cells was analyzed by flow cytometry two days later and the mean value of the resulting percentages of GFP positive cells for each illustrated virus sample was reported. Error bars indicate standard deviation.

SiaNAz labeled vectors were incubated with alkyne-PEG-folate (300 μM) in the presence of tris (100mM, pH 8.0), bathophenanthroline disulfonic acid disodium salt (3 mM) and CuBr (1 mM) in deoxygenated atmosphere for 6 hours at room temperature and used in transduction of 4T1 cells immediately after removal of excess ligand by size exclusion spin columns. Expression of the GFP transgene was analyzed by flow cytometry two days later. As controls, virus samples produced in the absence of Ac4ManNAz or incubated without alkyne-PEG-folate were assayed under otherwise identical conditions. Viral surface conjugation with the terminal alkyne-ligand enhanced the transduction efficiency toward target cells. Labeled vectors exhibited ~2-fold

increased levels of transgene expression, which was specific to both azide labeling and CuAAC

modification (Figure 3-9).

Phosphine-PEG-folate was used in surface modification of SINmu pseudotyped letiviral

vectors via Staudinger ligation. The transduction efficiency of the modified vectors was tested on

the FR over-expressing cell line ID8 (Figure 3-10).

Ac$_4$ManNAz (75 µM)	+	+	-	-
Phosphine-PEG-Folate (600 µM)	+	+	+	+
Folic acid inhibition (20 µM)	-	+	-	+
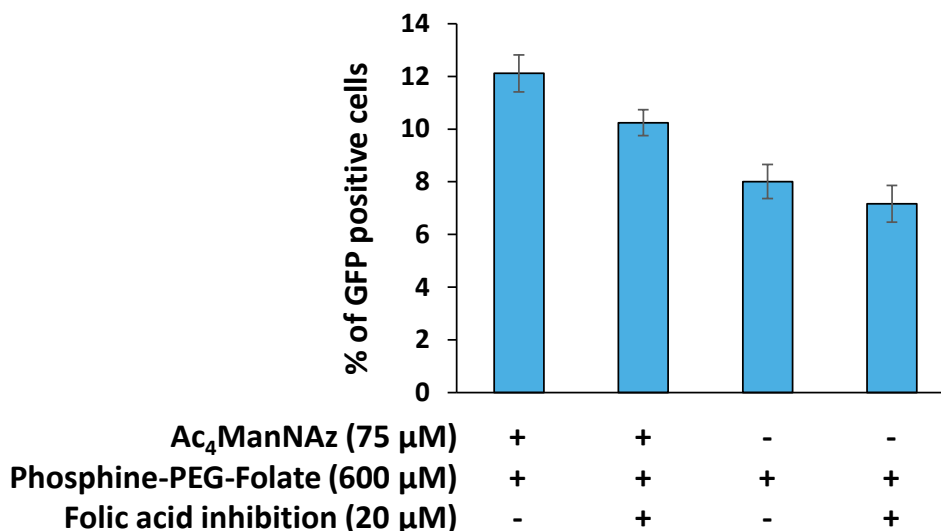
Figure 3-10. Modification of lentiviral vectors with phosphine-PEG-folate led to enhanced transduction of an FR over-expressing cell line ID8.

ID8 cells were cultivated in (-) folate media for two weeks, and seeded in 6-well plates at a density of 3.5×10^4 cells/well one day prior to transduction. 50 µL of concentrated SINmu pseudotyped lentivirus was used in each reaction with phosphine-PEG-folate. Reaction mixtures were incubated at room temperature for 5 hours. Each sample was then desalted by a size-exclusion spin column, and used immediately in the 3 hours infection of three wells of ID8 cells (6×10^4 cells/well). As a control, 20 µM of folic acid was added into six wells, three for SiaNAz (+) viruses and three for SiaNAz (-), and cells were incubated for 1 hour at 37 ˚C before infection to block cell surface receptors. Expression of the GFP transgene in transduced cells was analyzed by flow cytometry two days later and the mean value of the resulting percentages of GFP positive cells for each illustrated virus sample was reported. Error bars indicate standard deviation.

SINmu pseudotyped lentiviral vectors were incubated with phosphine-PEG-folate (600

µM) for 5 hours at room temperature and used in transduction of ID8 cells immediately after

removal of excess ligand by size exclusion spin columns. Expression of the GFP transgene was analyzed by flow cytometry two days later. As controls, 20 μM of folic acid was added into three wells of cells for (+) SiaNAz viruses and three wells for (-) SiaNAz viruses, and the cells were incubated for 1 hour at 37 ˚C before infection to block cell surface receptors. All reaction samples were assayed under otherwise identical conditions. Viral surface conjugation with the Staudinger ligand enhanced the transduction efficiency toward target cells, which was attenuated by incubation of the cells with folic acid (20 μM) as inhibitors one hour prior to infection (Figure 3-10).

3.3 Conclusion and discussion

Seven targeting ligands equipped with BCN, terminal alkyne or the Staudinger phosphine were introduced onto lentiviral viral surfaces via metabolically incorporated SiaNAz for higher transduction efficiency toward target cells. Four of these are small molecule ligands selective for prostate-specific membrane antigen (PSMA) or folate receptors (FRs), and the other three are peptides that are known to localize in angiogenic regions. In almost every case, simple and efficient bioorthogonal modification of viral surfaces significantly enhanced transduction toward cells bearing the targeted cell surface receptors. Notably, saturation of the cell surface receptor with free ligand prior to exposure to viruses only partially reduced ligand enhanced gene delivery. Presumably this is a result of the high local concentration of targeting ligands on the virus/cell interface associated with multidentate binding.

One merit of this two-step method is that it can serve as a general, flexible route to covalently introduce synthetic molecules. Bioorthogonal chemical modifications on the viral surface azide groups give access to virtually any kind of functionality, with excellent efficiency

and specificity. Three out of the five targeting molecules we have conjugated to the viral surface through bioorthogonal reactions, the c(RGDfK) peptide, the glutamate urea derivative and the folate, cannot be directly introduced by genetic insertion. In almost every case, excellent targeting was seen without any optimization in ligand concentration or reaction time. It may be advantageous to limit the number of ligands appended to viral surface, which can alter surface charge and aggregation propensity. Control over ligand density can easily be obtained by altering the level of SiaNAz incorporation, through changing the concentration of precursor azido sugar, or the efficiency of subsequent chemoselective modification, via change in modification time or ligand concentration.

The modified Sindbis virus envelope proteins we used as the pseudotype for the targeting assays include two glycoproteins, E1 and E2. E2 mediates binding to cellular receptors [182-185], while E1 is responsible for the fusion between the viral envelope and the cell membrane [186]. It is plausible that targeting ligands attached to aa 139 on E1 would interfere with its fusion function, especially in cases when the ligands are bulky. However, we do expect the ligand on E1 to contribute to the specific binding and increased transduction toward targeted cells. It has been shown that, when expressed in a high mannose structure, the glycan on E1 aa 139 alone can mediate higher transduction by binding to DC-SIGN, a cell surface lectin expressed on dendritic cells, just like the glycan on E2 aa 196 [121]. It might be interesting to introduce mutations at E2 aa 196 or E1 aa 139 to remove the glycan and observe the effect on our targeting system with different targeting ligands.

In summary, we have developed a general method for labeling Lentiviral surfaces that is both flexible and robust. This method lends itself to being applied to a wide variety of applications including expanded targeting, purification via modification with affinity tags, and

fluorescence/MRI/PET based particle tracking. Modification via azido sugar introduction can be widely applied to budded viruses. Lentiviral vectors were chosen for expediency, but in principle this method will be accessible with any virus bearing sialylated glycoproteins. Although most glycosylated viruses bear sialic acid residues, alternate methods for azide introduction include the use of other azido sugar precursors, azido amino acids and azido lipids.

3.4 Materials and methods

Synthesis of BCN-GGATWLPPR

(1*R*,8*S*,9*s*)-Bicyclo[6.1.0]non-4-yn-9ylmethyl (4-nitrophenyl) carbonate (*endo*-**2**) was synthesized as previously described [107]. The same protocol used in the synthesis of the FLAG-Cys peptide was followed to synthesize the VEGFR2 targeting peptide GGATWLPPR by Yoon Hyeun Oum using a CEM Liberty microwave peptide synthesizer (model No. 908505). To a solution of peptide GGATWLPPR (3.3 mg, 3.5 µmol) in DMSO (400 µL) was added triethylamine (9 µL) and *endo*-**2** (3.3 mg, 10.4 µmol). The reaction was then rotated at room temperature for 6 hours (Scheme 3-1). The resulting BCN-GGATWLPPR was purified by reversed-phase HPLC using a Varian C18 analytical column (250 x 4.6 mm, part No. R0086200C5), eluting with a gradient of acetonitrile in water (5% for 5 min, then 5-50% over 55 min, flow rate 1 ml/min). TFA (0.1%) was included in the mobile phase as the ion-pairing reagent. Subsequent removal of solvent by vacuum afforded purified BCN-GGATWLPPR (1.2 mg, 30%). MS (MALDI+): *m/z* calcd for $[C_{55}H_{80}N_{13}O_{13}]^+$ $[M + H]^+$: 1130.600, found: 1130.987 (Appendix 2).

Synthesis of BCN-GGRLVAYEGWV

The tyrosine kinase receptor Tie2 targeting peptide GGRLVAYEGWV was designed and synthesized by Yoon Hyeun Oum using a CEM Liberty microwave peptide synthesizer (model No. 908505), based on the description by H. J. Haisma, *et al.*[139, 187]. To a solution of peptide GGRLVAYEGWV (2.0 mg, 1.7 μmol) in DMSO (400 μL) was added TEA (9 μL) and (*endo*-**2**) (1.6 mg, 5 μmol). The reaction was then rotated at room temperature for 6 hours (Scheme 3-2). The resulting BCN- GGRLVAYEGWV was purified by reversed-phase HPLC using a Varian C18 analytical column (250 x 4.6 mm, part No. R0086200C5), eluting with a gradient of acetonitrile in water (5% for 5 min, then 5-50% over 55 min, flow rate 1 ml/min). TFA (0.1%) was included in the mobile phase as the ion-pairing reagent. Subsequent removal of solvent by vacuum afforded purified BCN-GGRLVAYEGWV (0.4 mg, 17%). MS (MALDI+): *m/z* calcd for $[C_{67}H_{96}N_{15}O_{17}]^+$ $[M + H]^+$: 1382.710, found: 1383.019 (Appendix 3).

Synthesis of BCN-c(RGDfK)

(1*R*,8*S*,9*r*)-Bicyclo[6.1.0]non-4-yn-9ylmethyl (4-nitrophenyl) carbonate (*exo*-**2**) was synthesized as previously described [107]. Cyclo (-Arg-Gly-Asp-D-Phe-Lys-) was synthesized manually by Yoon Hyeun Oum based on published procedures [141]. To a solution of c(-RGDfK-) (5.0 mg, 6.0 μmol) in DMF (500 μL) was added triethylamine (10 μL) and *exo*-**2** (7.3 mg, 20 μmol). The reaction was rotated at room temperature for 8 hours (Scheme 3-3). The resulting BCN-c(RGDfK) was purified by reversed-phase HPLC using a Varian C18 analytical column (250 x 4.6 mm, part No. R0086200C5), eluting with a gradient of acetonitrile in water (15-50% over 35 min, flow rate 1 ml/min). TFA (0.1%) was included in the mobile phase as the ion-pairing reagent.

Subsequent removal of solvent by vacuum afforded purified BCN-c(RGDfK) (1.9 mg, 40%). MS (ESI+): m/z calcd for $[C_{38}H_{54}N_9O_9]^+$ $[M + H]^+$: 780.404, found: 780.3 (Appendix 4).

Synthesis of BCN-PEG-glutamate urea

To a solution of 4-pentynoic acid (196.2 mg, 2mmol) and N-hydroxysuccinimide (230.2 mg, 2 mmol) in DCM (20 mL) at 0 °C was added N,N'-Dicyclohexylcarbodiimide (495.2 mg, 2.4 mmol). The resulting mixture was stirred at room temperature for 5 hours. The DCU precipitate was removed by filtration, and to the filtrate was added Trt-NH-$(PEG)_2$-NH_2 (105 mg, 0.227 mmol, Novabiochem, Cat. No. 01-63-0143). The reaction mixture was stirred for 13 hours, and filtered again. The product in the filtrate was purified by column chromatography on silica gel (EtOAc 100%). R_f = 0.2 (EtOAc 100%). All purified alkyne-PEG-NH-trt was dissolved in 20 mL dry DCM, and to the solution was added 1 mL TFA. The solution was then stirred at room temperature for 3 hours to remove the trityl group, and the crude product was concentrated over high vacuum (Scheme 3-4).

(S)-di-tertbutyl 2-(3-((S)-6-azido-1-tert-butoxy-1-oxohexan-2-yl)ureido)pentanedioate (**3**) was synthesized by Paul Gelfand following published procedures [147]. A mixture of **3** (10.5 mg, 20 μmol) and alkyne-PEG-NH_2 (crude, 15.8 mg) was dissolved in a mixture of *tert*-butanol (500 μL) and water (130 μL) in a 1.7 mL eppendorf tube. To this solution was added 50 mM sodium ascorbate (200 μL, 10 μmol), 50 mM copper (II) sulfate (20 μL, 1 μmol), 10 mM TBTA (100 μL, 1 μmol) in DMSO, and 1 M Tris buffer (pH 7.5, 50 μL, 50 μmol). The tube was then flushed with Ar and rotated at room temperature for 12 hours (Scheme 3-4). The resulting compound named *t*-butyl-glutamate urea-NH_2 was purified by reversed-phase HPLC using a Phenomenex Jupiter C12 semi-preparative column (250 x 10 mm, part No. 00G-4396-N0), eluting with a gradient of

53

acetonitrile in water (10-70% over 60 min, flow rate 4 ml/min). TFA (0.1%) was included in the mobile phase as the ion-pairing reagent. Subsequent removal of solvent by vacuum afforded purified t-butyl-glutamate urea-NH$_2$ (12.7 mg, 78%). MS (ESI+): m/z calcd for $[C_{39}H_{72}N_7O_{11}]^+$ [M + H]$^+$: 814.528, found: 814.5.

Purified t-butyl-glutamate urea-NH$_2$ (5.4 mg, 6.6 μmol) was treated by a mixture of 300 μL DCM and 700 μL TFA for 3 hours to remove the t-buty protecting groups. Solvent was then removed by vacuum. To a solution of the resulting crude glutamate urea-PEG-NH$_2$ in DMSO (400 μL) was added triethylamine (10 μL) and *endo*-**2** (6.3 mg, 20 μmol). Reaction was allowed to proceed at room temperature for 3 hours (Scheme 3-4). The product was purified by reversed-phase HPLC using a Varian C18 analytical column (250 x 4.6 mm, part No. R0086200C5), eluting with a gradient of acetonitrile in water (5% for 5 min, then 5-50% over 55 min, flow rate 1 ml/min). TFA (0.1%) was included in the mobile phase as the ion-pairing reagent. Subsequent removal of solvent by vacuum afforded purified BCN-PEG-glutamate urea (1.6 mg, 30%). MS (ESI+): m/z calcd for $[C_{38}H_{60}N_7O_{13}]^+$ [M + H]$^+$: 822.425, found: 823.1 (Appendix 5).

Synthesis of BCN-PEG-folate

Crude NH$_2$-PEG-folate was synthesized by Partha S. Banerjee. Folic acid was activated by NHS and DCC in dry DMSO. Trt-NH-(PEG)$_2$-NH$_2$ was added to the solution and stirred overnight, followed by filtration. The reaction was acidified by 1% TFA to remove protecting trityl group, and then vacuum concentrated to remove TFA.

The crude NH$_2$-PEG-folate was purified by reversed-phase HPLC using a Phenomenex Jupiter C12 semi-preparative column (250 x 10 mm, part No. 00G-4396-N0), eluting with a gradient of acetonitrile in water (10-18% over 24 min, flow rate 4 ml/min). TFA (0.1%) was

included in the mobile phase as the ion-pairing reagent. Subsequent removal of solvent by vacuum afforded purified NH$_2$-PEG-folate (6.0 mg, 9.4 μmol). MS (ESI+): *m/z* calcd for [C$_{29}$H$_{42}$N$_9$O$_8$]$^+$ [M + H]$^+$: 644.315, found: 644.3; and *m/z* calcd for [C$_{29}$H$_{43}$N$_9$O$_8$]$^{2+}$ [M + 2H]$^{2+}$: 322.661, found: 322.6.

To a solution of *exo*-**2** (3.9 mg, 12.4 μmol) in dry DMSO (200 μL), was added TEA (7 μL) and purified NH$_2$-PEG-folate (2.5 mg, 3.9 μmol). The reaction was agitated by rotation at room temperature for 15 hours. The resulting product was purified by reversed-phase HPLC using a Varian C18 analytical column (250 x 4.6 mm, part No. R0086200C5), eluting with a gradient of acetonitrile in water (10-50% over 40 min, flow rate 1 ml/min). TFA (0.1%) was included in the mobile phase as the ion-pairing reagent. Subsequent removal of solvent by vacuum afforded purified BCN-PEG-folate (0.5 mg, 16%). MS (ESI+): *m/z* calcd for [C$_{40}$H$_{54}$N$_9$O$_{10}$]$^+$ [M + H]$^+$: 820.399, found: 821.3; and *m/z* calcd for [C$_{40}$H$_{55}$N$_9$O$_{10}$]$^{2+}$ [M + 2H]$^{2+}$: 410.703, found: 410.7 (Appendix 6).

Cells and viruses

All cell lines used in this work were grown at 37 ˚C in a 5% CO$_2$ environment in a humidified incubator. HEK 293T cells (gift of Dr. Soosan Ghazizadeh, Stony Brook University) were maintained at low passage in Dulbecco's modified Eagle's medium (DMEM) with 10% fetal bovine serum (FBS), 100 U/ml penicillin and 100 μg/ml streptomycin. To produce VSV-G glycoprotein pseudotyped lentivirus, HEK 293T cells were seeded into 10-cm tissue culture dishes at the density of 3.3 x 10^6 cells per dish. Twenty four hours later, cells in each dish were transfected with 10 μg of pMD.G (VSV-G), 20 μg of pCMVΔR8.91, and 20 μg of pHR.EF1α.GFP.WPRE.sin (all three plasmids were gift of Dr. Soosan Ghazizadeh, Stony Brook University) using standard

calcium phosphate transfection [119]. For production of SiaNAz labeled virus, Ac4ManNAz in 50 mM stock solution was added into culture medium to the final concentration of 75 μM 7 hour after initiation of transfection. 16-18 hours after beginning of transfection, medium was removed by aspiration and cells were washed once with fresh medium before 7 ml of complete DMEM was added per dish. Again, for the production of SiaNAz labeled virus, 75 μM of Ac4ManNAz was included in culture medium. Virus containing medium was collected after another 48 hours and filtered through 0.45 μm sterile filter (VWR, Cat. No. 28145-481) to remove cell debris. Resulting virus samples was further concentrated by ultracentrifugation using a SW41 rotor for 2 hours 20 min at 25,000 rpm (82,700 g). The virus was stored at – 80 ˚C until use [114].

Sindbis virus glycoprotein pseudotyped lentivirus was produced by the same procedure, only the plasmid pMD.G (VSV-G) was replaced with the plasmid 2.2 1L1L (mutated Sindbis virus glycoprotein, gift of Dr. Irvin Chen, UCLA) [82], or the plasmid pSINmu (mutated Sindbis virus glycoprotein, gift of Dr. Pin Wang, USC) [95].

HUVEC cells were maintained at low passage in Endothelial Cell Growth Complete Medium (Lonza, Cat. No. CC-3024). U-87 MG cells were maintained at low passage in Eagle's Minimum Essential Medium (EMEM) with 10% fetal bovine serum (FBS), 100 U/ml penicillin and 100 μg/ml streptomycin. LNCaP, ID8 and 4T1 cells were maintained at low passage in RPMI-1640 Medium with 10% fetal bovine serum (FBS), 100 U/ml penicillin and 100 μg/ml streptomycin.

p24 ELISA assay

The p24 value of lentiviral vectors was obtained by an ELISA assay using the Lenti-X^{TM} p24 Rapid Titer Kit (Clontech, Cat. No. 632200), following the instruction provided in the kit. For

standard curve, a series of 2 fold dilutions of p24 protein (0 pg/ml, 12.5 pg/ml, 25 pg/ml, 50 pg/ml, 100 pg/ml, 200 pg/ml) were made with complete DMEM. To fit into the concentration range of the standards, unconcentrated virus samples were diluted 10^3 fold, and virus samples concentrated by ultracentrifugation were diluted 10^5 fold. Each dilution of standard was assayed in duplicate, and each virus sample was assayed in triplicate. Assay was read on a PerkinElmer VICTOR™ X5 Multilabel Plate Reader.

Western blotting

The BCN-PEG-FLAG peptide was used to selectively modify SiaNAz labeled lentiviruses. In each reaction, control or experimental, 16 ng p24 value of virus sample was suspended in 40 μl G1 reaction buffer (50 mM sodium citrate, pH 6.0, 10X buffer supplied with neuraminidase) and incubated in the presence or absence of 100 U of neuraminidase (New England BioLabs, Cat. No. P0720) at 37 ℃ for 1 hour. Each reaction was then run through a size-exclusion spin column (Princeton Separations, Cat. No. CS-901) equilibrated in PBS. BCN-FLAG at a final concentration of 300 μM was added into the corresponding reactions, and the total volume of each reaction was adjusted to 50 μl by PBS. The reaction mixtures were then incubated in room temperature for 6 hours before they were analyzed by electrophoresis on 10% SDS-polyacrylamide gels followed by western blotting. Monoclonal ANTI-FLAG® M2-Peroxidase (HRP) antibody (Sigma-Aldrich, Cat. No. A8592) was used to detect FLAG peptide labeled proteins.

Targeting assays

In the VEGFR2, $α_vβ_3$ integrin and PSMA targeting assays, 90 ng p24 value of concentrated 2.2 1L1L pseudotyped lentivirus was suspended in DMEM containing the corresponding BCN conjugated targeting reagent at a final concentration of 600 μM (stock solution: 10 mM in DMSO).

The reaction mixture therefore contained 6% DMSO originating from the stock solutions of the ligands. In negative controls, equal amount of DMSO instead of ligand stock was included in the reaction. Each reaction mixture was then incubated in room temperature for 6 hours, desalted by a size-exclusion spin column (Princeton Separations, Cat. No. CS-901) and used immediately in transduction. One-third of each reaction was used for infection of cells in one well of a 6-well plate. Cells were seeded one day prior to transduction and counted right before infection. For VEGFR targeting, 3×10^4 HUVEC cells per well were infected with 30 ng p24 value of BCN-GGATWLPPR labeled virus or corresponding negative controls for 2 hours. As a control, 300 μM of GGATWLPPR peptide was added into three wells of cells and incubated for 1 hour at 37 ˚C before infection to block cell surface receptors. For integrin $\alpha_v\beta_3$ targeting, 6×10^4 U-87 MG cells per well were infected with 30 ng p24 value of BCN-c(RGDfK) labeled virus or corresponding negative controls for 3 hours. As a control, 200 μM of c(RGDfK) peptide was added into three wells of cells and incubated for 1 hour at 37 ˚C before infection to block cell surface receptors. For PSMA targeting, 6×10^4 LNCaP cells per well were infected with 30 ng p24 value of BCN-PEG-glutamate urea labeled virus or corresponding negative controls for 3 hours. As a control, 300 μM of NH_2-PEG-glutamate-urea was added into three wells of cells and incubated for 1 hour at 37 ˚C before infection to block cell surface receptors.

In the Tie2 and FR targeting assays, the p24 titer of the stock viruses were not available. Therefore the quantity of the virus used in each reaction was determined in volume instead of p24 value.

In the Tie2 targeting assay, HUVEC cells were seeded in 6-well plates at a density of 1.2×10^4 cells/well one day prior to transduction. 29 μL of concentrated 2.2 1L1L pseudotyped lentivirus was used in each reaction, experimental or control, and incubated at room temperature

58

for 6 hours. Each sample was then desalted by a size-exclusion spin column, and used immediately in the 3 hours infection of three wells of HUVEC cells (3.6×10^4 cells/well).

In the FR targeting assays using BCN-PEG-folate, ID8 cells were cultivated in (-) folate media for two weeks, and seeded in 6-well plates at a density of 4×10^4 cells/well one day prior to transduction. 32 μL of concentrated 2.2 1L1L pseudotyped lentivirus was used in each reaction, experimental or control, and incubated at room temperature for 5 hours. Each sample was then desalted by a size-exclusion spin column, and used immediately in the 2-hour infection of three wells of ID8 cells (9.4×10^4 cells/well). As a control, 10 μM of folic acid was added into three wells, and cells were incubated for 1 hour at 37 ˚C before infection to block cell surface receptors.

In the FR targeting assays using alkyne-PEG-folate, 4T1 cells were cultivated in (-) folate media for two weeks, and then seeded in 6-well plates at a density of 5×10^4 cells/well one day prior to transduction. 50 μL of concentrated SINmu pseudotyped lentivirus was suspended in a reaction mixture (total vol. 100 μL) containing tris (100 mM, pH 8.0), bathophenanthroline disulfonic acid disodium salt (3 mM) and alkyne-PEG-folate (300 μM or 0 μM). Each reaction mixture was kept in a deoxygenated glove bag for 12 hours to ensure full exclusion of oxygen before CuBr (1 mM) was added, followed by incubation at room temperature for another 6 hours in deoxygenated atmosphere. Each sample was then desalted by a size-exclusion spin column, and used immediately in the 3 hours infection of three wells of 4T1 cells (5×10^4 cells/well).

In the FR targeting assays using phosphine-PEG-folate, ID8 cells were cultivated in (-) folate media for two weeks, and seeded in 6-well plates at a density of 3.5×10^4 cells/well one day prior to transduction. 50 μL of concentrated SINmu pseudotyped lentivirus was used in each reaction with phosphine-PEG-folate. Reaction mixtures were incubated at room temperature for 5

hours. Each sample was then desalted by a size-exclusion spin column, and used immediately in the 3 hours infection of three wells of ID8 cells (6×10^4 cells/well). As a control, 20 μM of folic acid was added into six wells, three for SiaNAz (+) viruses and three for SiaNAz (-), and cells were incubated for 1 hour at 37 ˚C before infection to block cell surface receptors.

In all assays, transduced cells were harvested 2 days after infection and analyzed by flow cytometry detecting expression of the GFP transgene.

Chapter 4. Surface modification of adeno-associated virus type 2 vectors via metabolically introduced azidohomoalanine

4.1 Introduction

4.1.1 The biology of AAV

Adeno-associated virus (AAV) is a small, nonenveloped virus that contains a single stranded DNA genome of approximately 4.7 kb [188-190]. It is a member of the family *Parvoviridae* and is designated in the genus *Dependovirus* due to the requirement of a helper virus such as adenovirus or herpesvirus for productive infection [191-193]. In the absence of helper viruses or helper functions, the viral DNA can be site-specifically integrated into the host chromosomal genome to establish a latent infection [194]. Numerous serotypes of AAV with differences in cellular tropism have been identified, among which the AAV serotype 2 (AAV-2) is the best characterized and most commonly used to construct recombinant AAV (rAAV) vectors [195-198].

The AAV genome contains two open reading frames (ORF), *rep* and *cap*, flanked by inverted terminal repeats (ITRs) [189] (Figure 4-1). The ITRs are essential for viral genome replication, integration, packaging, transcription and negative regulation under nonpermissive conditions [199-202]. The *rep* gene encodes four regulatory proteins called Rep78, Rep68, Rep52 and Rep40, which are involved in viral DNA replication, transcriptional control, site-specific integration processes and encapsidation of AAV genome [203-206]. Expression of Rep78 and Rep68 is driven by the promoter P5, whereas expression of Rep52 and Rep40 is driven by the promoter P19. The *cap* gene produces three viral capsid proteins (VP1, VP2, and VP3) using the

P40 promoter [196, 197]. These capsid proteins differ from each other at the N terminus as a result of alternative splicing and the use of an atypical start codon. The unspliced transcript produces VP1 (87 kDa), the largest of the capsid proteins. The spliced transcript produces VP2 (72 kDa) using a non-conventional start codon (ACG), whereas VP3 (62 kDa) is produced using a downstream conventional codon (AUG). VP1, VP2 and VP3 assemble in a molar ratio of 1:1:10 to form a viral capsid with 60 subunits arranged into an icosahedral structure [207].
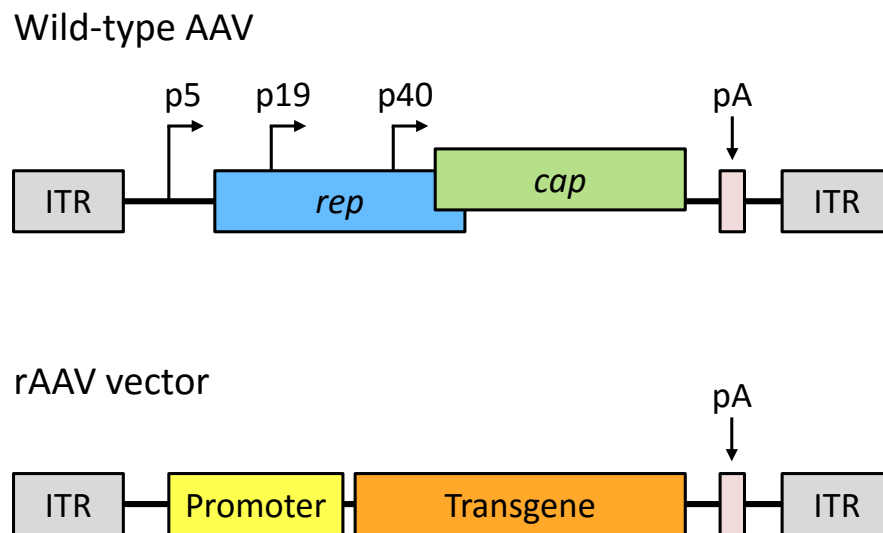
Figure 4-1. Genomic organization of wild type AAV and rAAV vectors.

The wild-type AAV genome consists of the viral genes *rep* and *cap* coding for the four Rep proteins (Rep78, Rep68, Rep52 and Rep40) and three capsid proteins (VP1, VP2 and VP3), the AAV promoters (p5, p19 and p40), the inverted terminal repeats (ITRs) and the polyadenylation site (pA). The p5 and p19 promoters regulate the transcription of the Rep proteins, whereas p40 controls expression of the VPs. In rAAV vectors, the viral *rep* and *cap* genes are replaced by a transgene cassette carrying the transgene and the respective eukaryotic promoter.

4.1.2 AAV-based gene vectors

AAV represents one of the most promising viral vector systems for gene therapy due to its many advantages: non-pathogenicity, relatively low immunogenicity, the ability to infect both dividing and non-dividing cells, persistent transgene expression, potential site-specific integration

without known side effects and many available serotypes [195-198, 208] (Table 4-1). AAV vectors have become increasingly common in clinical trials for gene therapy of many diseases such as cystic fibrosis [209], hemophilia B [210], muscular dystrophy [211] and Parkinson's disease [212].

Table 4-1. Advantages and disadvantages of adeno-associated viral vectors

Advantages	Disadvantages
Transduce non-dividing and dividing cells	Limited transgene capacity (~5Kbp)
Parental virus apathogenic	Site-specific integration lost following REP deletion
Wide cellular tropism	
Long-term transgene expression	
Potential site-specific integration	
Low immunogenicity	

Modified from reference [19].

In recombinant AAV (rAAV) vectors, the *rep* and *cap* ORFs in the wild-type viral genome are replaced by the transgene of interest and its eukaryotic promoter, leaving only the ITRs, which are the solely required *cis* elements for vector genome replication and packaging into viral particles [195-198] (Figure 4-1). The excised Rep and VP proteins can be provided in *trans* by another plasmid, which does not carry the ITR sequences [213]. Although wild-type AAV is capable of site-specific integration into the host genome on chromosome 19, the viral Rep proteins required for this integration are normally absent in current rAAV vectors. Thus, common rAAV vectors persist primarily as extrachromosomal elements (episomes), although they can also integrate into the host cell's genome at a low rate semi-randomly [214-217].

4.1.3 Engineering the AAV capsid

Despite many advantageous properties, AAV-based vectors still have problems that need to be addressed to improve the efficiency, specificity and thereby the safety for their utility in both laboratories and clinics. For example, *in vivo* application of rAAV vectors requires targeted gene delivery to specific cell types which is often limited by the virus's natural tropism. Many efforts have been made to manipulate capsid proteins to alter tropism and enhance transduction efficiency. Beside pseudotyping with the capsid of another serotype and the use of chimeric and mosaic capsids [218-222], various other rational and combinatorial targeting strategies have been developed, such as bridging with bi-specific adaptors [223, 224], chemical modification on surface lysine residues [224], and genetic introduction of a targeting peptide/protein [225-228] or an adaptor to recruit targeting ligands (e.g. an IgG binding domain to recruit antibodies) [229]. Although pseudotyping with capsids of novel AAV serotypes has extended rAAV delivery to many previously refractory cell types, it is unlikely to have a serotype with specificity toward a single cell type or tissue of interest [195]. The ratios between two serotypes in a mosaic capsid may vary from one production to another, and the mosaic capsid can potentially be inactivated by neutralizing antibodies directed against either serotype [218]. Although the bridging adaptor approach demonstrates wide substrate scope, it may require multistep procedures and the *in vivo* stability of some complexes is debatable [223, 224, 230]. Genetic modification of the AAV capsid can result in loss of virion integrity or function, and the type of motifs that can be introduced is limited. Chemical modification through the primary amino groups on lysine residues also allows access to a wide variety of effector moieties, however, efficiency is relatively low, specificity is problematic and the chemistry will be adversely affected by the presence of other nucleophiles in the sample. As a result, novel methods of viral surface functionalization that are flexible, efficient,

broadly applicable, and highly specific could aid in the development of superior AAV-based vectors.

4.1.4 Chemoselective modification of AAV vector surface via the metabolically introduced unnatural amino acid azidohomoalanine

The unnatural amino acid azidohomoalanine (Aha) can be metabolically incorporated into proteins in mammalian cells as a methionine (Met) surrogate through translational competition [30, 231]. In this work it was hypothesized that chemoselective modification of AAV vectors could be achieved through metabolic incorporation of Aha into the viral capsid. Two surface accessible methionine sites can be found on each AAV capsid protein when modeled using the program Visual Molecular Dynamics by Paul Gelfand. Residue-specific introduction of Aha into AAV capsid proteins can potentially be achieved by including Aha in methionine-depleted cell culture medium during virus production. Surface accessible Aha residues can then be selectively modified through bioorthogonal reactions such as CuAAC, SPAAC and Staudinger ligation to install various effector motifs including affinity ligands for targeted transduction (Figure 4-2).
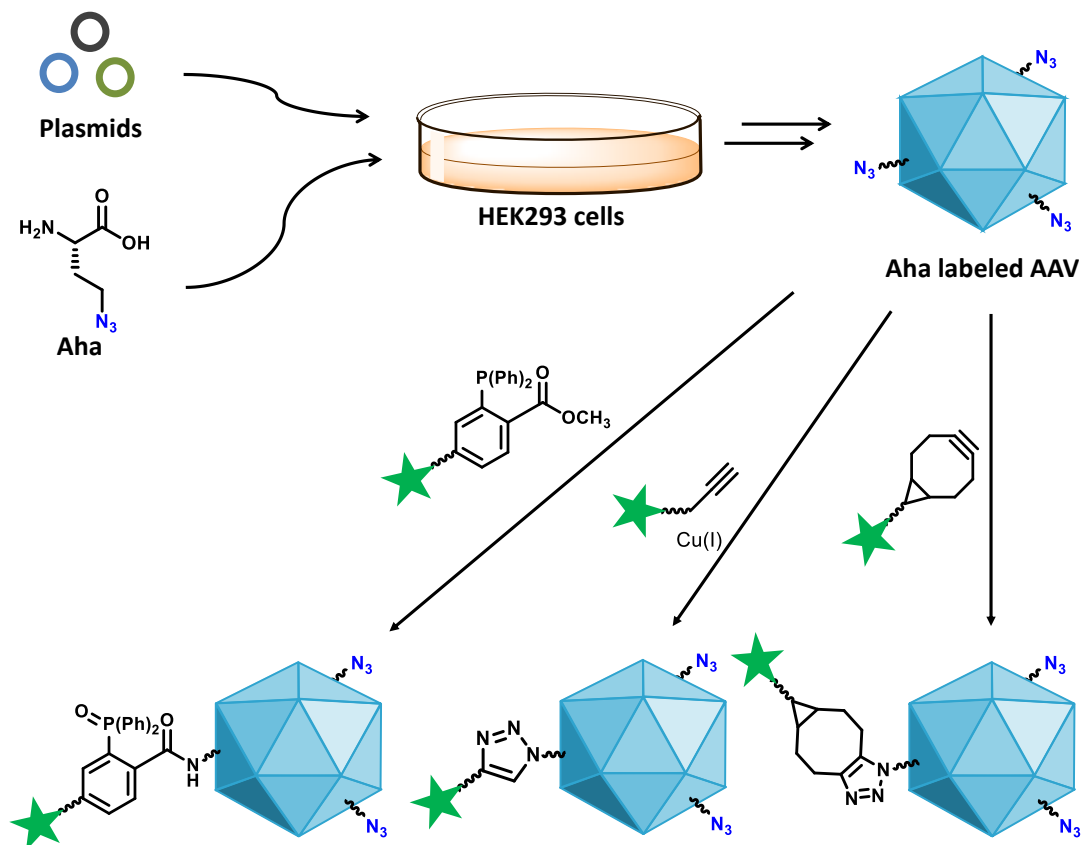
Figure 4-2. Metabolic incorporation of Aha into AAV capsid and subsequent chemoselective modification.

Residue-specific introduction of Aha into AAV capsid proteins by addition of Aha in methionine-depleted cell culture medium during virus production. Surface accessible Aha residues can then be selectively modified through bioorthogonal reactions such as Staudinger ligation, CuAAC, and SPAAC to install various effector molecules.

4.2 Results

4.2.1 Effect of Aha on viral production and transduction efficiency

To assess the effect of Aha on viral particle production and transduction efficiency, HEK293 cells were incubated for 10 hours with reconstituted DMEM containing either methionine (0.2 mM) or Aha (4 mM, 8 mM, 16 mM and 32 mM) during virus production. The resulting viruses, crude (cell lysates) or concentrated by $(NH_4)_2SO_4$ fractional precipitation, were analyzed

by quantitative real time PCR assays for the viral particle titer, and infection assays for the functional titer. With increasing concentration of Aha in the cell medium, viral particle titer and transductional titer both exhibited gradual reduction (Figure 4-3). Surprisingly, virus samples produced in the presence of 4 mM and 8 mM Aha scored higher in both assays compared to viruses produced without methionine substitution. This is possibly a result of experimental inconsistency caused by handling big numbers of samples with lengthy procedures during harvesting.
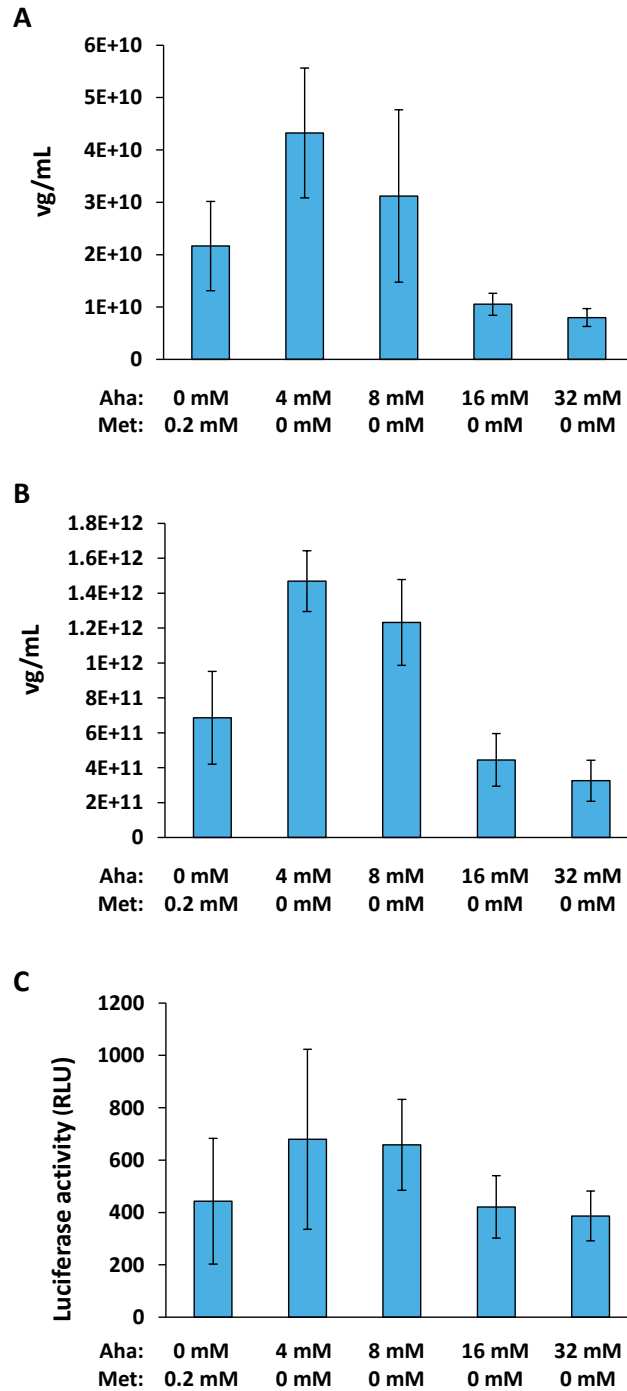
Figure 4-3. Effect of Aha on viral production and transduction efficiency.

Transfected HEK 293 cells were incubated in media containing methionine (0.2 mM) or Aha (4 mM, 8 mM, 16 mM and 32 mM) for 10 hours during virus production. Three independent productions were made for each condition. (A) Virus containing cell lysates and (B) virus samples concentrated by $(NH_4)_2SO_4$ fractional precipitation were quantified by qPCR after treatment with DNase I and proteinase K. (C) 20 μL of each concentrated virus sample was used in a 3 hour

transduction of 2 x 10^4 HeLa cells. 24 hours after transduction, cells were analyzed using the Bright-Glo™ Luciferase Assay System. Background signal by uninfected HeLa cells was subtracted from each column. For each Aha concentration the average value of all three independent productions was reported. Error bars indicate standard deviation.

4.2.2 Aha incorporation onto viral surface

To confirm Aha incorporation onto viral surface, concentrated AAV samples produced in the presence of 0 mM, 8 mM or 32 mM Aha were modified by CuAAC reactions with alkyne-PEG-FLAG. AAV capsid proteins were then immunoprecipitated by anti-VP1, -VP2, and -VP3 monoclonal antibody (B1) and Protein G PLUS-Agarose. After elution by boiling directly in SDS-PAGE loading buffer, capsid proteins were separated by gel and detected by silver staining, anti-FLAG tag western blotting and anti-AAV VP western blotting. As shown in Figure 4-4, anti-FLAG tag western blotting exhibited the same pattern of bands as anti-AAV VP western blotting, with slightly shifted molecular weight possibly due to addition of the charged FLAG tag to the VPs. This result suggested successful incorporation of Aha onto viral capsids. Yet, because the silver staining revealed unsatisfying purity of the VP samples, the identities of the proteins detected on the anti-FLAG tag western blotting were rendered inconclusive. AAV samples with enhanced purity may be needed for reliable confirmation of Aha incorporation.
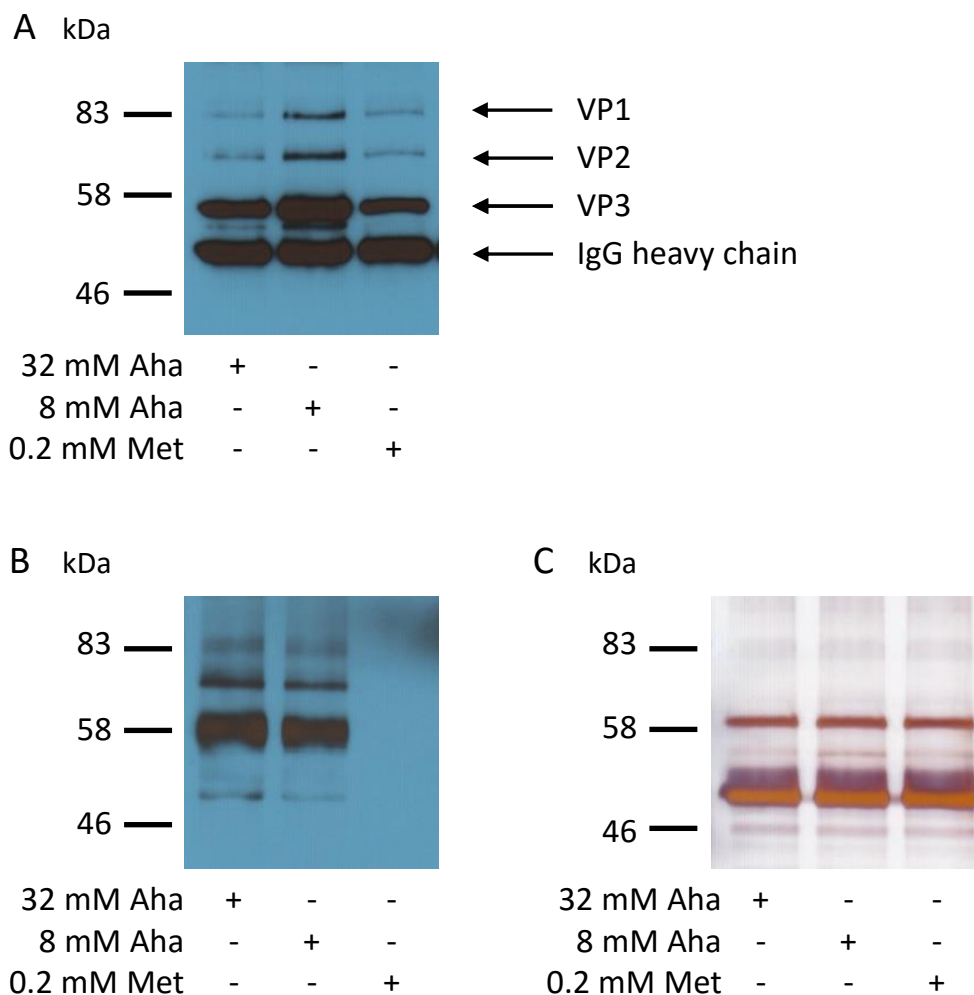
Figure 4-4. Confirming Aha incorporation onto AAV capsid.

Concentrated AAV samples produced in the presence of 0 mM, 8 mM or 32 mM Aha were modified by CuAAC reactions with alkyne-PEG-FLAG. AAV capsid proteins were then immunoprecipitated by anti-VP1, -VP2, and -VP3 monoclonal antibody (B1) and Protein G PLUS-Agarose. Proteins in each elution were analyzed by SDS-PAGE followed by detection using (A) anti-AAV VP western blot, (B) anti-FLAG tag western blot and (C) silver staining.

4.3 Conclusion and future direction

10 hour incubation of AAV producing HEK 293 cells with media containing Aha in the concentration rage from 4 mM to 32 mM did not cause significant negative impact on viral particle production, although viral titer gradually decrease with rising amount of Aha. Despite the drop in

viral particle count, the transduction function of the vectors did not seem to be affected. Confirmation of Aha incorporation onto viral capsid under these conditions was hindered by the presence of contaminating cellular proteins, therefore virus samples with higher purity is needed. To this end, an alternative production protocol featuring larger production scale and improved pre-purification by PEG 8000 precipitation was used to generate cleaner AAV samples. Other purification methods such as enrichment by heparin-agarose are also available. Enhanced purity will facilitate more reliable assessment of Aha incorporation by immunoblotting and mass spectrometry.

Azide groups displayed on the AAV capsid facilitate a wide variety of applications including expanded targeting, immune evasion, and visualization/tracking of viral particles by fluorescence/MRI/PET. Modification via azido sugar introduction can be widely applied to budded viruses. Many ligands capable of selective modification of azide have been developed for the lentiviral and adenoviral platform in our lab, which can be easily applied to the Aha labeled AAV vectors.

4.4 Materials and methods

Cells and viruses

HEK 293 cells were maintained at low passage in Dulbecco's modified Eagle's medium (DMEM) with 10% fetal bovine serum (FBS), 100 U/ml penicillin and 100 µg/ml streptomycin at 37 ˚C in a 5% CO_2 environment in a humidified incubator. To produce AAV-2 vectors HEK 293 cells were seeded into 15-cm tissue culture dishes at the density of 1.3×10^7 cells per dish. Twenty two hours later, the medium was replaced with 25 ml per dish of complete IMDM/10% FBS. After another 3 hours of incubation, each dish of cells were transfected with 22.5 µg of pXX6-80

(adenoviral helper plasmid), 7.5 μg of pTR-CMV-LUC (rAAV vector plasmid containing the luciferase gene), and 7.5 μg of pXR2 (AAV-2 helper plasmid) using standard calcium phosphate transfection. 14 hours after initiation of transfection, cells were washed twice with 10 ml of methionine-depleted DMEM per dish, and medium was replaced with 13 ml of reconstituted DMEM containing either methionine (0.2 mM) or Aha (4 mM, 8 mM, 16 mM or 32 mM). Medium was again replaced with complete DMEM containing 2% FBS 24 hours post-transfection, and viruses were harvested 65 hours post-transfection by lysis of cells using freeze/thaw and sonication. Three independent productions were made for each condition. Virus containing cell lysates were either used directly in quantification assays or concentrated and partially purified by $(NH_4)_2SO_4$ fractional precipitation [232].

Quantitative real time PCR assay

Virus containing cell lysates (crude/dilute virus) and concentrated virus samples were quantified by quantitative real time PCR (qPCR) after treatment with DNase I and proteinase K. A 200 bp fragment of the CMV promoter sequence was amplified by PCR. Increase of the PCR product was monitored by SYBR Green. Primers: forward 5'-GGGACTTT-CCTACTTGGCA-3', reverse 5'-GGCGGAGTTGTTACGACAT-3' [233]. Conditions used for the reactions were as follow: 1 cycle at 95 ℃ for 15 min; 45 cycles at 94 ℃ for 10 s, 55 ℃ for 20 s, and 72 ℃ for 30 s.

Transduction assay

20 μL of each concentrated virus sample was used in a 3 hour transduction of 2×10^4 HeLa cells. 24 hours after transduction, cells were analyzed using the Bright-Glo™ Luciferase Assay System. Uninfected HeLa cells were used as controls to subtracted background signal from each readout.

Confirming Aha incorporation onto viral surface using CuAAC and western blotting

Concentrated AAV samples produced in the presence of 0 mM, 8 mM or 32 mM Aha were modified by CuAAC reactions with alkyne-FLAG. Each virus sample was suspended in a reaction mixture containing tris (100mM, pH 8.0), bathophenanthroline disulfonic acid disodium salt (final conc. 1 mM, MP Biomedicals, Cat. No. 150112) and alkyne-FLAG (final conc. 600 μM). Each reaction mixture was kept in a deoxygenated glove bag for 12 hours to ensure full exclusion of oxygen, before CuBr (final conc. 1 mM, Alfa Aecar, Cat. No. 40752, 50 mM stock in DMSO freshly made before reaction) was added. The reaction mixtures were then incubated for another 12 hours at room temperature in deoxygenated atmosphere. AAV capsid proteins in each reaction sample were then immunoprecipitated by anti-VP1, -VP2, and -VP3 monoclonal antibody (B1) (Acris, BM5015) and Protein G PLUS-Agarose. After elution by boiling in SDS-PAGE loading buffer, capsid proteins were analyzed by electrophoresis on 10% SDS-polyacrylamide gels followed by silver staining, and western blotting with monoclonal ANTI-FLAG® M2-Peroxidase (HRP) antibody (Sigma-Aldrich, Cat. No. A8592) to detect FLAG tag labeled proteins, or with anti-VP1, -VP2, and -VP3 monoclonal antibody (B1) to detect AAV VP proteins.

References

1. Kay, M.A. State-of-the-art gene-based therapies: the road ahead. *Nature Reviews Genetics* **12**, 316-328 (2011).

2. Blaese, R.M. The ADA human gene therapy clinical protocol. *Human Gene Therapy* **1**, 327-362 (1990).

3. Rosenberg, S.A., Aebersold, P., Cornetta, K., Kasid, A., Morgan, R.A., Moen, R., Karson, E.M., Lotze, M.T., Yang, J.C., Topalian, S.L., Merino, M.J., Culver, K., Miller, A.D., Blaese, R.M. & Anderson, W.F. Gene transfer into humans — immunotherapy of patients with advanced melanoma, using tumor-infiltrating lymphocytes modified by retroviral gene transduction. *New England Journal of Medicine* **323**, 570-578 (1990).

4. Cevher, E., Çağlar, E.Ş. & Sezer, A.D. Gene delivery systems: recent progress in viral and non-viral therapy (2012).

5. Newman, C.M.H. & Bettinger, T. Gene therapy progress and prospects: Ultrasound for gene transfer. *Gene Therapy* **14**, 465-475 (2007).

6. Mehier-Humbert, S. & Guy, R.H. Physical methods for gene transfer: improving the kinetics of gene delivery into cells. *Advanced Drug Delivery Reviews* **57**, 733-753 (2005).

7. Wells, D.J. Gene therapy progress and prospects: electroporation and other physical methods. *Gene Therapy* **11**, 1363-1369 (2004).

8. Plank, C., Schillinger, U., Scherer, F., Bergemann, C., Remy, J.S., Krotz, F., Anton, M., Lausier, J. & Rosenecker, J. The magnetofection method: Using magnetic force to enhance gene delivery. *Biological Chemistry* **384**, 737-747 (2003).

9. Mintzer, M.A. & Simanek, E.E. Nonviral vectors for gene delivery. *Chemical Reviews* **109**, 259-302 (2009).

10. Li, W. & Szoka, F., Jr. Lipid-based nanoparticles for nucleic acid delivery. *Pharmaceutical Research* **24**, 438-449 (2007).

11. Pack, D.W., Hoffman, A.S., Pun, S. & Stayton, P.S. Design and development of polymers for gene delivery. *Nature Reviews Drug Discovery* **4**, 581-593 (2005).

12. Thomas, M. & Klibanov, A.M. Non-viral gene therapy: polycation-mediated DNA delivery. *Applied Microbiology and Biotechnology* **62**, 27-34 (2003).

13. Lee, C.C., MacKay, J.A., Frechet, J.M.J. & Szoka, F.C. Designing dendrimers for biological applications. *Nature Biotechnology* **23**, 1517-1526 (2005).

14. Discher, D.E. & Ahmed, F. Polymersomes. *Annual Review of Biomedical Engineering* **8**, 323-341 (2006).

15. Martin, M. & Rice, K. Peptide-guided gene delivery. *The AAPS Journal* **9**, E18-E29 (2007).

16. Sokolova, V. & Epple, M. Inorganic nanoparticles as carriers of nucleic acids into cells. *Angewandte Chemie International Edition* **47**, 1382-1395 (2008).

17. Yin, H., Kanasty, R.L., Eltoukhy, A.A., Vegas, A.J., Dorkin, J.R. & Anderson, D.G. Non-viral vectors for gene-based therapy. *Nature Reviews Genetics* **15**, 541-555 (2014).

18. He, C.-X., Tabata, Y. & Gao, J.-Q. Non-viral gene delivery carrier and its three-dimensional transfection system. *International Journal of Pharmaceutics* **386**, 232-242 (2010).

19. Vannucci, L., Lai, M., Chiuppesi, F., Ceccherini-Nelli, L. & Pistello, M. Viral vectors: a look back and ahead on gene transfer technology. *New Microbiologica* **36**, 1-22 (2013).

20. Baum, C., Kustikova, O., Modlich, U., Li, Z. & Fehse, B. Mutagenesis and oncogenesis by chromosomal insertion of gene transfer vectors. *Human Gene Therapy* **17**, 253-263 (2006).

21. Bessis, N., GarciaCozar, F.J. & Boissier, M.C. Immune responses to gene therapy vectors: influence on vector function and effector mechanisms. *Gene Therapy* **11**, S10-S17 (2004).

22. Waehler, R., Russell, S.J. & Curiel, D.T. Engineering targeted viral vectors for gene therapy. *Nature Reviews Genetics* **8**, 573-587 (2007).

23. Thomas, C.E., Ehrhardt, A. & Kay, M.A. Progress and problems with the use of viral vectors for gene therapy. *Nature Reviews Genetics* **4**, 346-358 (2003).

24. Bouard, D., Alazard-Dany, N. & Cosset, F.L. Viral vectors: from virology to transgene expression. *British Journal of Pharmacology* **157**, 153-165 (2009).

25. Zheng, M.M., Zheng, L., Zhang, P.Y., Li, J.B. & Zhang, Y. Development of bioorthogonal reactions and their applications in bioconjugation. *Molecules* **20**, 3190-3205 (2015).

26. McKay, C.S. & Finn, M.G. Click chemistry in complex mixtures: bioorthogonal bioconjugation. *Chemistry & Biology* **21**, 1075-1101 (2014).

27. Ramil, C.P. & Lin, Q. Bioorthogonal chemistry: strategies and recent developments. *Chemical Communications* **49**, 11007-11022 (2013).

28. Rao, H., Tanpure, A.A., Sawant, A.A. & Srivatsan, S.G. Enzymatic incorporation of an azide-modified UTP analog into oligoribonucleotides for post-transcriptional chemical functionalization. *Nature Protocols* **7**, 1097-1112 (2012).

29. Dube, D.H. & Bertozzi, C.R. Metabolic oligosaccharide engineering as a tool for glycobiology. *Current Opinion in Chemical Biology* **7**, 616-625 (2003).

30. Dieterich, D.C., Link, A.J., Graumann, J., Tirrell, D.A. & Schuman, E.M. Selective identification of newly synthesized proteins in mammalian cells using bioorthogonal noncanonical amino acid tagging (BONCAT). *Proceedings of the National Academy of Sciences of the United States of America* **103**, 9482-9487 (2006).

31. Davis, L. & Chin, J.W. Designer proteins: applications of genetic code expansion in cell biology. *Nature Reviews Molecular Cell Biology* **13**, 168-182 (2012).

32. Liu, C.C. & Schultz, P.G. Adding new chemistries to the genetic code. *Annual Review of Biochemistry* **79**, 413-444 (2010).

33. Prescher, J.A. & Bertozzi, C.R. Chemistry in living systems. *Nature Chemical Biology* **1**, 13-21 (2005).

34. Hang, H.C., Yu, C., Kato, D.L. & Bertozzi, C.R. A metabolic labeling approach toward proteomic analysis of mucin-type O-linked glycosylation. *Proceedings of the National Academy of Sciences of the United States of America* **100**, 14846-14851 (2003).

35. Saxon, E. & Bertozzi, C.R. Cell surface engineering by a modified Staudinger reaction. *Science* **287**, 2007-2010 (2000).

36. Rostovtsev, V.V., Green, L.G., Fokin, V.V. & Sharpless, K.B. A stepwise huisgen cycloaddition process: copper(I)-catalyzed regioselective "ligation" of azides and terminal alkynes. *Angewandte Chemie* **114**, 2708-2711 (2002).

37. Agard, N.J., Prescher, J.A. & Bertozzi, C.R. A strain-promoted [3 + 2] azide-alkyne cycloaddition for covalent modification of biomolecules in living systems. *Journal of the American Chemical Society* **126**, 15046-15047 (2004).

38. Blackman, M.L., Royzen, M. & Fox, J.M. Tetrazine ligation: fast bioconjugation based on inverse-electron-demand Diels-Alder reactivity. *Journal of the American Chemical Society* **130**, 13518-13519 (2008).

39. Devaraj, N.K., Weissleder, R. & Hilderbrand, S.A. Tetrazine-based cycloadditions: application to pretargeted live cell imaging. *Bioconjugate Chemistry* **19**, 2297-2299 (2008).

40. Stockmann, H., Neves, A.A., Stairs, S., Brindle, K.M. & Leeper, F.J. Exploring isonitrile-based click chemistry for ligation with biomolecules. *Organic & Biomolecular Chemistry* **9**, 7303-7305 (2011).

41. Yang, J., Šečkutė, J., Cole, C.M. & Devaraj, N.K. Live-cell imaging of cyclopropene tags with fluorogenic tetrazine cycloadditions. *Angewandte Chemie International Edition* **51**, 7476-7479 (2012).

42. Kaya, E., Vrabel, M., Deiml, C., Prill, S., Fluxa, V.S. & Carell, T. A genetically encoded norbornene amino acid for the mild and selective modification of proteins in a copper-free click reaction. *Angewandte Chemie International Edition* **51**, 4466-4469 (2012).

43.   Song, W., Wang, Y., Qu, J., Madden, M.M. & Lin, Q. A photoinducible 1,3-dipolar cycloaddition reaction for rapid, selective modification of tetrazole-containing proteins. *Angewandte Chemie International Edition* **47**, 2832-2835 (2008).

44.   Yu, Z., Pan, Y., Wang, Z., Wang, J. & Lin, Q. Genetically encoded cyclopropene directs rapid, photoclick-chemistry-mediated protein labeling in mammalian cells. *Angewandte Chemie International Edition* **51**, 10600-10604 (2012).

45.   McKay, C.S., Moran, J. & Pezacki, J.P. Nitrones as dipoles for rapid strain-promoted 1,3-dipolar cycloadditions with cyclooctynes. *Chemical Communications* **46**, 931-933 (2010).

46.   Debets, M.F., van Hest, J.C.M. & Rutjes, F.P.J.T. Bioorthogonal labelling of biomolecules: new functional handles and ligation methods. *Organic & Biomolecular Chemistry* **11**, 6439-6455 (2013).

47.   Patterson, D.M., Nazarova, L.A. & Prescher, J.A. Finding the right (bioorthogonal) chemistry. *ACS Chemical Biology* **9**, 592-605 (2014).

48.   van Berkel, S.S., Dirks, A.J., Debets, M.F., van Delft, F.L., Cornelissen, J.J.L.M., Nolte, R.J.M. & Rutjes, F.P.J.T. Metal-free triazole formation as a tool for bioconjugation. *ChemBioChem* **8**, 1504-1508 (2007).

49.   Walther, W. & Stein, U. Viral vectors for gene transfer - A review of their use in the treatment of human diseases. *Drugs* **60**, 249-271 (2000).

50.   Gendelman, H.E., Narayan, O., Molineaux, S., Clements, J.E. & Ghotbi, Z. Slow, persistent replication of lentiviruses: role of tissue macrophages and macrophage precursors in bone marrow. *Proceedings of the National Academy of Sciences of the United States of America* **82**, 7086-7090 (1985).

51.   Bukrinsky, M.I., Haggerty, S., Dempsey, M.P., Sharova, N., Adzhubei, A., Spitz, L., Lewis, P., Goldfarb, D., Emerman, M. & Stevenson, M. A nuclear localization signal within HIV-1 matrix protein that governs infection of non-dividing cells. *Nature* **365**, 666-669 (1993).

52.   Freed, E.O. & Martin, M.A. HIV-1 infection of non-dividing cells. *Nature* **369**, 107-108 (1994).

53.   Naldini, L., Blömer, U., Gallay, P., Ory, D., Mulligan, R., Gage, F.H., Verma, I.M. & Trono, D. In vivo gene delivery and stable transduction of nondividing cells by a lentiviral vector. *Science* **272**, 263-267 (1996).

54.   Bukrinsky, M. A hard way to the nucleus. *Molecular Medicine* **10**, 1-5 (2004).

55.   Curran, M.A., Kaiser, S.M., Achacoso, P.L. & Nolan, G.P. Efficient transduction of nondividing cells by optimized feline immunodeficiency virus vectors. *Molecular Therapy* **1**, 31-38 (2000).

56. Poeschla, E.M., Wong-Staal, F. & Looney, D.J. Efficient transduction of nondividing human cells by feline immunodeficiency virus lentiviral vectors. *Nature Medicine* **4**, 354-357 (1998).

57. Mitrophanous, K.A., Yoon, S., Rohll, J.B., Patil, D., Wilkes, F.J., Kim, V.N., Kingsman, S.M., Kingsman, A.J. & Mazarakis, N.D. Stable gene transfer to the nervous system using a non-primate lentiviral vector. *Gene Therapy* **6**, 1808-1818 (1999).

58. Mangeot, P.-E., Nègre, D., Dubois, B., Winter, A.J., Leissner, P., Mehtali, M., Kaiserlian, D., Cosset, F.-L. & Darlix, J.-L. Development of minimal lentivirus vectors derived from simian immunodeficiency virus (SIVmac251) and their use for gene transfer into human dendritic cells. *Journal of Virology* **74**, 8307-8315 (2000).

59. Sakuma, T., Barry, M.A. & Ikeda, Y. Lentiviral vectors: basic to translational. *Biochemical Journal* **443**, 603-618 (2012).

60. Dropulic, B. Lentiviral vectors: their molecular design, safety, and use in laboratory and preclinical research. *Human Gene Therapy* **22**, 649-657 (2011).

61. Joshi, S. & Joshi, R.L. Molecular biology of human immunodeficiency virus Type-1. *Transfusion Science* **17**, 351-378 (1996).

62. Nielsen, M.H., Pedersen, F.S. & Kjems, J. Molecular strategies to inhibit HIV-1 replication. *Retrovirology* **2**, 10-10 (2005).

63. Cronin, J., Zhang, X.Y. & Reiser, J. Altering the tropism of lentiviral vectors through pseudotyping. *Current Gene Therapy* **5**, 387-398 (2005).

64. Emeagi, P.U., Goyvaerts, C., Maenhout, S., Pen, J., Thielemans, K. & Breckpot, K. Lentiviral vectors: a versatile tool to fight cancer. *Current Molecular Medicine* **13**, 602-625 (2013).

65. Montini, E., Cesana, D., Schmidt, M., Sanvito, F., Bartholomae, C.C., Ranzani, M., Benedicenti, F., Sergi, L.S., Ambrosi, A., Ponzoni, M., Doglioni, C., Di Serio, C., von Kalle, C. & Naldini, L. The genotoxic potential of retroviral vectors is strongly modulated by vector design and integration site selection in a mouse model of HSC gene therapy. *The Journal of Clinical Investigation* **119**, 964-975 (2009).

66. Montini, E., Cesana, D., Schmidt, M., Sanvito, F., Ponzoni, M., Bartholomae, C., Sergi, L.S., Benedicenti, F., Ambrosi, A., Di Serio, C., Doglioni, C., von Kalle, C. & Naldini, L. Hematopoietic stem cell gene transfer in a tumor-prone mouse model uncovers low genotoxicity of lentiviral vector integration. *Nature Biotechnology* **24**, 687-696 (2006).

67. De Meyer, S.F., Vanhoorelbeke, K., Chuah, M.K., Pareyn, I., Gillijns, V., Hebbel, R.P., Collen, D., Deckmyn, H. & VandenDriessche, T. Phenotypic correction of von Willebrand disease type 3 blood-derived endothelial cells with lentiviral vectors expressing von Willebrand factor. *Blood* **107**, 4728-4736 (2006).

68. Naldini, L. Lentiviruses as gene transfer agents for delivery to non-dividing cells. *Current Opinion in Biotechnology* **9**, 457-463 (1998).

69. Wagemaker, G. Lentiviral hematopoietic stem cell gene therapy in inherited metabolic disorders. *Human Gene Therapy* **25**, 862-865 (2014).

70. Leyva, F., Anzinger, J., McCoy, J.P. & Kruth, H. Evaluation of transduction efficiency in macrophage colony-stimulating factor differentiated human macrophages using HIV-1 based lentiviral vectors. *BMC Biotechnology* **11**, 13 (2011).

71. Hutson, T.H., Foster, E., Moon, L.D.F. & Yáñez-Muñoz, R.J. Lentiviral vector-mediated RNA silencing in the central nervous system. *Human Gene Therapy Methods* **25**, 14-32 (2014).

72. Liechtenstein, T., Perez-Janices, N. & Escors, D. Lentiviral vectors for cancer immunotherapy and clinical applications. *Cancers* **5**, 815-837 (2013).

73. Cartier, N., Hacein-Bey-Abina, S., Bartholomae, C.C., Veres, G., Schmidt, M., Kutschera, I., Vidaud, M., Abel, U., Dal-Cortivo, L., Caccavelli, L., Mahlaoui, N., Kiermer, V., Mittelstaedt, D., Bellesme, C., Lahlou, N., Lefrère, F., Blanche, S., Audit, M., Payen, E., Leboulch, P., l'Homme, B., Bougnères, P., Von Kalle, C., Fischer, A., Cavazzana-Calvo, M. & Aubourg, P. Hematopoietic stem cell gene therapy with a lentiviral vector in X-linked adrenoleukodystrophy. *Science* **326**, 818-823 (2009).

74. Cavazzana-Calvo, M., Payen, E., Negre, O., Wang, G., Hehir, K., Fusil, F., Down, J., Denaro, M., Brady, T., Westerman, K., Cavallesco, R., Gillet-Legrand, B., Caccavelli, L., Sgarra, R., Maouche-Chretien, L., Bernaudin, F., Girot, R., Dorazio, R., Mulder, G.-J., Polack, A., Bank, A., Soulier, J., Larghero, J., Kabbara, N., Dalle, B., Gourmel, B., Socie, G., Chretien, S., Cartier, N., Aubourg, P., Fischer, A., Cornetta, K., Galacteros, F., Beuzard, Y., Gluckman, E., Bushman, F., Hacein-Bey-Abina, S. & Leboulch, P. Transfusion independence and HMGA2 activation after gene therapy of human β-thalassaemia. *Nature* **467**, 318-322 (2010).

75. Kalos, M., Levine, B.L., Porter, D.L., Katz, S., Grupp, S.A., Bagg, A. & June, C.H. T cells with chimeric antigen receptors have potent antitumor effects and can establish memory in patients with advanced leukemia. *Science Translational Medicine* **3**, 95ra73 (2011).

76. Coutant, F., Sanchez David, R.Y., Félix, T., Boulay, A., Caleechurn, L., Souque, P., Thouvenot, C., Bourgouin, C., Beignon, A.-S. & Charneau, P. A nonintegrative lentiviral vector-based vaccine provides long-term sterile protection against malaria. *Plos One* **7**, e48644 (2012).

77. Tebas, P., Stein, D., Binder-Scholl, G., Mukherjee, R., Brady, T., Rebello, T., Humeau, L., Kalos, M., Papasavvas, E., Montaner, L.J., Schullery, D., Shaheen, F., Brennan, A.L., Zheng, Z., Cotte, J., Slepushkin, V., Veloso, E., Mackley, A., Hwang, W.-T., Aberra, F., Zhan, J., Boyer, J., Collman, R.G., Bushman, F.D., Levine, B.L. & June, C.H. Antiviral effects of autologous CD4 T cells genetically modified with a conditionally replicating lentiviral vector expressing long antisense to HIV. *Blood* **121**, 1524-1533 (2013).

78. Manjunath, N., Wu, H., Subramanya, S. & Shankar, P. Lentiviral delivery of short hairpin RNAs. *Advanced Drug Delivery Reviews* **61**, 732-745 (2009).

79. Sumimoto, H. & Kawakami, Y. Lentiviral vector-mediated RNAi and its use for cancer research. *Future Oncology* **3**, 655-664 (2007).

80. Hu, B., Tai, A. & Wang, P. Immunization delivered by lentiviral vectors for cancer and infectious diseases. *Immunological Reviews* **239**, 45-61 (2011).

81. Morizono, K., Xie, Y., Ringpis, G.-E., Johnson, M., Nassanian, H., Lee, B., Wu, L. & Chen, I.S.Y. Lentiviral vector retargeting to P-glycoprotein on metastatic melanoma through intravenous injection. *Nature Medicine* **11**, 346-352 (2005).

82. Morizono, K., Pariente, N., Xie, Y. & Chen, I.S.Y. Redirecting lentiviral vectors by insertion of integrin-tageting peptides into envelope proteins. *The Journal of Gene Medicine* **11**, 549-558 (2009).

83. Morizono, K., Xie, Y., Helguera, G., Daniels, T.R., Lane, T.F., Penichet, M.L. & Chen, I.S.Y. A versatile targeting system with lentiviral vectors bearing the biotin-adaptor peptide. *The Journal of Gene Medicine* **11**, 655-663 (2009).

84. Anliker, B., Abel, T., Kneissl, S., Hlavaty, J., Caputi, A., Brynza, J., Schneider, I.C., Munch, R.C., Petznek, H., Kontermann, R.E., Koehl, U., Johnston, I.C.D., Keinanen, K., Muller, U.C., Hohenadl, C., Monyer, H., Cichutek, K. & Buchholz, C.J. Specific gene transfer to neurons, endothelial cells and hematopoietic progenitors with lentiviral vectors. *Nature Methods* **7**, 929-935 (2010).

85. Lei, Y., Joo, K.-I., Zarzar, J., Wong, C. & Wang, P. Targeting lentiviral vector to specific cell types through surface displayed single chain antibody and fusogenic molecule. *Virology Journal* **7**, 35 (2010).

86. Liang, M., Yan, M., Lu, Y.F. & Chen, I.S.Y. Retargeting vesicular stomatitis virus glycoprotein pseudotyped lentiviral vectors with enhanced stability by in situ synthesized polymer shell. *Human Gene Therapy Methods* **24**, 11-18 (2013).

87. Yu, J.H. & Schaffer, D.V. Selection of novel vesicular stomatitis virus glycoprotein variants from a peptide insertion library for enhanced purification of retroviral and lentiviral vectors. *Journal of Virology* **80**, 3285-3292 (2006).

88. Croyle, M.A., Callahan, S.M., Auricchio, A., Schumer, G., Linse, K.D., Wilson, J.M., Brunner, L.J. & Kobinger, G.P. PEGylation of a vesicular stomatitis virus G pseudotyped lentivirus vector prevents inactivation in serum. *Journal of Virology* **78**, 912-921 (2004).

89. Hwang, B.Y. & Schaffer, D.V. Engineering a serum-resistant and thermostable vesicular stomatitis virus G glycoprotein for pseudotyping retroviral and lentiviral vectors. *Gene Therapy* **20**, 807-815 (2013).

90.   Morizono, K., Bristol, G., Xie, Y.-m., Kung, S.K.-P. & Chen, I.S.Y. Antibody-directed targeting of retroviral vectors via cell surface antigens. *Journal of Virology* **75**, 8016-8020 (2001).

91.   Funke, S., Maisner, A., Muhlebach, M.D., Koehl, U., Grez, M., Cattaneo, R., Cichutek, K. & Buchholz, C.J. Targeted cell entry of lentiviral vectors. *Molecular Therapy* **16**, 1427-1436 (2008).

92.   Munch, R.C., Muhlebach, M.D., Schaser, T., Kneissl, S., Jost, C., Pluckthun, A., Cichutek, K. & Buchholz, C.J. DARPins: an efficient targeting domain for lentiviral vectors. *Molecular Therapy* **19**, 686-693 (2011).

93.   Höfig, I., Barth, S., Salomon, M., Jagusch, V., Atkinson, M.J., Anastasov, N. & Thirion, C. Systematic improvement of lentivirus transduction protocols by antibody fragments fused to VSV-G as envelope glycoprotein. *Biomaterials* **35**, 4204-4212 (2014).

94.   Lei, Y., Joo, K.-I. & Wang, P. Engineering fusogenic molecules to achieve targeted transduction of enveloped lentiviral vectors. *Journal of Biological Engineering* **3**, 8 (2009).

95.   Yang, L., Bailey, L., Baltimore, D. & Wang, P. Targeting lentiviral vectors to specific cell types in vivo. *Proceedings of the National Academy of Sciences of the United States of America* **103**, 11479-11484 (2006).

96.   Eleftheriadou, I., Trabalza, A., Ellison, S.M., Gharun, K. & Mazarakis, N.D. Specific retrograde transduction of spinal motor neurons using lentiviral vectors targeted to presynaptic NMJ receptors. *Molecular Therapy* **22**, 1285-1298 (2014).

97.   Lee, C.-L., Dang, J., Joo, K.-I. & Wang, P. Engineered lentiviral vectors pseudotyped with a CD4 receptor and a fusogenic protein can target cells expressing HIV-1 envelope proteins. *Virus Research* **160**, 340-350 (2011).

98.   Tornøe, C.W., Christensen, C. & Meldal, M. Peptidotriazoles on solid phase: [1,2,3]-triazoles by regiospecific copper(i)-catalyzed 1,3-dipolar cycloadditions of terminal alkynes to azides. *The Journal of Organic Chemistry* **67**, 3057-3064 (2002).

99.   Baskin, J.M., Prescher, J.A., Laughlin, S.T., Agard, N.J., Chang, P.V., Miller, I.A., Lo, A., Codelli, J.A. & Bertozzi, C.R. Copper-free click chemistry for dynamic in vivo imaging. *Proceedings of the National Academy of Sciences of the United States of America* **104**, 16793-16797 (2007).

100.   Sletten, E.M. & Bertozzi, C.R. A hydrophilic azacyclooctyne for Cu-free click chemistry. *Organic Letters* **10**, 3097-3099 (2008).

101.   Laughlin, S.T. & Bertozzi, C.R. Metabolic labeling of glycans with azido sugars and subsequent glycan-profiling and visualization via Staudinger ligation. *Nature Protocols* **2**, 2930-2944 (2007).

102. Chang, P.V., Chen, X., Smyrniotis, C., Xenakis, A., Hu, T., Bertozzi, C.R. & Wu, P. Metabolic labeling of sialic acids in living animals with alkynyl sugars. *Angewandte Chemie International Edition* **48**, 4030-4033 (2009).

103. Kho, Y., Kim, S.C., Jiang, C., Barma, D., Kwon, S.W., Cheng, J., Jaunbergs, J., Weinbaum, C., Tamanoi, F., Falck, J. & Zhao, Y. A tagging-via-substrate technology for detection and proteomics of farnesylated proteins. *Proceedings of the National Academy of Sciences of the United States of America* **101**, 12479-12484 (2004).

104. Neef, A.B. & Luedtke, N.W. Dynamic metabolic labeling of DNA in vivo with arabinosyl nucleosides. *Proceedings of the National Academy of Sciences of the United States of America* **108**, 20404-20409 (2011).

105. Prescher, J.A., Dube, D.H. & Bertozzi, C.R. Chemical remodelling of cell surfaces in living animals. *Nature* **430**, 873-877 (2004).

106. Luchansky, S.J., Hang, H.C., Saxon, E., Grunwell, J.R., Yu, C., Dube, D.H. & Bertozzi, C.R. in Methods in Enzymology (eds. Yuan, C.L. & Reiko, T.L.) 249-272 (Academic Press, 2003).

107. Dommerholt, J., Schmidt, S., Temming, R., Hendriks, L.J.A., Rutjes, F.P.J.T., van Hest, J.C.M., Lefeber, D.J., Friedl, P. & van Delft, F.L. Readily accessible bicyclononynes for bioorthogonal labeling and three-dimensional imaging of living cells. *Angewandte Chemie International Edition* **49**, 9422-9425 (2010).

108. Puri, A., Grimaldi, S. & Blumenthal, R. Role of viral envelope sialic acid in membrane fusion mediated by the vesicular stomatitis virus envelope glycoprotein. *Biochemistry* **31**, 10108-10113 (1992).

109. Etchison, J.R., Robertson, J.S. & Summers, D.F. Host cell-dependent differences in the oligosaccharide moieties of the VSV G protein. *Journal of General Virology* **57**, 43-52 (1981).

110. Saxon, E., Luchansky, S.J., Hang, H.C., Yu, C., Lee, S.C. & Bertozzi, C.R. Investigating cellular metabolism of synthetic azidosugars with the Staudinger ligation. *Journal of the American Chemical Society* **124**, 14893-14902 (2002).

111. Oetke, C., Hinderlich, S., Brossmer, R., Reutter, W., Pawlita, M. & Keppler, O.T. Evidence for efficient uptake and incorporation of sialic acid by eukaryotic cells. *European Journal of Biochemistry* **268**, 4553-4561 (2001).

112. Oetke, C., Brossmer, R., Mantey, L.R., Hinderlich, S., Isecke, R., Reutter, W., Keppler, O.T. & Pawlita, M. Versatile biosynthetic engineering of sialic acid in living cells using synthetic sialic acid analogues. *Journal of Biological Chemistry* **277**, 6688-6695 (2002).

113. Luchansky, S.J., Goon, S. & Bertozzi, C.R. Expanding the diversity of unnatural cell-surface sialic acids. *ChemBioChem* **5**, 371-374 (2004).

114. Kutner, R.H., Zhang, X.-Y. & Reiser, J. Production, concentration and titration of pseudotyped HIV-1-based lentiviral vectors. *Nature Protocols* **4**, 495-505 (2009).

115. Batard, P., Jordan, M. & Wurm, F. Transfer of high copy number plasmid into mammalian cells by calcium phosphate transfection. *Gene* **270**, 61-68 (2001).

116. Cannon, K.S., Hebert, D.N. & Helenius, A. Glycan-dependent and -independent Association of Vesicular Stomatitis Virus G Protein with Calnexin. *Journal of Biological Chemistry* **271**, 14280-14284 (1996).

117. Luchansky, S.J., Argade, S., Hayes, B.K. & Bertozzi, C.R. Metabolic functionalization of recombinant glycoprotein. *Biochemistry* **43**, 12358-12366 (2004).

118. Luchansky, S.J., Hang, H.C., Saxon, E., Grunwell, J.R., Danielle, C.Y., Dube, D.H. & Bertozzi, C.R. in Recognition of Carbohydrates in Biological Systems Pt A: General Procedures 249-272 (Academic Press Inc, San Diego, 2003).

119. Ghazizadeh, S., Katz, A.B., Harrington, R. & Taichman, L.B. Lentivirus-mediated gene transfer to human epidermis. *Journal of Investigative Dermatology Symposium Proceedings* **9**, 269-275 (2004).

120. von Bonsdorff, C.H. & Harrison, S.C. Sindbis virus glycoproteins form a regular icosahedral surface lattice. *Journal of Virology* **16**, 141-145 (1975).

121. Morizono, K., Ku, A., Xie, Y., Harui, A., Kung, S.K.P., Roth, M.D., Lee, B. & Chen, I.S.Y. Redirecting lentiviral vectors pseudotyped with Sindbis virus-derived envelope proteins to DC-SIGN by modification of N-linked glycans of envelope proteins. *Journal of Virology* **84**, 6923-6934 (2010).

122. Diaz, R.M., Bateman, A., Emiliusen, L., Fielding, A., Trono, D., Russell, S.J. & Vile, R.G. A lentiviral vector expressing a fusogenic glycoprotein for cancer gene therapy. *Gene Therapy* **7**, 1656-1663 (2000).

123. Huszthy, P.C., Giroglou, T., Tsinkalovsky, O., Euskirchen, P., Skaftnesmo, K.O., Bjerkvig, R., von Laer, D. & Miletic, H. Remission of invasive, cancer stem-like glioblastoma xenografts using lentiviral vector-mediated suicide gene therapy. *Plos One* **4** (2009).

124. Ravet, E., Lulka, H., Gross, F., Casteilla, L., Buscail, L. & Cordelier, P. Using lentiviral vectors for efficient pancreatic cancer gene therapy. *Cancer Gene Therapy* **17**, 315-324 (2010).

125. Breckpot, K., Aerts, J.L. & Thielemans, K. Lentiviral vectors for cancer immunotherapy: transforming infectious particles into therapeutics. *Gene Therapy* **14**, 847-862 (2007).

126. Burke, D. & Keegstra, K. Carbohydrate structure of Sindbis virus glycoprotein E2 from virus grown in hamster and chicken cells. *Journal of Virology* **29**, 546-554 (1979).

127. Carmeliet, P. Angiogenesis in life, disease and medicine. *Nature* **438**, 932-936 (2005).

128. Kowanetz, M. & Ferrara, N. Vascular endothelial growth factor signaling pathways: therapeutic perspective. *Clinical Cancer Research* **12**, 5018-5022 (2006).

129. Binetruy-Tournaire, R., Demangel, C., Malavaud, B., Vassy, R., Rouyre, S., Kraemer, M., Plouet, J., Derbin, C., Perret, G. & Mazie, J.C. Identification of a peptide blocking vascular endothelial growth factor (VEGF)-mediated angiogenesis. *The EMBO Journal* **19**, 1525-1533 (2000).

130. Martin, V., Liu, D., Fueyo, J. & Gomez-Manzano, C. Tie2: A journey from normal angiogenesis to cancer and beyond. *Histology and Histopathology* **23**, 773-780 (2008).

131. Peters, K.G., Coogan, A., Berry, D., Marks, J., Iglehart, J.D., Kontos, C.D., Rao, P., Sankar, S. & Trogan, E. Expression of Tie2/Tek in breast tumour vasculature provides a new marker for evaluation of tumour angiogenesis. *British Journal of Cancer* **77**, 51-56 (1998).

132. Takahama, M., Tsutsumi, M., Tsujiuchi, T., Nezu, K., Kushibe, K., Taniguchi, S., Kotake, Y. & Konishi, Y. Enhanced expression of Tie2, its ligand angiopoietin-1, vascular endothelial growth factor, and CD31 in human non-small cell lung carcinomas. *Clinical Cancer Research* **5**, 2506-2510 (1999).

133. Tanaka, S., Sugimachi, K., Yamashita, Y.I., Ohga, T., Shirabe, K., Shimada, M., Wands, J.R. & Sugimachi, K. Tie2 vascular endothelial receptor expression and function in hepatocellular carcinoma. *Hepatology* **35**, 861-867 (2002).

134. Lewis, C.E., De Palma, M. & Naldini, L. Tie2-expressing monocytes and tumor angiogenesis: regulation by hypoxia and angiopoietin-2. *Cancer Research* **67**, 8429-8432 (2007).

135. Zadeh, G., Qian, B.P., Okhowat, A., Sabha, N., Kontos, C.D. & Guha, A. Targeting the Tie2/Tek receptor in astrocytomas. *American Journal of Pathology* **164**, 467-476 (2004).

136. Muller, A., Lange, K., Gaiser, T., Hofmann, M., Bartels, H., Feller, A.C. & Merz, H. Expression of angiopoietin-1 and its receptor TEK in hematopoietic cells from patients with myeloid leukemia. *Leukemia Research* **26**, 163-168 (2002).

137. Schliemann, C., Bieker, R., Padro, T., Kessler, T., Hintelmann, H., Buchner, T., Berdel, W.E. & Mesters, R.M. Expression of angiopoietins and their receptor Tie2 in the bone marrow of patients with acute myeloid leukemia. *Haematologica-the Hematology Journal* **91**, 1203-1211 (2006).

138. Kukk, E., Wartiovaara, U., Gunji, Y., Kaukonen, J., Buhring, H.J., Rappold, I., Matikainen, M.T., Vihko, P., Partanen, J., Palotie, A., Alitalo, K. & Alitalo, R. Analysis of Tie receptor tyrosine kinase in haemopoietic progenitor and leukaemia cells. *British Journal of Haematology* **98**, 195-203 (1997).

139. Deng, S.J., Liu, W., Simmons, C.A., Moore, J.T. & Tian, G.C. Identifying substrates for endothelium-specific Tie-2 receptor tyrosine kinase from phage-displayed peptide libraries

for high throughput screening. *Combinatorial Chemistry & High Throughput Screening* **4**, 525-533 (2001).

140. Haubner, R., Gratias, R., Diefenbach, B., Goodman, S.L., Jonczyk, A. & Kessler, H. Structural and functional aspects of RGD-containing cyclic pentapeptides as highly potent and selective integrin αVβ3 antagonists. *Journal of the American Chemical Society* **118**, 7461-7472 (1996).

141. Dai, X., Su, Z. & Liu, J.O. An improved synthesis of a selective αvβ3-integrin antagonist cyclo(-RGDfK-). *Tetrahedron Letters* **41**, 6295-6298 (2000).

142. Wright Jr, G.L., Haley, C., Beckett, M.L. & Schellhammer, P.F. Expression of prostate-specific membrane antigen in normal, benign, and malignant prostate tissues. *Urologic Oncology: Seminars and Original Investigations* **1**, 18-28 (1995).

143. Kawakami, M. & Nakayama, J. Enhanced expression of prostate-specific membrane antigen gene in prostate cancer as revealed by in situ hybridization. *Cancer Research* **57**, 2321-2324 (1997).

144. Silver, D.A., Pellicer, I., Fair, W.R., Heston, W.D. & Cordon-Cardo, C. Prostate-specific membrane antigen expression in normal and malignant human tissues. *Clinical Cancer Research* **3**, 81-85 (1997).

145. Chang, S.S., O'Keefe, D.S., Bacich, D.J., Reuter, V.E., Heston, W.D.W. & Gaudin, P.B. Prostate-specific membrane antigen is produced in tumor-associated neovasculature. *Clinical Cancer Research* **5**, 2674-2681 (1999).

146. Kozikowski, A.P., Zhang, J., Nan, F., Petukhov, P.A., Grajkowska, E., Wroblewski, J.T., Yamamoto, T., Bzdega, T., Wroblewska, B. & Neale, J.H. Synthesis of urea-based inhibitors as active site probes of glutamate carboxypeptidase II: efficacy as analgesic agents. *Journal of Medicinal Chemistry* **47**, 1729-1738 (2004).

147. Murelli, R.P., Zhang, A.X., Michel, J., Jorgensen, W.L. & Spiegel, D.A. Chemical control over immune recognition: a class of antibody-recruiting small molecules that target prostate cancer. *Journal of the American Chemical Society* **131**, 17090-17092 (2009).

148. Gonen, N. & Assaraf, Y.G. Antifolates in cancer therapy: Structure, activity and mechanisms of drug resistance. *Drug Resistance Updates* **15**, 183-210 (2012).

149. Assaraf, Y.G., Leamon, C.P. & Reddy, J.A. The folate receptor as a rational therapeutic target for personalized cancer treatment. *Drug Resistance Updates* **17**, 89-95 (2014).

150. Zhao, R. & Goldman, I.D. The proton-coupled folate transporter: Physiological and pharmacological roles. *Current Opinion in Pharmacology* **13**, 875-880 (2013).

151. Desmoulin, S.K., Hou, Z., Gangjee, A. & Matherly, L.H. The human proton-coupled folate transporter: Biology and therapeutic applications to cancer. *Cancer Biology & Therapy* **13**, 1355-1373 (2012).

152. Qiu, A., Jansen, M., Sakaris, A., Min, S.H., Chattopadhyay, S., Tsai, E., Sandoval, C., Zhao, R., Akabas, M.H. & Goldman, I.D. Identification of an intestinal folate transporter and the molecular basis for hereditary folate malabsorption. *Cell* **127**, 917-928 (2006).

153. Zhao, R. & Goldman, I.D. The molecular identity and characterization of a Proton-Coupled Folate Transporter—PCFT; biological ramifications and impact on the activity of pemetrexed. *Cancer and Metastasis Reviews* **26**, 129-139 (2007).

154. Nakai, Y., Inoue, K., Abe, N., Hatakeyama, M., Ohta, K.-y., Otagiri, M., Hayashi, Y. & Yuasa, H. Functional characterization of human proton-coupled folate transporter/heme carrier protein 1 heterologously expressed in mammalian cells as a folate transporter. *Journal of Pharmacology and Experimental Therapeutics* **322**, 469-476 (2007).

155. Matherly, L., Hou, Z. & Deng, Y. Human reduced folate carrier: translation of basic biology to cancer etiology and therapy. *Cancer and Metastasis Reviews* **26**, 111-128 (2007).

156. Della-Longa, S. & Arcovito, A. Structural and functional insights on folate receptor a (FRa) by homology modeling, ligand docking and molecular dynamics. *Journal of Molecular Graphics and Modelling* **44**, 197-207 (2013).

157. Elnakat, H. & Ratnam, M. Role of folate receptor genes in reproduction and related cancers. *Frontiers in Bioscience* **11**, 506-519 (2006).

158. Parker, N., Turk, M.J., Westrick, E., Lewis, J.D., Low, P.S. & Leamon, C.P. Folate receptor expression in carcinomas and normal tissues determined by a quantitative radioligand binding assay. *Analytical Biochemistry* **338**, 284-293 (2005).

159. Low, P.S., Henne, W.A. & Doorneweerd, D.D. Discovery and development of folic-acid-based receptor targeting for imaging and therapy of cancer and inflammatory diseases. *Accounts of Chemical Research* **41**, 120-129 (2008).

160. Hilgenbrink, A.R. & Low, P.S. Folate receptor-mediated drug targeting: from therapeutics to diagnostics. *Journal of Pharmaceutical Sciences* **94**, 2135-2146 (2005).

161. Low, P.S. & Kularatne, S.A. Folate-targeted therapeutic and imaging agents for cancer. *Current Opinion in Chemical Biology* **13**, 256-262 (2009).

162. Rijnboutt, S., Jansen, G., Posthuma, G., Hynes, J.B., Schornagel, J.H. & Strous, G.J. Endocytosis of GPI-linked membrane folate receptor-alpha. *Journal of Cell Biology* **132**, 35-47 (1996).

163. Sabharanjak, S. & Mayor, S. Folate receptor endocytosis and trafficking. *Advanced Drug Delivery Reviews* **56**, 1099-1109 (2004).

164. Elnakat, H. & Ratnam, M. Distribution, functionality and gene regulation of folate receptor isoforms: implications in targeted therapy. *Advanced Drug Delivery Reviews* **56**, 1067-1084 (2004).

165. Chancy, C.D., Kekuda, R., Huang, W., Prasad, P.D., Kuhnel, J.-M., Sirotnak, F.M., Roon, P., Ganapathy, V. & Smith, S.B. Expression and differential polarization of the reduced-folate transporter-1 and the folate receptor alpha in mammalian retinal pigment epithelium. *Journal of Biological Chemistry* **275**, 20676-20684 (2000).

166. Weitman, S.D., Lark, R.H., Coney, L.R., Fort, D.W., Frasca, V., Zurawski Jr, V.R. & Kamen, B.A. Distribution of the folate receptor GP38 in normal and malignant cell lines and tissues. *Cancer Research* **52**, 3396-3401 (1992).

167. Reddy, J.A., Haneline, L.S., Srour, E.F., Antony, A.C., Clapp, D.W. & Low, P.S. Expression and functional characterization of the β-isoform of the folate receptor on CD34+ cells. *Blood* **93**, 3940-3948 (1999).

168. Nakashima-Matsushita, N., Homma, T., Yu, S., Matsuda, T., Sunahara, N., Nakamura, T., Tsukano, M., Ratnam, M. & Matsuyama, T. Selective expression of folate receptor beta and its possible role in methotrexate transport in synovial macrophages from patients with rheumatoid arthritis. *Arthritis & Rheumatism* **42**, 1609-1616 (1999).

169. Van Der Heijden, J.W., Oerlemans, R., Dijkmans, B.A.C., Qi, H., Laken, C.J.V.D., Lems, W.F., Jackman, A.L., Kraan, M.C., Tak, P.P., Ratnam, M. & Jansen, G. Folate receptor β as a potential delivery route for novel folate antagonists to macrophages in the synovial tissue of rheumatoid arthritis patients. *Arthritis & Rheumatism* **60**, 12-21 (2009).

170. Xia, W., Hilgenbrink, A.R., Matteson, E.L., Lockwood, M.B., Cheng, J.X. & Low, P.S. A functional folate receptor is induced during macrophage activation and can be used to target drugs to activated macrophages. *Blood* **113**, 438-446 (2009).

171. Wu, M., Gunning, W. & Ratnam, M. Expression of folate receptor type alpha in relation to cell type, malignancy, and differentiation in ovary, uterus, and cervix. *Cancer Epidemiology Biomarkers & Prevention* **8**, 775-782 (1999).

172. Bueno, R., Appasani, K., Mercer, H., Lester, S. & Sugarbaker, D. The α folate receptor is highly activated in malignant pleural mesothelioma. *Journal of Thoracic and Cardiovascular Surgery* **121**, 225-233 (2001).

173. Christoph, D.C., Asuncion, B.R., Hassan, B., Tran, C., Maltzman, J.D., O'Shannessy, D.J., Wynes, M.W., Gauler, T.C., Wohlschlaeger, J., Hoiczyk, M., Schuler, M., Eberhardt, W.E. & Hirsch, F.R. Significance of folate receptor alpha and thymidylate synthase protein expression in patients with non-small-cell lung cancer treated with pemetrexed. *Journal of Thoracic Oncology* **8**, 19-30 (2013).

174. Crane, L.A., Arts, H.G., van Oosten, M., Low, P., van der Zee, A.J., van Dam, G. & Bart, J. The effect of chemotherapy on expression of folate receptor-alpha in ovarian cancer. *Cellular Oncology* **35**, 9-18 (2012).

175. Nunez, M.I., Behrens, C., Woods, D.M., Lin, H., Suraokar, M., Kadara, H., Hofstetter, W., Kalhor, N., Lee, J.J., Franklin, W., Stewart, D.J. & Wistuba, I.I. High expression of folate

receptor alpha in lung cancer correlates with adenocarcinoma histology and mutation. *Journal of Thoracic Oncology* **7**, 833-840 (2012).

176. Ross, J.F., Chaudhuri, P.K. & Ratnam, M. Differential regulation of folate receptor isoforms in normal and malignant tissues in vivo and in established cell lines. Physiologic and clinical implications. *Cancer* **73**, 2432-2443 (1994).

177. Toffoli, G., Cernigoi, C., Russo, A., Gallo, A., Bagnoli, M. & Boiocchi, M. Overexpression of folate binding protein in ovarian cancers. *International Journal of Cancer* **74**, 193-198 (1997).

178. Pan, X.Q., Zheng, X., Shi, G., Wang, H., Ratnam, M. & Lee, R.J. Strategy for the treatment of acute myelogenous leukemia based on folate receptor β–targeted liposomal doxorubicin combined with receptor induction using all-trans retinoic acid. *Blood* **100**, 594-602 (2002).

179. Banerjee, P.S., Zuniga, E.S., Ojima, I. & Carrico, I.S. Targeted and armed oncolytic adenovirus via chemoselective modification. *Bioorganic & Medicinal Chemistry Letters* **21**, 4985-4988 (2011).

180. Banerjee, P.S., Ostapchuk, P., Hearing, P. & Carrico, I.S. Unnatural amino acid incorporation onto adenoviral (Ad) coat proteins facilitates chemoselective modification and retargeting of Ad type 5 vectors. *Journal of Virology* **85**, 7546-7554 (2011).

181. Banerjee, P.S., Ostapchuk, P., Hearing, P. & Carrico, I. Chemoselective attachment of small molecule effector functionality to human adenoviruses facilitates gene delivery to cancer cells. *Journal of the American Chemical Society* **132**, 13615-13617 (2010).

182. Wang, K.S., Kuhn, R.J., Strauss, E.G., Ou, S. & Strauss, J.H. High-affinity laminin receptor is a receptor for Sindbis virus in mammalian cells. *Journal of Virology* **66**, 4992-5001 (1992).

183. Byrnes, A.P. & Griffin, D.E. Binding of Sindbis virus to cell surface heparan sulfate. *Journal of Virology* **72**, 7349-7356 (1998).

184. Klimstra, W.B., Heidner, H.W. & Johnston, R.E. The furin protease cleavage recognition sequence of Sindbis virus PE2 can mediate virion attachment to cell surface heparan sulfate. *Journal of Virology* **73**, 6299-6306 (1999).

185. Myles, K.M., Pierro, D.J. & Olson, K.E. Deletions in the putative cell receptor-binding domain of Sindbis virus strain MRE16 E2 glycoprotein reduce midgut infectivity in Aedes aegypti. *Journal of Virology* **77**, 8872-8881 (2003).

186. Sanz, M.A., Rejas, M., amp, x, a, T. & Carrasco, L. Individual expression of Sindbis virus glycoproteins. E1 alone promotes cell fusion. *Virology* **305**, 463-472 (2003).

187. Haisma, H.J., Kamps, G.K., Bouma, A., Geel, T.M., Rots, M.G., Kariath, A. & Bellu, A.R. Selective targeting of adenovirus to αvβ3 integrins, VEGFR2 and Tie2 endothelial

receptors by angio-adenobodies. *International Journal of Pharmaceutics* **391**, 155-161 (2010).

188. Weitzman, M.D. & Linden, R.M. in Adeno-Associated Virus (eds. Snyder, R.O. & Moullier, P.) 1-23 (Humana Press, 2011).

189. Srivastava, A., Lusby, E.W. & Berns, K.I. Nucleotide sequence and organization of the adeno-associated virus 2 genome. *Journal of Virology* **45**, 555-564 (1983).

190. Büeler, H. in Biological Chemistry 613 (1999).

191. Weindler, F.W. & Heilbronn, R. A subset of herpes simplex virus replication genes provides helper functions for productive adeno-associated virus replication. *Journal of Virology* **65**, 2476-2483 (1991).

192. Richardson, W.D. & Westphal, H. Requirement for either early region 1a or early region 1b adenovirus gene products in the helper effect for adeno-associated virus. *Journal of Virology* **51**, 404-410 (1984).

193. Conway, J.E., Zolotukhin, S., Muzyczka, N., Hayward, G.S. & Byrne, B.J. Recombinant adeno-associated virus type 2 replication and packaging is entirely supported by a herpes simplex virus type 1 amplicon expressing Rep and Cap. *Journal of Virology* **71**, 8780-8789 (1997).

194. Kotin, R.M., Siniscalco, M., Samulski, R.J., Zhu, X.D., Hunter, L., Laughlin, C.A., McLaughlin, S., Muzyczka, N., Rocchi, M. & Berns, K.I. Site-specific integration by adeno-associated virus. *Proceedings of the National Academy of Sciences of the United States of America* **87**, 2211-2215 (1990).

195. Kwon, I. & Schaffer, D.V. Designer gene delivery vectors: Molecular engineering and evolution of adeno-associated viral vectors for enhanced gene transfer. *Pharmaceutical Research* **25**, 489-499 (2008).

196. Daya, S. & Berns, K.I. Gene therapy using adeno-associated virus vectors. *Clinical Microbiology Reviews* **21**, 583-593 (2008).

197. Coura, R.D. & Nardi, N.B. A role for adeno-associated viral vectors in gene therapy. *Genetics and Molecular Biology* **31**, 1-11 (2008).

198. Buning, H., Perabo, L., Coutelle, O., Quadt-Humme, S. & Hallek, M. Recent developments in adeno-associated virus vector technology. *Journal of Gene Medicine* **10**, 717-733 (2008).

199. McLaughlin, S.K., Collis, P., Hermonat, P.L. & Muzyczka, N. Adeno-associated virus general transduction vectors: analysis of proviral structures. *Journal of Virology* **62**, 1963-1973 (1988).
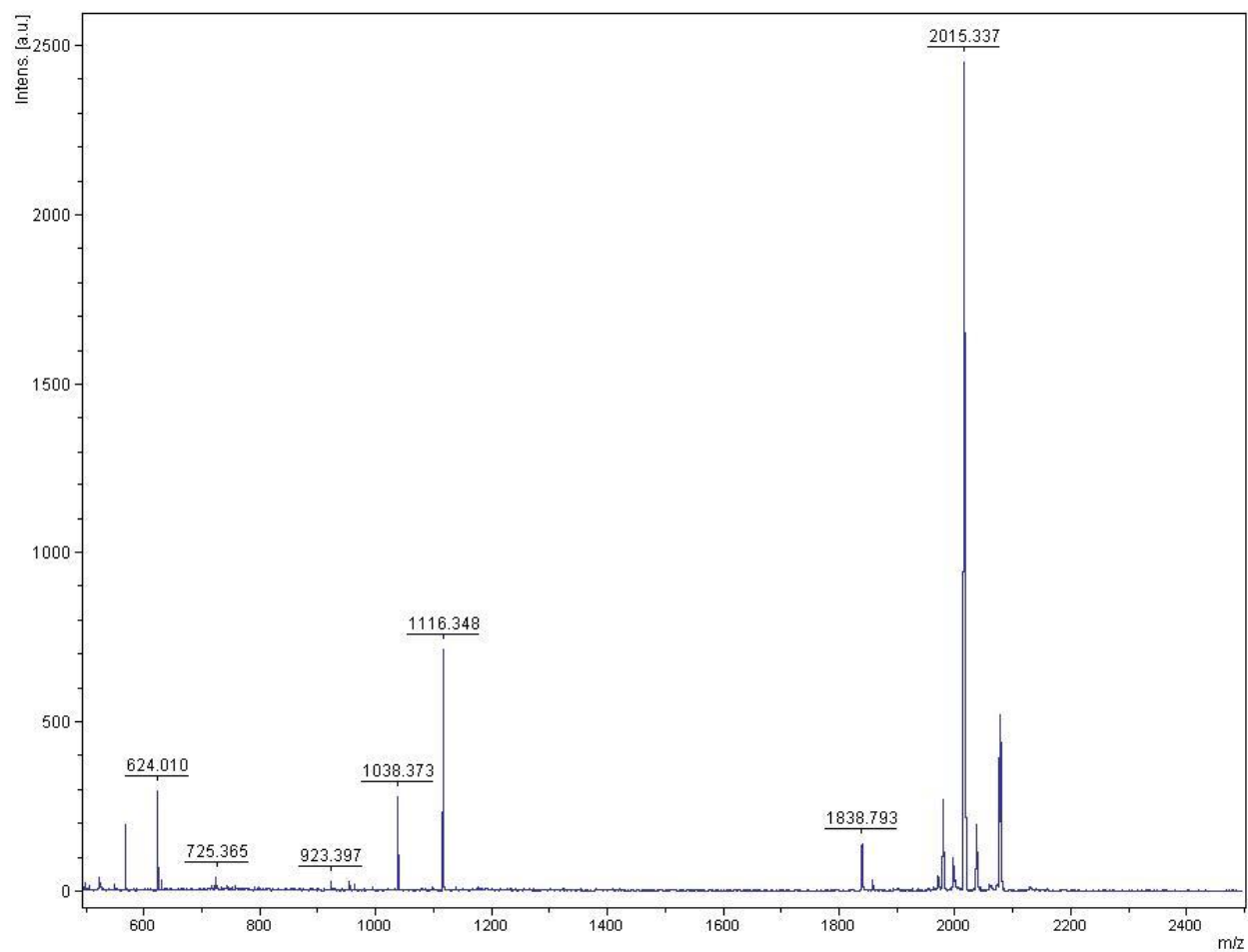
200. Snyder, R.O., Samulski, R.J. & Muzyczka, N. In vitro resolution of covalently joined AAV chromosome ends. *Cell* **60**, 105-113 (1990).

201. Snyder, R.O., Im, D.S., Ni, T., Xiao, X., Samulski, R.J. & Muzyczka, N. Features of the adeno-associated virus origin involved in substrate recognition by the viral Rep protein. *Journal of Virology* **67**, 6096-6104 (1993).

202. McCarty, D.M., Ryan, J.H., Zolotukhin, S., Zhou, X. & Muzyczka, N. Interaction of the adeno-associated virus Rep protein with a sequence within the A palindrome of the viral terminal repeat. *Journal of Virology* **68**, 4998-5006 (1994).

203. Smith, R.H. & Kotin, R.M. The Rep52 gene product of adeno-associated virus is a DNA helicase with 3'-to-5' polarity. *Journal of Virology* **72**, 4874-4881 (1998).

204. King, J.A., Dubielzig, R., Grimm, D. & Kleinschmidt, J.A. DNA helicase-mediated packaging of adeno-associated virus type 2 genomes into preformed capsids. *The EMBO Journal* **20**, 3282-3291 (2001).

205. Dubielzig, R., King, J.A., Weger, S., Kern, A. & Kleinschmidt, J.A. Adeno-associated virus type 2 protein interactions: formation of pre-encapsidation complexes. *Journal of Virology* **73**, 8989-8998 (1999).

206. Kyösti ö, S.R., Owens, R.A., Weitzman, M.D., Antoni, B.A., Chejanovsky, N. & Carter, B.J. Analysis of adeno-associated virus (AAV) wild-type and mutant Rep proteins for their abilities to negatively regulate AAV p5 and p19 mRNA levels. *Journal of Virology* **68**, 2947-2957 (1994).

207. Sonntag, F., Schmidt, K. & Kleinschmidt, J.A. A viral assembly factor promotes AAV2 capsid formation in the nucleolus. *Proceedings of the National Academy of Sciences of the United States of America* **107**, 10220-10225 (2010).

208. Mueller, C. & Flotte, T.R. Clinical gene therapy using recombinant adeno-associated virus vectors. *Gene Therapy* **15**, 858-863 (2008).

209. Martini, S.V., Rocco, P.R.M. & Morales, M.M. Adeno-associated virus for cystic fibrosis gene therapy. *Brazilian Journal of Medical and Biological Research* **44**, 1097-1104 (2011).

210. Nathwani, A.C., Tuddenham, E.G.D., Rangarajan, S., Rosales, C., McIntosh, J., Linch, D.C., Chowdary, P., Riddell, A., Pie, A.J., Harrington, C., O'Beirne, J., Smith, K., Pasi, J., Glader, B., Rustagi, P., Ng, C.Y.C., Kay, M.A., Zhou, J., Spence, Y., Morton, C.L., Allay, J., Coleman, J., Sleep, S., Cunningham, J.M., Srivastava, D., Basner-Tschakarjan, E., Mingozzi, F., High, K.A., Gray, J.T., Reiss, U.M., Nienhuis, A.W. & Davidoff, A.M. Adenovirus-associated virus vector-mediated gene transfer in hemophilia B. *New England Journal of Medicine* **365**, 2357-2365 (2011).

211. Bowles, D.E., McPhee, S.W.J., Li, C., Gray, S.J., Samulski, J.J., Camp, A.S., Li, J., Wang, B., Monahan, P.E., Rabinowitz, J.E., Grieger, J.C., Govindasamy, L., Agbandje-McKenna,

M., Xiao, X. & Samulski, R.J. Phase 1 gene therapy for Duchenne muscular dystrophy using a translational optimized AAV vector. *Molecular Therapy* **20**, 443-455 (2012).

212.   Kaplitt, M.G., Feigin, A., Tang, C., Fitzsimons, H.L., Mattis, P., Lawlor, P.A., Bland, R.J., Young, D., Strybing, K., Eidelberg, D. & During, M.J. Safety and tolerability of gene therapy with an adeno-associated virus (AAV) borne GAD gene for Parkinson's disease: an open label, phase I trial. *The Lancet* **369**, 2097-2105 (2007).

213.   Tal, J. Adeno-associated virus-based vectors in gene therapy. *Journal of Biomedical Science* **7**, 279-291 (2000).

214.   Nakai, H., Wu, X., Fuess, S., Storm, T.A., Munroe, D., Montini, E., Burgess, S.M., Grompe, M. & Kay, M.A. Large-scale molecular characterization of adeno-associated virus vector integration in mouse liver. *Journal of Virology* **79**, 3606-3614 (2005).

215.   Duan, D., Sharma, P., Yang, J., Yue, Y., Dudus, L., Zhang, Y., Fisher, K.J. & Engelhardt, J.F. Circular intermediates of recombinant adeno-associated virus have defined structural characteristics responsible for long-term episomal persistence in muscle tissue. *Journal of Virology* **72**, 8568-8577 (1998).

216.   Nakai, H., Yant, S.R., Storm, T.A., Fuess, S., Meuse, L. & Kay, M.A. Extrachromosomal recombinant adeno-associated virus vector genomes are primarily responsible for stable liver transduction in vivo. *Journal of Virology* **75**, 6969-6976 (2001).

217.   Schnepp, B.C., Clark, K.R., Klemanski, D.L., Pacak, C.A. & Johnson, P.R. Genetic fate of recombinant adeno-associated virus vector genomes in muscle. *Journal of Virology* **77**, 3495-3504 (2003).

218.   Hauck, B., Chen, L. & Xiao, W. Generation and characterization of chimeric recombinant AAV vectors. *Molecular Therapy* **7**, 419-425 (2003).

219.   Rabinowitz, J.E., Bowles, D.E., Faust, S.M., Ledford, J.G., Cunningham, S.E. & Samulski, R.J. Cross-dressing the virion: the transcapsidation of adeno-associated virus serotypes functionally defines subgroups. *Journal of Virology* **78**, 4421-4432 (2004).

220.   Gigout, L., Rebollo, P., Clement, N., Warrington, K.H., Muzyczka, N., Linden, R.M. & Weber, T. Altering AAV tropism with mosaic viral capsids. *Molecular Therapy* **11**, 856-865 (2005).

221.   Stachler, M.D. & Bartlett, J.S. Mosaic vectors comprised of modified AAV1 capsid proteins for efficient vector purification and targeting to vascular endothelial cells. *Gene Therapy* **13**, 926-931 (2006).

222.   Grimm, D., Pandey, K., Nakai, H., Storm, T.A. & Kay, M.A. Liver transduction with recombinant adeno-associated virus is primarily restricted by capsid serotype not vector genotype. *Journal of Virology* **80**, 426-439 (2006).

223. Bartlett, J.S., Kleinschmidt, J., Boucher, R.C. & Samulski, R.J. Targeted adeno-associated virus vector transduction of nonpermissive cells mediated by a bispecific F(ab'γ)2 antibody. *Nature Biotechnology* **17**, 181-186 (1999).

224. Ponnazhagan, S., Mahendra, G., Kumar, S., Thompson, J.A. & Castillas, J., Mark. Conjugate-based targeting of recombinant adeno-associated virus type 2 vectors by using avidin-linked ligands. *Journal of Virology* **76**, 12900-12907 (2002).

225. Girod, A., Ried, M., Wobus, C., Lahm, H., Leike, K., Kleinschmidt, J., Deleage, G. & Hallek, M. Genetic capsid modifications allow efficient re-targeting of adeno-associated virus type 2. *Nature Medicine* **5**, 1052-1056 (1999).

226. Shi, W. & Bartlett, J.S. RGD inclusion in VP3 provides adeno-associated virus type 2 (AAV2)-based vectors with a heparan sulfate-independent cell entry mechanism. *Molecular Therapy* **7**, 515-525 (2003).

227. White, S.J., Nicklin, S.A., Büning, H., Brosnan, M.J., Leike, K., Papadakis, E.D., Hallek, M. & Baker, A.H. Targeted gene delivery to vascular tissue in vivo by tropism-modified adeno-associated virus vectors. *Circulation* **109**, 513-519 (2004).

228. Munch, R.C., Janicki, H., Volker, I., Rasbach, A., Hallek, M., Buning, H. & Buchholz, C.J. Displaying high-affinity ligands on adeno-associated viral vectors enables tumor cell-specific and safe gene transfer. *Molecular Therapy* **21**, 109-118 (2013).

229. Ried, M.U., Girod, A., Leike, K., Büning, H. & Hallek, M. Adeno-associated virus capsids displaying immunoglobulin-binding domains permit antibody-mediated vector retargeting to specific cell surface receptors. *Journal of Virology* **76**, 4559-4566 (2002).

230. Arnold, G.S., Sasser, A.K., Stachler, M.D. & Bartlett, J.S. Metabolic biotinylation provides a unique platform for the purification and targeting of multiple AAV vector serotypes. *Molecular Therapy* **14**, 97-106 (2006).

231. Lang, K. & Chin, J.W. Cellular incorporation of unnatural amino acids and bioorthogonal labeling of proteins. *Chemical Reviews* **114**, 4764-4806 (2014).

232. Choi, V.W., Asokan, A., Haberman, R.A. & Samulski, R.J. in Current Protocols in Molecular Biology (John Wiley & Sons, Inc., 2001).

233. Rohr, U.-P., Wulf, M.-A., Stahn, S., Steidl, U., Haas, R. & Kronenwett, R. Fast and reliable titration of recombinant adeno-associated virus type-2 using quantitative real-time PCR. *Journal of Virological Methods* **106**, 81-88 (2002).
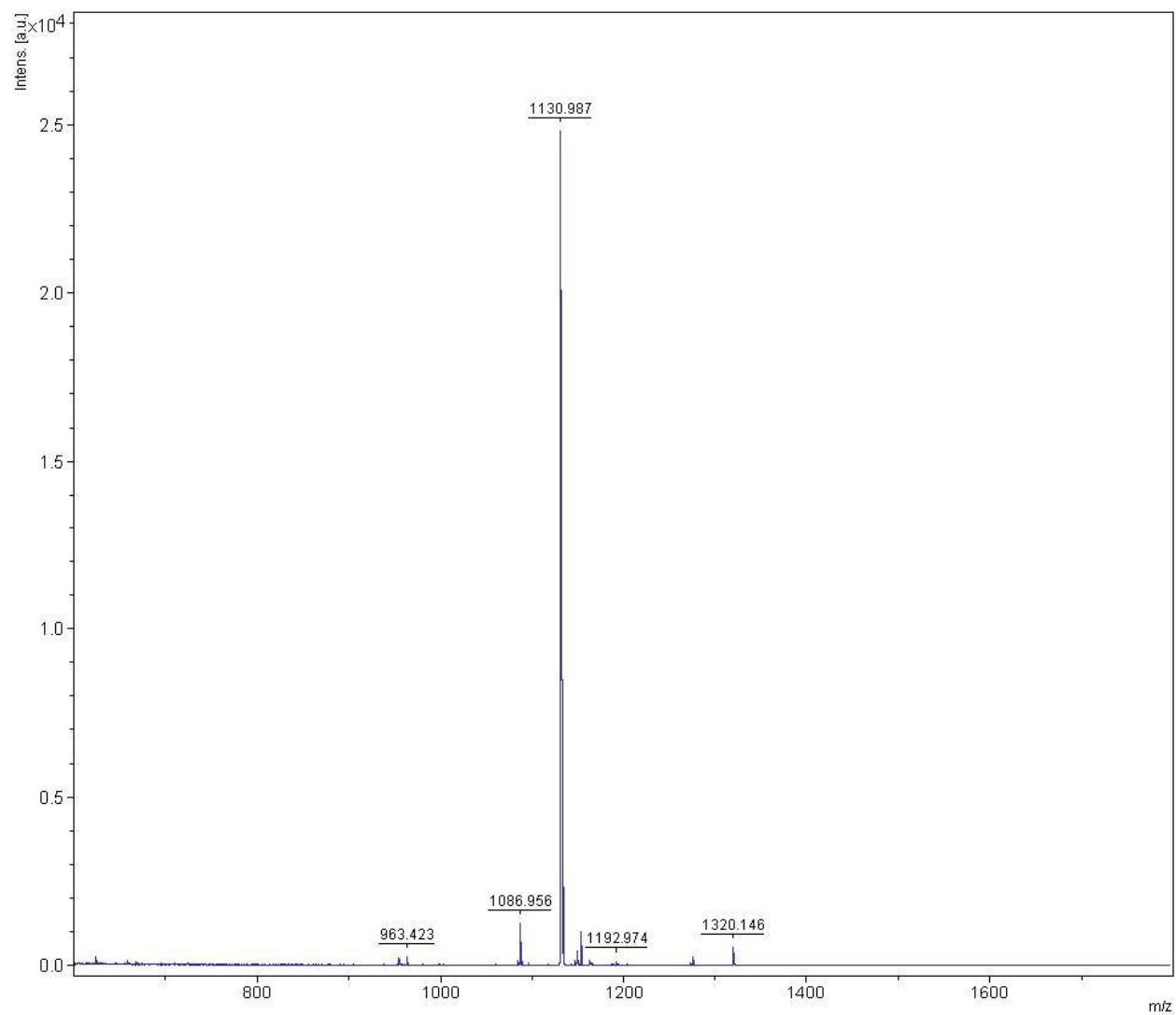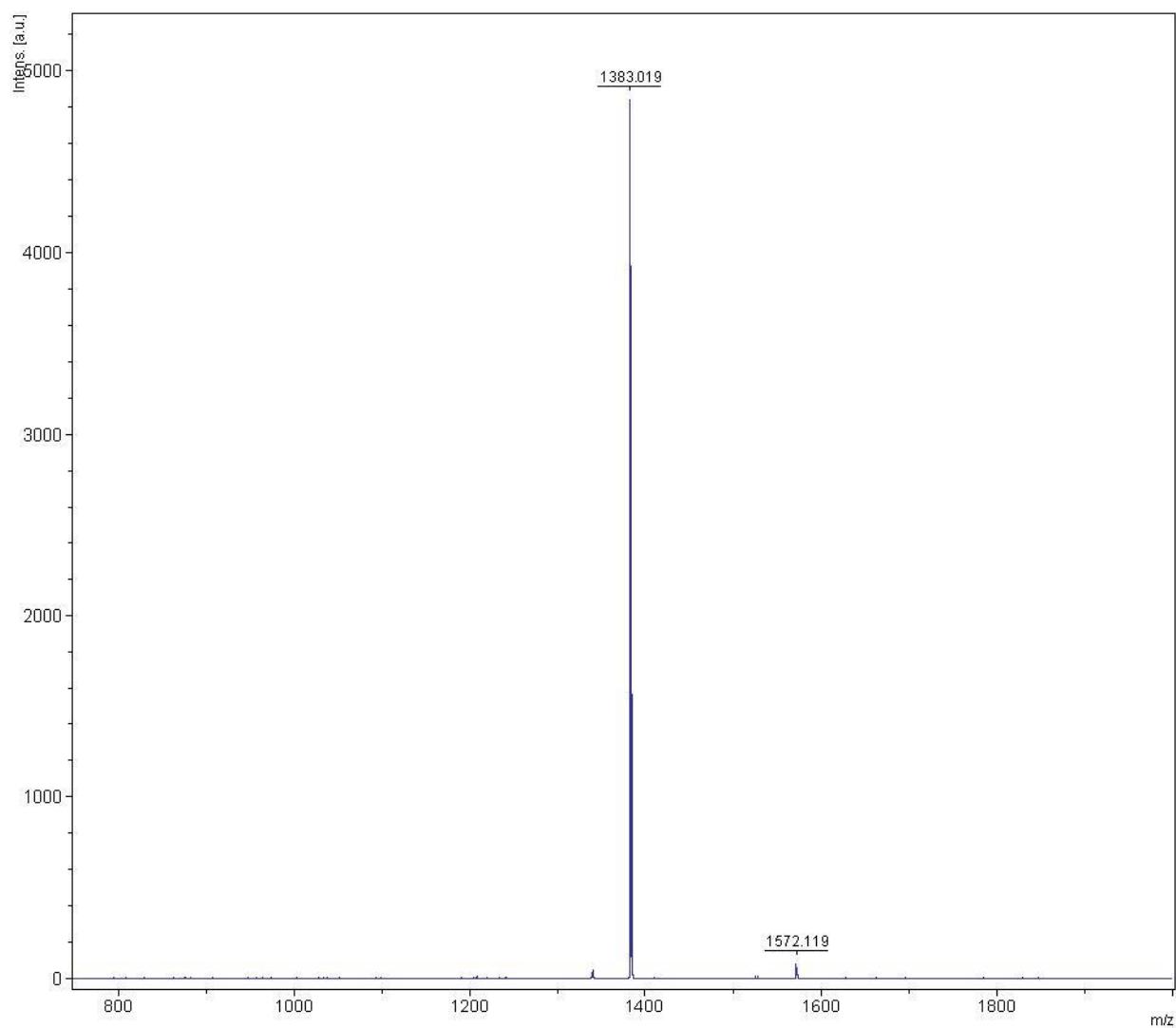
Appendix

Appendix 1. Mass Spectrum (MALDI+) of BCN-PEG-FLAG.
m/z calcd for $[C_{87}H_{136}N_{15}O_{37}S]^+$ $[M + H]^+$: 2014.894, found: 2015.337.
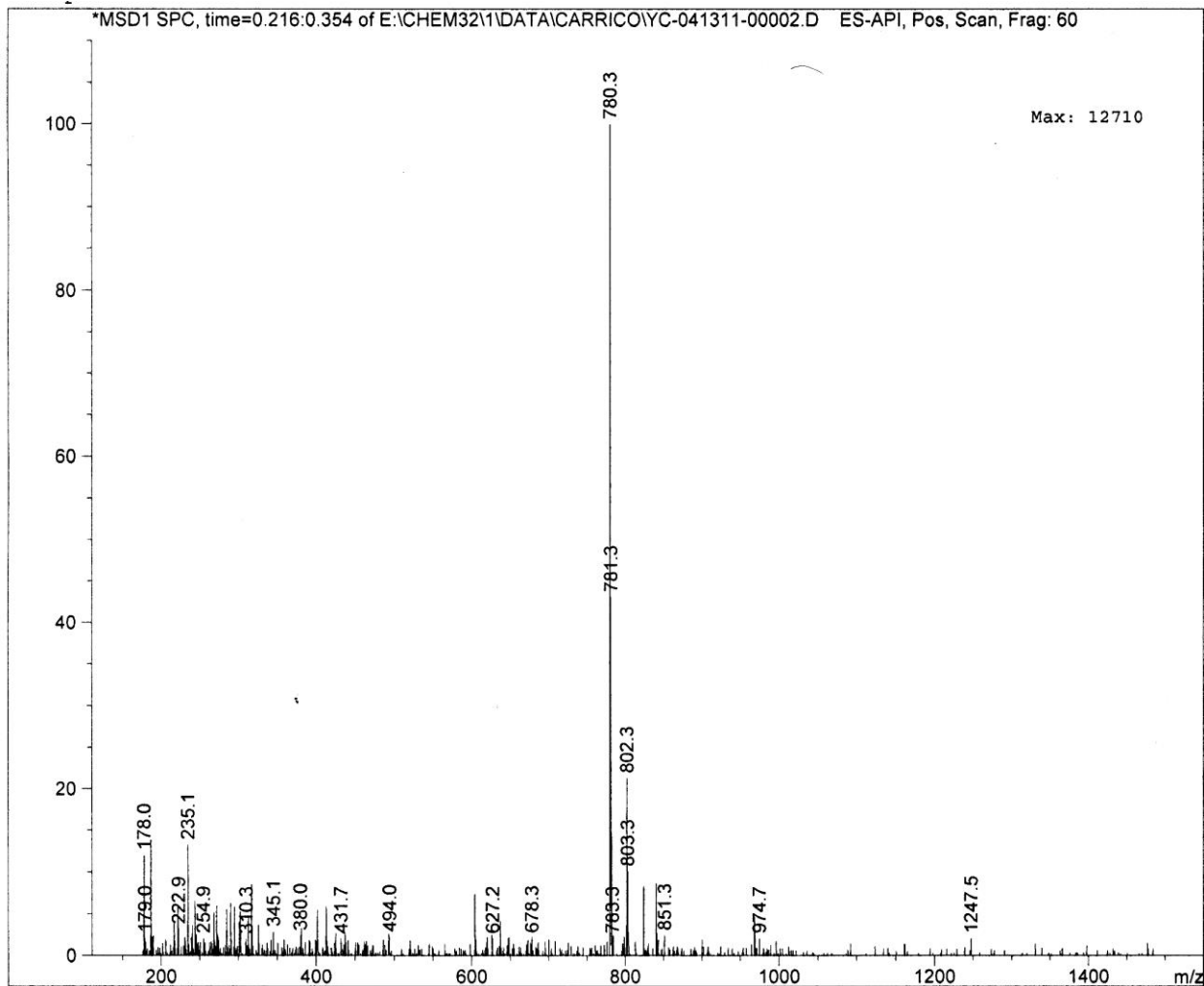
Appendix 2. Mass spectrum (MALDI+) of BCN-GGATWLPPR.

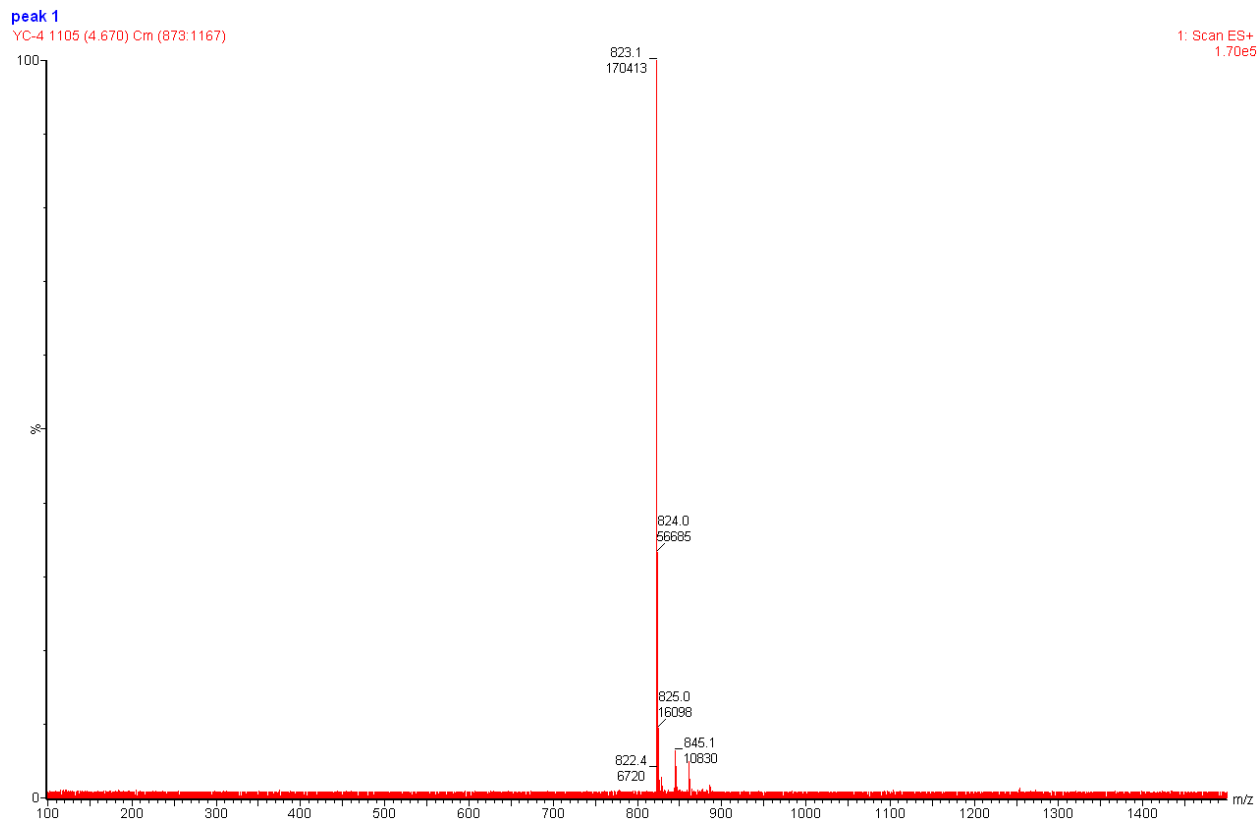*m/z* calcd for $[C_{55}H_{80}N_{13}O_{13}]^+$ $[M + H]^+$: 1130.600, found: 1130.987.

Appendix 3. Mass spectrum (MALDI+) of BCN-GGRLVAYEGWV.

m/z calcd for $[C_{67}H_{96}N_{15}O_{17}]^+$ $[M + H]^+$: 1382.710, found: 1383.019.
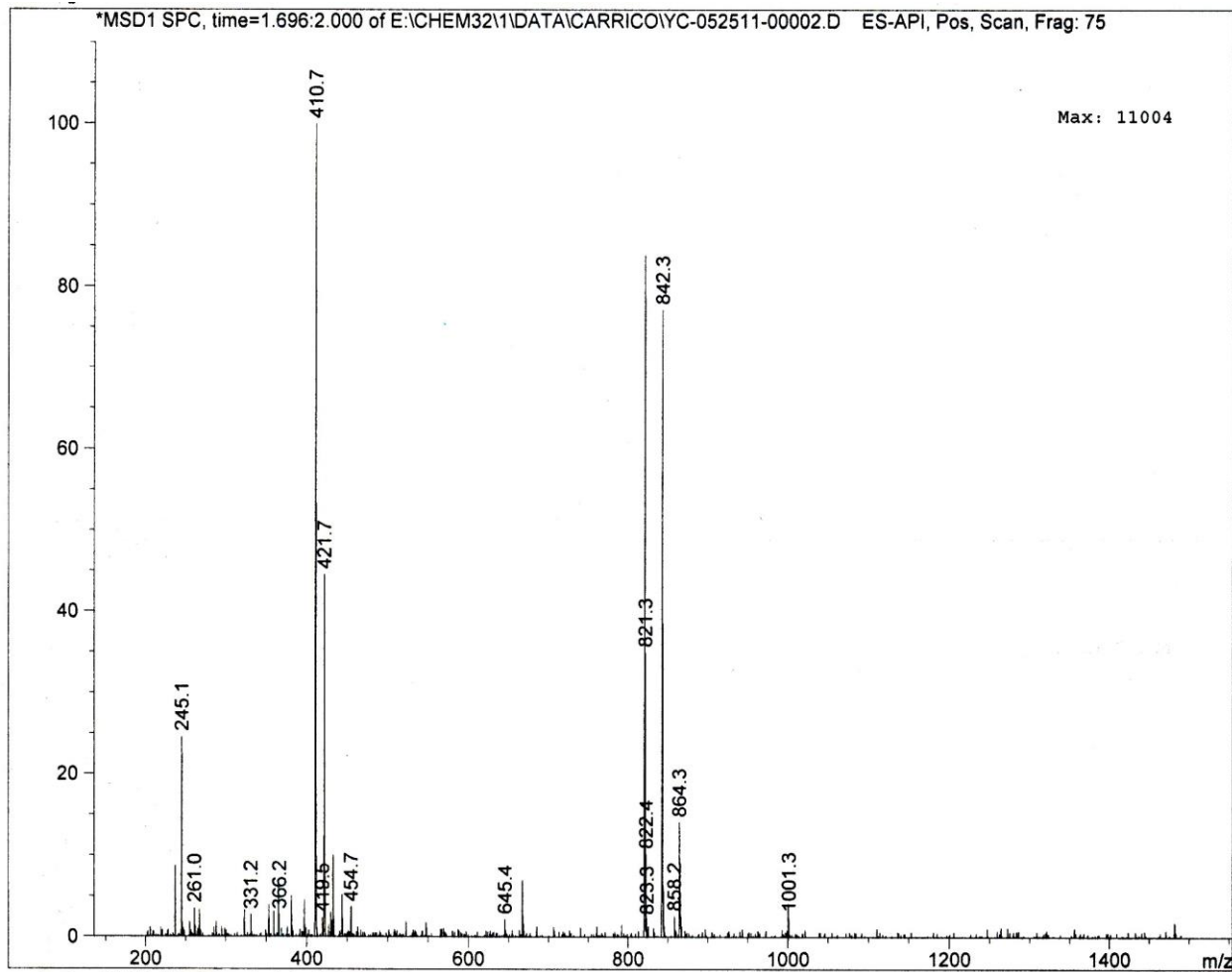
Appendix 4. Mass spectrum (ESI+) of BCN-c(RGDfK).

m/z calcd for $[C_{38}H_{54}N_9O_9]^+$ $[M + H]^+$: 780.404, found: 780.3.

Appendix 5. Mass spectrum (ESI+) of BCN-PEG-glutamate urea.

m/z calcd for $[C_{38}H_{60}N_7O_{13}]^+$ $[M + H]^+$: 822.425, found: 823.1.

Appendix 6. Mass spectrum (ESI+) of BCN-PEG-folate.

m/z calcd for $[C_{40}H_{54}N_9O_{10}]^+$ $[M + H]^+$: 820.399, found: 821.3; and m/z calcd for $[C_{40}H_{55}N_9O_{10}]^{2+}$ $[M + 2H]^{2+}$: 410.703, found: 410.7.